

UNIVERSITY OF MINNESOTA  
ST. ANTHONY FALLS HYDRAULIC LABORATORY

Project Report No. 316

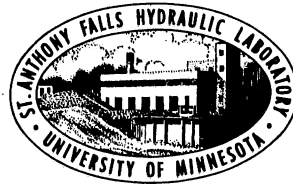
Numerical Simulation of Stratification Dynamics  
and Mixing in Wastewater Stabilization Ponds

by

Ruochuan Gu

and

Heinz G. Stefan



Prepared for

LEGISLATIVE COMMISSION ON MINNESOTA RESOURCES  
St. Paul, Minnesota

June 1991

**Minneapolis, Minnesota**



## Table of Contents

	<u>PAGE NO.</u>
List of Figures	ii
1. Introduction	1
2. Simulation of natural stratification and mixing dynamics	6
2.1 Overview of model development	6
2.2 Diurnal effects	6
2.3 Estimation of vertical thermal diffusivity	8
2.4 Input data	10
2.5 Model calibration	11
2.6 Model verification	25
3. Simulation of inflow jet mixing and water transfer	29
3.1 Jet entrainment and mixing	29
3.2 Water transfer	32
4. Simulation of stratification dynamics with jet mixing and water transfer	33
5. Evaluation of stratification and mixing dynamics	62
6. Summary	75
References	76
Appendix A Statistical Parameters of Error Analysis	79
Appendix B Definitions and Values of Model Coefficients	81
Appendix C Program Listings	84
Appendix D Water Temperature and Weather Data (on disk, by request)	102

The University of Minnesota is committed to the policy that all persons shall have equal access to its programs, facilities, and employment without regard to race religion, color, sex, national origin, handicap, age, or veteran status.

## List of Figures

- Fig. 1 Flow pattern and jet behavior of the wastewater discharge in pond 1 (mid-summer conditions)
- Fig. 2 Schematic of wastewater inflow into pond 1 and water transfer between pond 1 and pond 2
- Fig. 3 Schematic of water transfer between pond 2 and pond 3 and outflow from pond 3
- Fig. 4 Measured and simulated water temperatures in pond 3 at 6:00 am, Aug. 4, 1989, timestep = 24 hours
- Fig. 5 Measured and simulated water temperatures in pond 3 at 6:00 am, Aug. 13, 1989, timestep = 24 hours
- Fig. 6 Measured and simulated water temperatures in pond 3 at 6:00 am, Sept. 4, 1989, timestep = 24 hours
- Fig. 7 Measured and simulated water temperatures in pond 3 at 6:00 am, Sept. 13, 1989, timestep = 24 hours
- Fig. 8 Measured and simulated water temperatures in pond 3 at 6:00 am, Oct. 13, 1989, timestep = 24 hours
- Fig. 9 Measured and simulated water temperatures in pond 3, 1989, timestep = 12 hours, probe #1 (surface)
- Fig. 10 Measured and simulated water temperatures in pond 3, 1989, timestep = 12 hours, probe #2
- Fig. 11 Measured and simulated water temperatures in pond 3, 1989, timestep = 12 hours, probe #3
- Fig. 12 Measured and simulated water temperatures in pond 3, 1989, timestep = 12 hours, probe #4
- Fig. 13 Measured and simulated water temperatures in pond 3, 1989, timestep = 12 hours, probe #5
- Fig. 14 Measured and simulated water temperatures in pond 3, 1989, timestep = 12 hours, probe #6 (bottom)
- Fig. 15 Measured and simulated Diurnal cycle of water temperature stratification, pond 3, Aug. 4, 1989
- Fig. 16 Measured and simulated Diurnal cycle of water temperature stratification, pond 3, Aug. 13, 1989
- Fig. 17 Measured and simulated Diurnal cycle of water temperature stratification, pond 3, Aug. 22, 1989
- Fig. 18 Measured and simulated Diurnal cycle of water temperature stratification, pond 3, Sept. 2, 1989
- Fig. 19 Measured and simulated Diurnal cycle of water temperature stratification, pond 3, Sept. 25, 1989
- Fig. 20 Measured and simulated Diurnal cycle of water temperature stratification, pond 3, Oct. 13, 1989
- Fig. 21 Measured and simulated Diurnal cycle of water temperature stratification, pond 3, Oct. 21, 1989
- Fig. 22 a) Water depth and b) estimated net flow rate of inflow (positive) and outflow (negative), pond 3, 1989
- Fig. 23 a) Water depth and b) estimated net flow rate of inflow (positive) and outflow (negative), pond 3, 1990



## List of Figures (Cont'd)

- Fig. 24 Measured and simulated water temperatures in pond 3, 1990, timestep = 12 hours, probe #1 (surface)
- Fig. 25 Measured and simulated water temperatures in pond 3, 1990, timestep = 12 hours, probe #2
- Fig. 26 Measured and simulated water temperatures in pond 3, 1990, timestep = 12 hours, probe #3
- Fig. 27 Measured and simulated water temperatures in pond 3, 1990, timestep = 12 hours, probe #4
- Fig. 28 Measured and simulated water temperatures in pond 3, 1990, timestep = 12 hours, probe #5
- Fig. 29 Measured and simulated water temperatures in pond 3, 1990, timestep = 12 hours, probe #6 (bottom)
- Fig. 30 Variation of inflow, outflow, rainfall, evaporation and storage with time, pond 1, Aug. 1 - Nov. 30, 1989
- Fig. 31 Variation of inflow, outflow, rainfall, evaporation and storage with time, pond 1, April, 7 - Oct. 31, 1990
- Fig. 32 Total volumes of inflow, outflow, rainfall, evaporation and change in storage, Aug. 1 - Nov. 30, 1989
- Fig. 33 Total volumes of inflow, outflow, rainfall, evaporation and change in storage, April 7 - Oct. 31, 1990
- Fig. 34 Water balance for pond 1, Aug. 1 - Nov. 30, 1989
- Fig. 35 Water balance for pond 1, April 7, - Oct. 31, 1990
- Fig. 36 Measured and calculated water depth, pond 1, Aug. 1-Nov. 30, 1989
- Fig. 37 Calculated flow rate of entrainment by inflow jet in pond 1, 1989
- Fig. 38 Measured and calculated water depth, pond 1, April 7-Oct. 31, 1990
- Fig. 39 Calculated flow rate of entrainment by inflow jet in pond 1, 1990
- Fig. 40 Measured inflow temperature and simulated spreading flow temperature, pond 1, 1989
- Fig. 41 Calculated depth of intruding interflow (equilibrium layer), pond 1, 1989
- Fig. 42 Measured inflow temperature and simulated spreading flow temperature, pond 1, 1990
- Fig. 43 Calculated depth of intruding interflow (equilibrium layer), pond 1, 1990
- Fig. 44 Comparison of water temperature profiles simulated with jet and without jet, pond 1, 6:00 pm, July 3, 1990
- Fig. 45 Comparison of temperature-depth profiles simulated with jet and without jet, pond 1, 6:00 pm, Aug. 29, 1990
- Fig. 46 Measured and simulated water temperatures in pond 1, 1989 timestep = 12 hours, probe #1
- Fig. 47 Measured and simulated water temperatures in pond 1, 1989 timestep = 12 hours, probe #2
- Fig. 48 Measured and simulated water temperatures in pond 1, 1989 timestep = 12 hours, probe #3
- Fig. 49 Measured and simulated water temperatures in pond 1, 1989 timestep = 12 hours, probe #4
- Fig. 50 Measured and simulated water temperatures in pond 1, 1989 timestep = 12 hours, probe #5
- Fig. 51 Measured and simulated water temperatures in pond 1, 1989 timestep = 12 hours, probe #6

## List of Figures (Cont'd)

- Fig. 52 Measured and simulated water temperatures in pond 1, 1990  
timestep = 12 hours, probe #1
- Fig. 53 Measured and simulated water temperatures in pond 1, 1990  
timestep = 12 hours, probe #2
- Fig. 54 Measured and simulated water temperatures in pond 1, 1990  
timestep = 12 hours, probe #3
- Fig. 55 Measured and simulated water temperatures in pond 1, 1990  
timestep = 12 hours, probe #4
- Fig. 56 Measured and simulated water temperatures in pond 1, 1990  
timestep = 12 hours, probe #5
- Fig. 57 Measured and simulated water temperatures in pond 1, 1990  
timestep = 12 hours, probe #6
- Fig. 58 Simulated water temperatures, pond 1, August, 1989
- Fig. 59 Simulated water temperatures, pond 1, September, 1989
- Fig. 60 Simulated water temperatures, pond 1, October, 1989
- Fig. 61 Simulated water temperatures, pond 1, November, 1989
- Fig. 62 Simulated water temperatures, pond 1, April, 1990
- Fig. 63 Simulated water temperatures, pond 1, May, 1990
- Fig. 64 Simulated water temperatures, pond 1, June, 1990
- Fig. 65 Simulated water temperatures, pond 1, July, 1990
- Fig. 66 Simulated water temperatures, pond 1, August, 1990
- Fig. 67 Simulated water temperatures, pond 1, September, 1990
- Fig. 68 Simulated water temperatures, pond 1, October, 1990
- Fig. 69 Simulated water temperatures, pond 3, August, 1989
- Fig. 70 Simulated water temperatures, pond 3, September, 1989
- Fig. 71 Simulated water temperatures, pond 3, October, 1989
- Fig. 72 Simulated water temperatures, pond 3, April, 1990
- Fig. 73 Simulated water temperatures, pond 3, May, 1990
- Fig. 74 Simulated water temperatures, pond 3, June, 1990
- Fig. 75 Simulated water temperatures, pond 3, July, 1990
- Fig. 76 Simulated water temperatures, pond 3, August, 1990
- Fig. 77 Simulated water temperatures, pond 3, September, 1990
- Fig. 78 Simulated water temperatures, pond 3, October, 1990

# 1. Introduction

Stabilization ponds are an economical and efficient method of waste water treatment in small communities. This form of wastewater treatment relies upon the natural ability of a body of water to achieve self-purification. Self-purification means reduction of fecal coliform bacteria, biochemical oxygen demand, and organic content, and returning the dissolved oxygen level to desirable levels. Overall efficiency of waste stabilization ponds is a function of many interacting processes. To gain a better understanding of the important factors and for insight into methods of stabilization pond management, a study of the physical, chemical and biological processes has been initiated. In an earlier report (Luck and Stefan, 1990) field observations on water temperature and dissolved oxygen stratification in the Harris, Minnesota, wastewater stabilization ponds were reported. The alternating mixing and restratification of these ponds over periods of hours or days were documented. These physical processes which are in response to time-variable weather underlie the water chemistry and phytoplankton growth.

The ultimate goal of the study is to develop a water quality model for wastewater stabilization ponds, in order to predict the effluent water quality at the time of release. As a first step a water temperature model, including stratification is developed herein. This report describes that model and its ability to predict observed temperature distributions and stratification periods in the ponds. Intermittent stratification, sometimes lasting several days, has a strong effect on sediment/water interaction and vertical transport of dissolved oxygen, nutrients and phytoplankton in the pond. It is therefore considered necessary to first develop a model to simulate stratification and mixing as a basis for a dynamic water quality model.

The wastewater treatment facility at Harris, Minnesota consists of three stabilization ponds and was selected for a case study. Wastewater is pumped underground through a 4 inch diameter ductile iron pipe and discharged vertically in the center of pond 1 (Fig. 1). Fig. 2 and Fig. 3 schematically illustrate the water transfer system between ponds and inflow to pond 1 and outflow from pond 3. The outlet pipes withdraw water from an elevation two feet above the pond bottom. During the summer months the ponds are operated in series. As water accumulates in pond 1 it is intermittently transferred to pond 2, and eventually to pond 3. This water transfer is gravity driven with the flow rate controlled by the use of various sized gates in the control structures. In wintertime, the water flows freely between pond 1 and 2 as the control gate between them is kept open. Pond 3 is discharged intermittently, mostly during the spring and again during the fall, into a ditch that flows into Goose Creek and then into the St. Croix River.

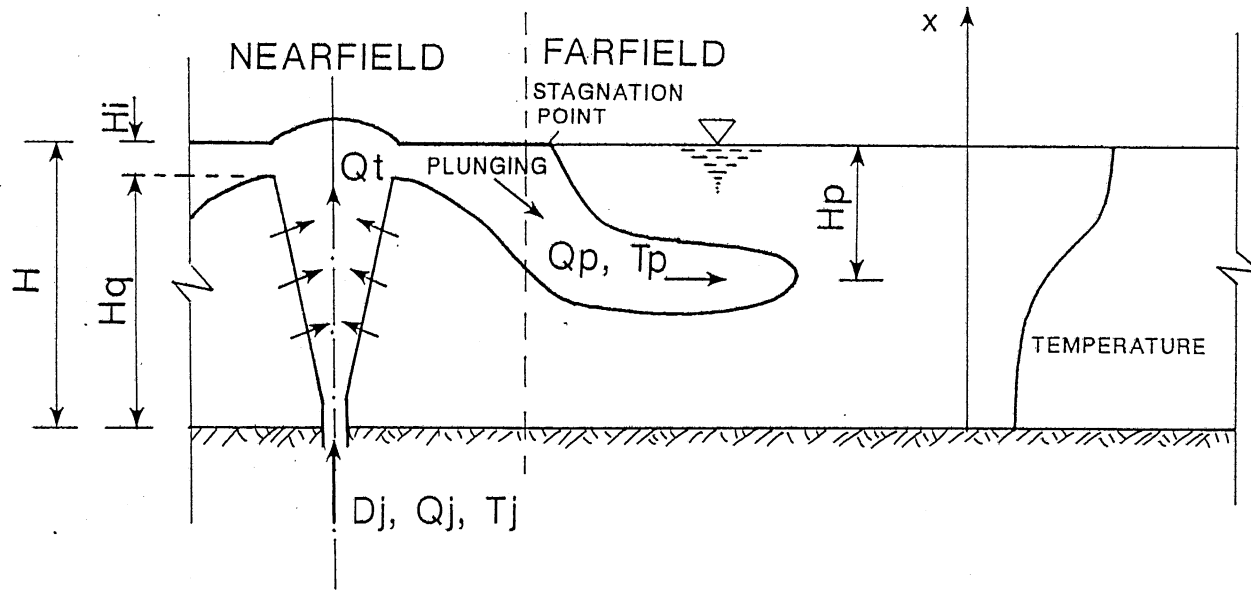


Fig. 1 Flow pattern and jet behavior of the wastewater discharge in pond 1 (mid-summer conditions)

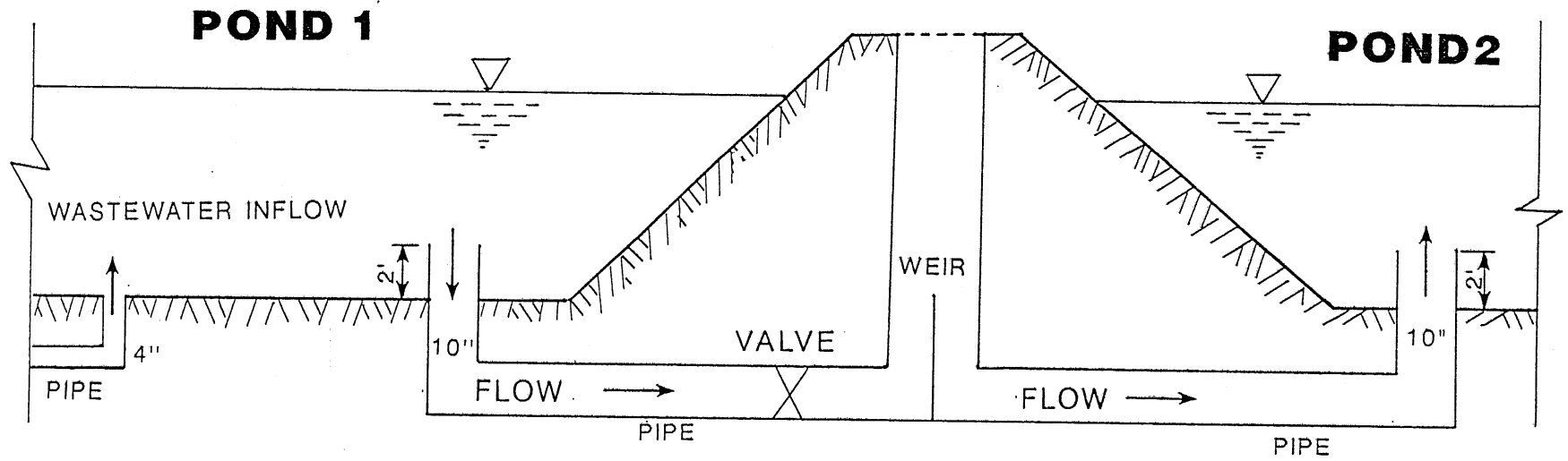


Fig. 2 Schematic of wastewater inflow into pond 1 and water transfer between pond 1 and pond 2

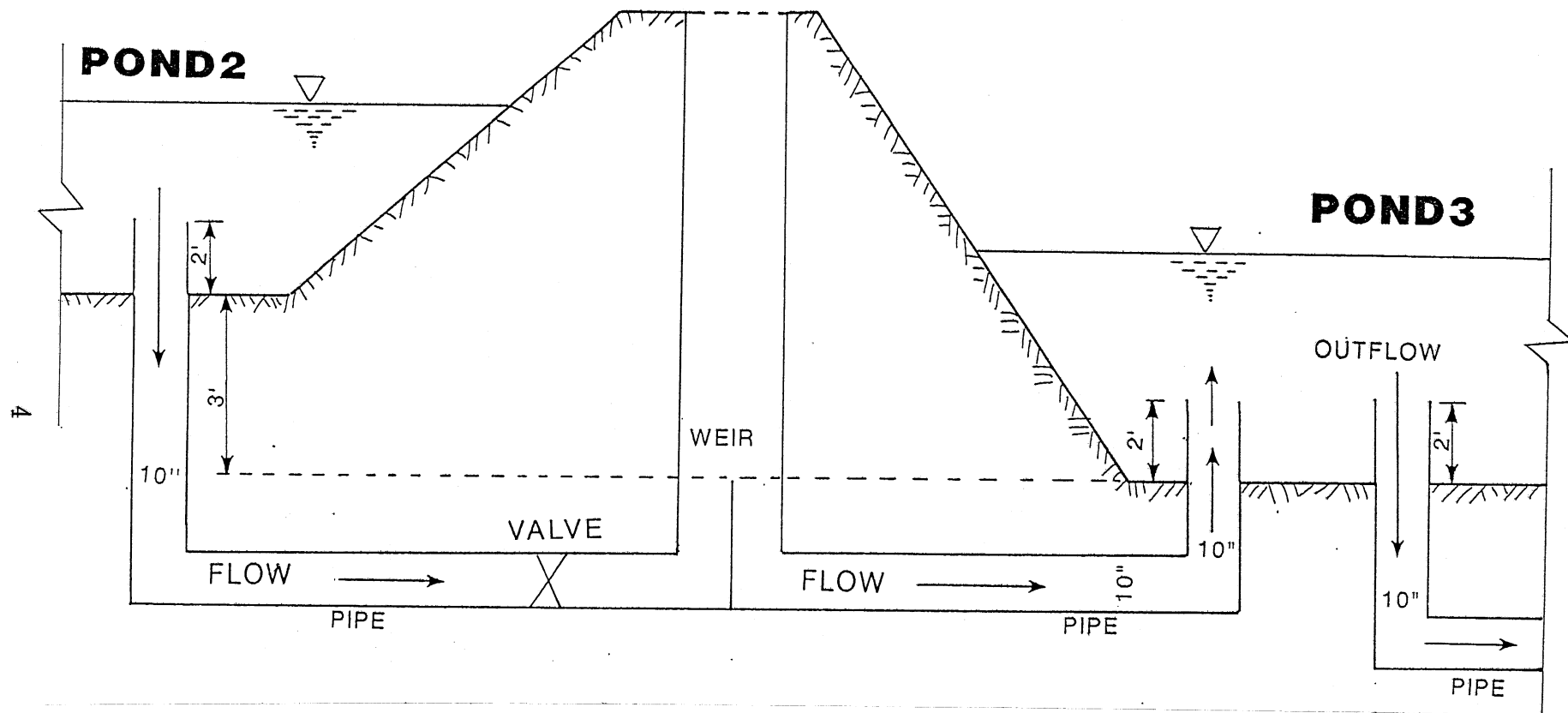


Fig. 3 Schematic of water transfer between pond 2 and pond 3 and outflow from pond 3

The physical limnology of the ponds was investigated by Luck and Stefan (1990) through field studies including continuous recordings of meteorological and thermal parameters, occasional measurements of underwater light, dissolved oxygen and secchi depth and observations of ice thicknesses and snow cover in winter. The information was collected as part of a broader, joint program in which researchers from the Minnesota Pollution Control Agency is measuring biological and chemical parameters on a similar schedule. By analysis of the data it is intended to gain an understanding of water quality dynamics and the interacting processes in such ponds and to obtain data for the calibration of a dynamic pond water quality simulation model. The starting point for this model was the MINLAKE program (Riley and Stefan, 1988) which was developed to simulate eutrophication parameters in lakes. By substantial modification and extension of the model an application to ponds is deemed possible, particularly to explore pond management alternatives. Both field studies and numerical modeling of pond water quality dynamics are necessary to study pond problems and improvement of operation and performance of ponds.

During two years of field studies Luck and Stefan (1990) documented hydrothermal (physical) features in the Harris wastewater stabilization ponds in detail at timescales of minutes. Based on the observed water temperature, inflow and weather data collected on site, a numerical simulation of mixing and stratification was accomplished. The frequency and dynamics of stratification will be described, and the model to simulate them will be presented in this report.

A pond is usually smaller and more shallow than a lake. Therefore modifications of the water temperature simulation model originally developed by Stefan and Ford (1975), Ford and Stefan (1980) and Stefan et al. (1982) and used by Riley et al. (1988) had to be made. In particular the time step in the numerical simulation had to be reduced in order to capture the stratification and destratification dynamics of the ponds. For pond 1, inflow was analyzed to develop a simple jet mixing model. This model was incorporated as a submodel into the main model to simulate the jet entrainment from ambient water, depth of flow intrusion and forced mixing of the pond water. A sub-surface inflow and outflow model was developed to evaluate the water balance and to simulate the effects of water transfer between ponds on the stratification.

In this report the adaptation of the MINLAKE model to a pond including modification of the model and the use of input data are described. Simulation results including model calibration and verification with data for pond 3 (1989 and 1990) are presented. The jet entrainment and mixing model and its incorporation into the pond model are described. Finally an application of the extended model to pond 1 for the summer periods of 1989 and 1990 is made and numerically simulated results are compared to measured field data.

## 2. Simulation of Natural Stratification and Mixing Dynamics

### 2.1 Overview of Model Development

The MINLAKE model was developed earlier to simulate principal hydrothermal, chemical and biological processes in a lake on a daily time scale over a summer season (Riley and Stefan, 1987, Riley, 1988). This model was extended by Gu and Stefan (1990) to accomplish year-round temperature simulation. New submodels for winter covers and for the heat exchange with lake bottom sediments were incorporated into the main model for the extension. The output of the MINLAKE program consists of daily vertical distribution of water temperature, dissolved oxygen, suspended solids, phosphorus and phytoplankton. Simulations can be carried out over periods of months without changes in parameters.

In the modification of the MINLAKE program for the Harris Ponds, the difference between a pond and a lake had to be considered. Primary differences are in size and nutrient loading. A pond has a shallow depth and smaller area than a lake. Therefore maximum and minimum layer thicknesses, specified in the input data file of the model and minimum volume of a layer, set in the program have to be varied. The effect of wind to vertical diffusion and mixing in the pond are much less than in a lake. Higher nutrient loading into the pond causes more phytoplankton growth and hence more light attenuation.

### 2.2 Diurnal Effects

In order to simulate the onset and the disappearance of temperature stratification in the pond, a time step smaller than one day has to be used in the simulation. The MINLAKE program was originally designed for a fixed time step of one day. The time step did not appear explicitly in the subroutines implementing the governing equations. Variable time step was therefore not available in the program. Changing from the original one-day time step to a 12 hour or 6 hour timestep required modification of the program and rearrangement of input and output data. To make the least change of the program and its operation, the year calendar operating system was kept. A new type of calendar unit with half-days or quarter-days was generated. The half day calendar has 24 months and 730 or 732 (for leap year) units (half days), as shown in Table 1. With this new operating system, input parameters containing time dimensions of  $(\text{day})^{-1}$  are replaced by  $(\text{half day})^{-1}$ . The weather parameters in the meteorological data file are also reorganized for a time interval of a half day. Equations having implicit time parameters in the form of 86400 seconds or 24 hours are multiplied by a factor  $\Delta t/24$  in unit of hours or  $\Delta t/1.0$  in unit of days. The governing equations for state variables (Riley and Stefan, 1987) are kept the same as before since the time step,  $\Delta t$ , is absorbed by parameters in input data



Table 1 Year calendar for 12h timestep

Half Days	Month																							
	1	2	3	4	5	6	7	8	9	10	11	12	13	14	15	16	17	18	19	20	21	22	23	24
1	1	32	63	91	119	150	181	211	241	272	303	333	363	394	425	456	487	517	547	578	609	639	669	700
2	2	33	64	92	120	151	182	212	242	273	304	334	364	395	426	457	488	518	548	579	610	640	670	701
3	3	34	65	93	121	152	183	213	243	274	305	335	365	396	427	458	489	519	549	580	611	641	671	702
4	4	35	66	94	122	153	184	214	244	275	306	336	366	397	428	459	490	520	550	581	612	642	672	703
5	5	36	67	95	123	154	185	215	245	276	307	337	367	398	429	460	491	521	551	582	613	643	673	704
6	6	37	68	96	124	155	186	216	246	277	308	338	368	399	430	461	492	522	552	583	614	644	674	705
7	7	38	69	97	125	156	187	217	247	278	309	339	369	400	431	462	493	523	553	584	615	645	675	706
8	8	39	70	98	126	157	188	218	248	279	310	340	370	401	432	463	494	524	554	585	616	646	676	707
9	9	40	71	99	127	158	189	219	249	280	311	341	371	402	433	464	495	525	555	586	617	647	677	708
10	10	41	72	100	128	159	190	220	250	281	312	342	372	403	434	465	496	526	556	587	618	648	678	709
11	11	42	73	101	129	160	191	221	251	282	313	343	373	404	435	466	497	527	557	588	619	649	679	710
12	12	43	74	102	130	161	192	222	252	283	314	344	374	405	436	467	498	528	558	589	620	650	680	711
13	13	44	75	103	131	162	193	223	253	284	315	345	375	406	437	468	499	529	559	590	621	651	681	712
14	14	45	76	104	132	163	194	224	254	285	316	346	376	407	438	469	500	530	560	591	622	652	682	713
15	15	46	77	105	133	164	195	225	255	286	317	347	377	408	439	470	501	531	561	592	623	653	683	714
16	16	47	78	106	134	165	196	226	256	287	318	348	378	409	440	471	502	532	562	593	624	654	684	715
17	17	48	79	107	135	166	197	227	257	288	319	349	379	410	441	472	503	533	563	594	625	655	685	716
18	18	49	80	108	136	167	198	228	258	289	320	350	380	411	442	473	504	534	564	595	626	656	686	717
19	19	50	81	109	137	168	199	229	259	290	321	351	381	412	443	474	505	535	565	596	627	657	687	718
20	20	51	82	110	138	169	200	230	260	291	322	352	382	413	444	475	506	536	566	597	628	658	688	719
21	21	52	83	111	139	170	201	231	261	292	323	353	383	414	445	476	507	537	567	598	629	659	689	720
22	22	53	84	112	140	171	202	232	262	293	324	354	384	415	446	477	508	538	568	599	630	660	690	721
23	23	54	85	113	141	172	203	233	263	294	325	355	385	416	447	478	509	539	569	600	631	661	691	722
24	24	55	86	114	142	173	204	234	264	295	326	356	386	417	448	479	510	540	570	601	632	662	692	723
25	25	56	87	115	143	174	205	235	265	296	327	357	387	418	449	480	511	541	571	602	633	663	693	724
26	26	57	88	116	144	175	206	236	266	297	328	358	388	419	450	481	512	542	572	603	634	664	694	725
27	27	58	89	117	145	176	207	237	267	298	329	359	389	420	451	482	513	543	573	604	635	665	695	726
28	28	59	90	118	146	177	208	238	268	299	330	360	390	421	452	483	514	544	574	605	636	666	696	727
29	29	60			147	178	209	239	269	300	331	361	391	422	453	484	515	545	575	606	637	667	697	728
30	30	61			148	179	210	240	270	301	332	362	392	423	454	485	516	546	576	607	638	668	698	729
31	31	62			149	180			271	302			393	424	455	486			577	608			699	730

Note: Add 1 to values of month 4 and add 2 to all values after day 29 of month 4 during leap years.

through the factor  $\Delta t/1.0$  (day), and is set equal to one (half day). This modification and rearrangement makes it possible to do numerical simulations with a variable time step of 24, 12 or 6 hours, i.e. full, half or quarter day.

In the original program, light distribution was assumed to be symmetrical about a midday (noon) maximum with a photo period in the range of 10 to 14 hours. These aspects had to be considered also in the simulation with smaller time steps. For the half-day time step used in this study, the light subroutines are not modified since the half-day timesteps from 6:00 am to 6:00 pm and 6:00 pm to 6:00 am are also symmetrical about midday and midnight, respectively. If a smaller than 12 hour timestep is used, the light distribution over different time intervals within a one-day period has to be reevaluated in a different way and the photosynthesis submodel needs to be further modified.

### 2.3 Estimation of Vertical Thermal Diffusivity

The circulation in a lake or a pond is normally driven by wind stresses at the water surface or natural convection due to cooling. Flow mechanisms contributing to vertical transport and mixing are currents, breaking internal waves, and seiche-induced shear instability. In the model vertical transport is simulated by turbulent vertical diffusion and the vertical diffusion coefficient has to be specified. The parameters to which the vertical diffusion coefficient  $K_z$  can be related are surface area,  $A$ , maximum depth,  $H$ , strength of stratification represented by Brunt-Vaisala frequency,  $N$ , and wind speed,  $W$ .

The diffusion coefficient,  $K_z$ , in the epilimnion was related to wind speed,  $W$ , by a function (Filatov, et al, 1981, Riley and Stefan, 1987)

$$K_z = C_k W^b \quad (2.1a)$$

where  $C_k$  and  $b$  are constant coefficients,  $W$  is in mph and  $K_z$  is in  $m^2/day$ . Typical values for the empirical coefficients used in lakes are  $C_k = 28$  and  $b = 1.3$ . Appendix B gives a summary of coefficients used in various lake simulations.

The hypolimnetic diffusion coefficient in lakes is determined from

$$K_z = \min \left[ K_{zmax}, K_{zmax} CN^{-1} \right] \quad (2.1b)$$

where  $K_{zmax}$  = maximum hypolimnetic diffusion coefficient estimated from surface area of the lake and  $C$  = minimum value of  $N$  at which the  $K_{zmax}$

occurs taken to be  $8.66 \times 10^{-3} \text{ sec}^{-1}$  (Jassby and Powell, 1975). Effects of  $N$  on  $K_z$  in the hypolimnion were discussed by Ward (1977), Riley and Stefan (1988), Jassby and Powell (1975) and Hondzo, et al (1990).

Eqs. 2.1a and 2.1b suggest that wind speed is of dominant importance for epilimnetic diffusion; stratification affects the vertical diffusion in hypolimnia strongly. Since a high diffusion rate due to strong wind mixing produces nearly uniform distributions of temperature and concentrations of dissolved and suspended substances within the mixed layer, effects of  $N$  on  $K_z$  in lake epilimnia could be neglected. Effects of surface area on  $K_z$  are included in the empirical coefficients  $C_k$  and  $b$  for epilimnia and  $K_{z\text{max}}$  for hypolimnia.  $K_{z\text{max}}$  takes account of wind effects in a deep lake.

In the application of the MINLAKE model to the Harris ponds it was found that the  $C_k$  value of 28 is not suitable for a pond with a much smaller surface area than a lake. Large  $K_z$  values result in complete mixing in the pond. A  $C_k$  value in the range of 0.1 to 0.3 is suggested based on the model calibration. In this study of the Harris ponds the empirical coefficients  $C_k$  and  $K_{z\text{max}}$  are among several calibration parameters for the model. The previously developed formulation for the vertical diffusion coefficient (Eq. 2.1a for hypolimnia and Eq. 2.1b for epilimnia) are followed in computations for the ponds with different values of the empirical coefficients (calibration parameters). A value of  $0.1 \text{ m}^2/\text{day}$  was used for  $K_{z\text{max}}$  (see Appendix B for comparison).

When the model is applied to other ponds which have no field data, the fitting technique and the calibration procedure cannot be employed to determine the empirical coefficients,  $C_k$  and  $K_{z\text{max}}$ . The dependence of epilimnetic  $K_z$  on surface area  $A$ , therefore, has to be quantified to estimate  $C_k$  and  $K_{z\text{max}}$  in this situation. It has been shown that a correlation exists between vertical diffusion coefficient and lake surface area (Ward, 1977, Hondzo, et al, 1990). Ward concluded from data for two man-made African lakes and measurements in thirteen lakes by previous investigators that lake surface area is the dominant factor for vertical diffusion in lake hypolimnia. Hondzo, et al (1990) gave a  $K_z$  versus  $A^{0.56}$  correlation in hypolimnia based on data for six Minnesota lakes. Dimensional analysis performed by Ward (1977) gave a linear relationship,  $K_z$  versus  $A^{0.5}$ , for lake hypolimnia. Similarly, by eliminating  $N$  in the dimensional analysis, a  $K_z$  versus  $A^{0.75}$  correlation is obtained herein for lake epilimnia with a reference parameter  $A^{0.5}/H$ , the ratio of approximate lake width to depth.

## 2.4 Input Data

Field data were available to carry out the simulation of temperature stratification. The data include water temperature profiles and meteorological parameters averaged from 2 minute measurements over 20 minute intervals and weekly intermittent data on light attenuation, Secchi depth and pond stage or depth. Input requirements for water temperature simulation include the initial conditions, lake geometry, the meteorological data file and the inflow outflow data file (Riley and Stefan, 1987). All data files are reorganized in the new type of calendar system for the half day time steps. Parameters changed are those related to time dimensions such as the diffusion coefficient, heat fluxes and wind speed. Data files are given in Appendix D (disk).

In the input data file, the measured values for the light attenuation coefficient are used directly. The measured attenuation coefficient includes the effects of suspended solids such as phytoplankton.

Measurements of sunshine percentage were not available. The sunshine percentage is used to calculate cloud cover in the program. Estimation of cloud cover was therefore based on solar radiation measurements by using the relationships (Baker and Enz, 1979)

$$Cr = 100 - S \quad (2.2)$$

$$S = a \frac{H_s}{H_{smax}} \times 100 \quad (2.3)$$

where  $Cr$  = percentage of cloud cover,  $S$  = percentage of sunshine,  $a$  = coefficient,  $H_s$  = total solar radiation and  $H_{smax}$  = maximum solar radiation (clear day). The mean value of coefficient  $a$  was determined from Twin City weather data for 1971-1972 and 1982 to be equal 0.952.  $H_{smax}$  is used as an input weather parameter instead of sunshine percentage in the meteorological data file. Calculation of  $Cr$  is incorporated into the program.

There was no direct measurement of inflow or outflow flow rate, or water quality for pond 3. Flow rate was therefore evaluated from the water budget equation

$$\frac{dV(z)}{dt} = Q_i - Q_o \pm Q_g - Q_e + Q_p \quad (2.4)$$

and the volume depth relation, where  $V$  = storage volume of the pond,  $t$  = time,  $z$  = depth,  $Q$  = flow rate with subscripts "i", "o", "g", "e" and "p" indicating inflow, outflow, groundwater or seepage, evaporation and precipitation, respectively. Flux from or to groundwater or seepage was neglected (Luck and Stefan, 1990, MPCA and CECM, 1989). Outflow temperature from the pond is assumed to be water temperature in the pond at the level of withdrawal. Inflow temperature to pond 3 is the water temperature in pond 2 at the level of withdrawal.

## 2.5 Model Calibration

Temperature stratification in the Harris wastewater stabilization pond 3 was simulated for the period from Aug. 1 to Oct. 31, 1989, using two time steps, one day (24 hours) and one half day (12 hours) and Apr. 7 to Oct. 31, 1990, using a time step of 12 hours. The simulation for 1989 served to calibrate the model. The model was verified against 1990 data.

Figs. 4 through 8 show numerical results with a one day time step and comparison with measured 6:00 am temperature profiles. The applicability of the simulation model to a pond is demonstrated by the small error between field data and simulated water temperatures (see Appendix A for definition of statistical parameters). 110 pairs of data were analyzed, giving a regression slope of 0.99, a regression coefficient of 0.98, and a standard error of 0.56 °C. Values of maximum hypolimnetic diffusion coefficient, wind function coefficient and wind sheltering coefficient, which were defined by Riley and Stefan (1988), were calibrated to be 0.1 m<sup>2</sup>/day, 20 and 0.1 respectively. The coefficient  $C_k$  in the Eq. 2.1b for  $K_z$  is set to be 0.2.

Strong diurnal cycles of temperature stratification/destratification during the summer period had been illustrated in the recorded field data (Luck and Stefan, 1990). During the day time, absorption of solar radiation in the surface layers causes stratification to occur. The stratification gradually becomes stronger, beginning in the morning. A convective isothermal surface mixed layer develops during the night. These processes cannot be described by numerical simulation with one day time step. To gain insight into the cycle of daytime stratification and night mixing, a half day time step instead of one day time step was used in the simulation.

Shown in Figs. 9 through 14 are the measured and simulated temperature variations at 6 hrs (6 am) and 18 hrs (6 pm) of every day and at different depths where probes were located. The time interval between the measured points in the figures is half a day (12 hours). The morning temperatures (6:00 hrs) mark the bottom boundary of the temperature envelope, after night cooling. The evening temperatures (18:00 hrs) follow the top boundary after day heating. The temperature difference between morning and evening has its maximum value in the surface layers, is less with depth and becomes very small at the bottom. The diurnal cycle of stratification and mixing can be more clearly seen in Figs. 15 through 21.

Estimated net inflow rates (outflow if negative) for 1989 which were derived from pond water depths and used as input in the simulation are shown in Fig. 22. Water depths and net flow rates for 1990 are presented in Fig. 23. An example of weather data used as input is shown in Fig. 23. The complete weather and temperature records are displayed graphically in the report by Luck and Stefan (1990). The analysis of errors between field data and model simulations for 1989 was based on 800 pairs of water temperature data (Table 2). Slope of model to data regression is 1.00.

# HARRIS POND #3, AUG. 4, 1989:

## TEMPERATURE STRATIFICATION SIMULATION

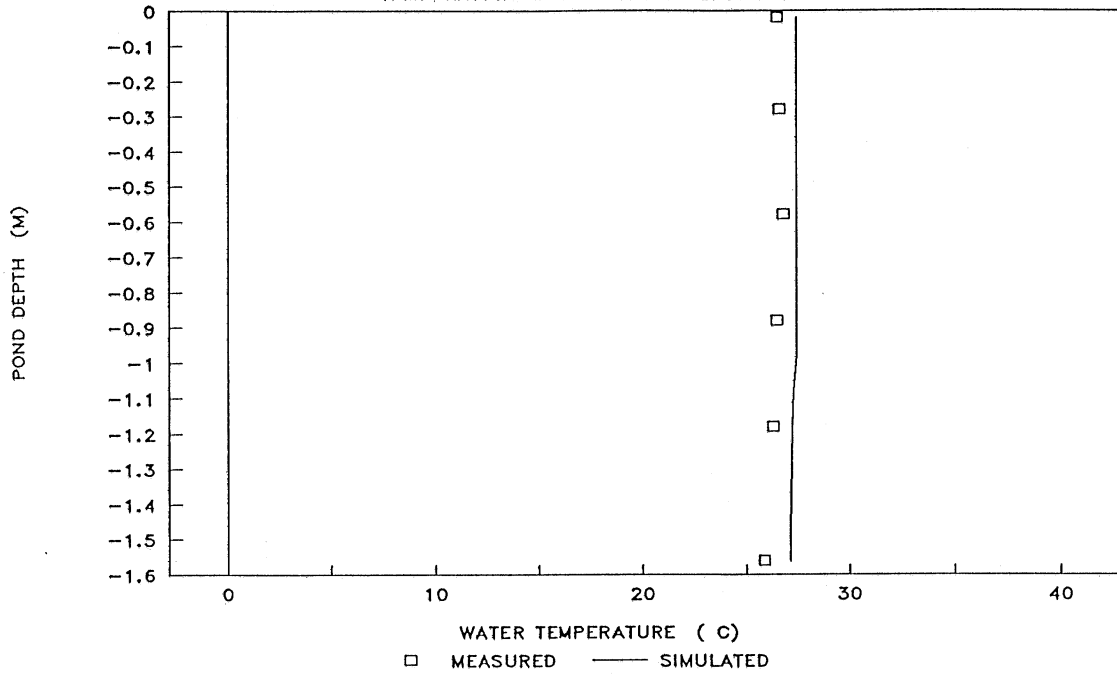


Fig. 4 Measured and simulated water temperatures in pond 3 at 6:00 am, Aug. 4, 1989, timestep = 24 hours

### HARRIS POND #3, AUG. 13, 1989:

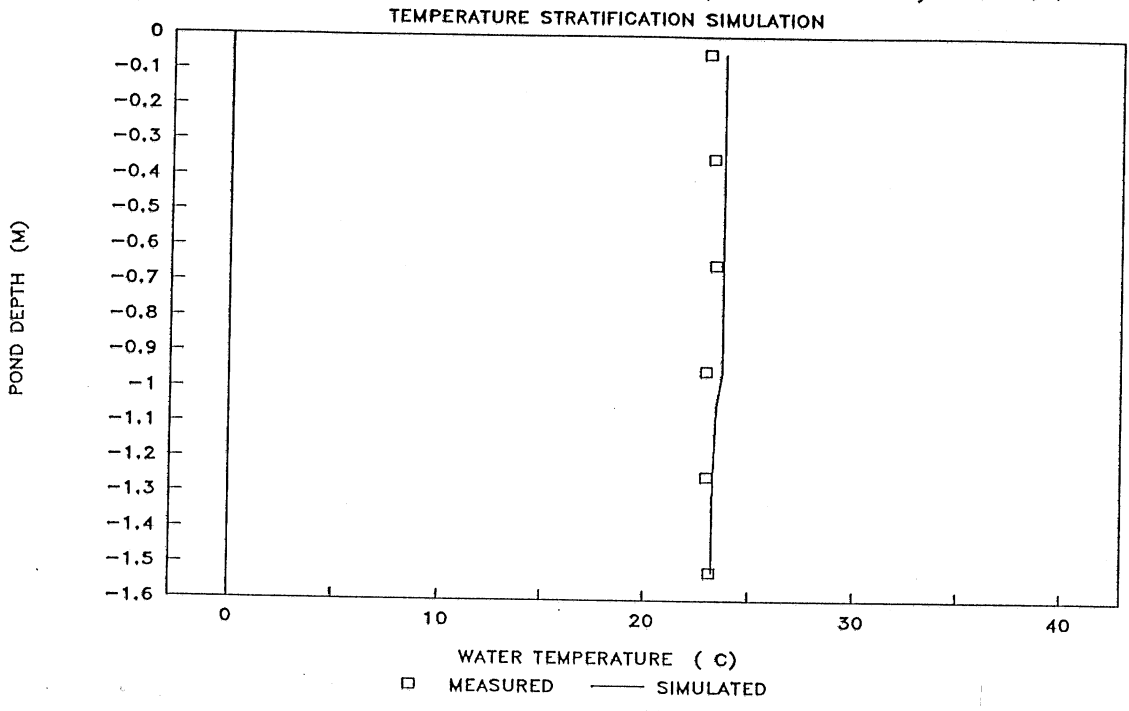


Fig. 5 Measured and simulated water temperatures in pond 3 at 6:00 am, Aug. 13, 1989, timestep = 24 hours

### HARRIS POND #3, SEPT. 2, 1989:

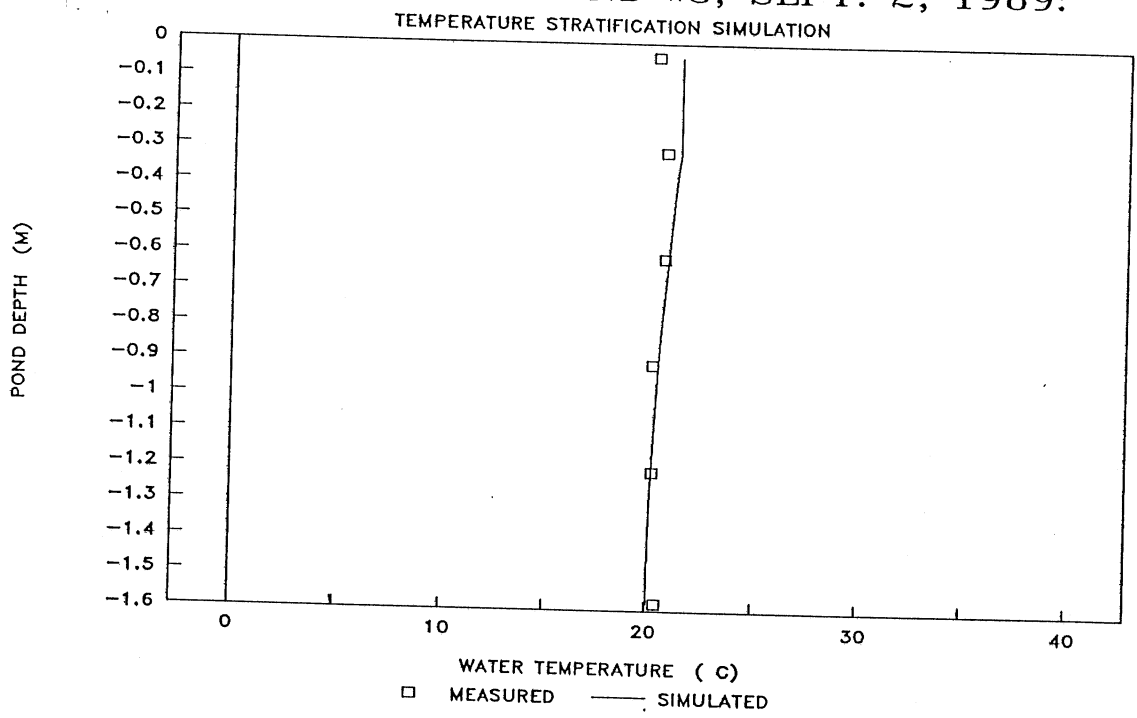


Fig. 6 Measured and simulated water temperatures in pond 3 at 6:00 am, Sept. 4, 1989, timestep = 24 hours

### HARRIS POND #3, SEPT. 13, 1989:

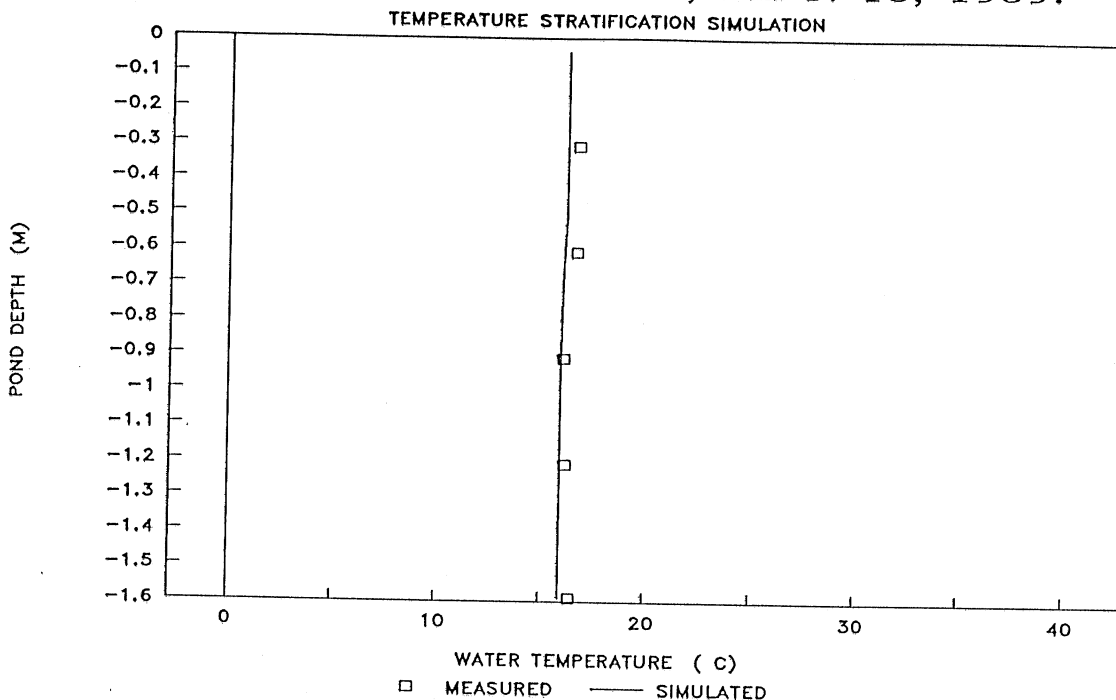


Fig. 7 Measured and simulated water temperatures in pond 3 at 6:00 am, Sept. 13, 1989, timestep = 24 hours

### HARRIS POND #3, OCT. 13, 1989:

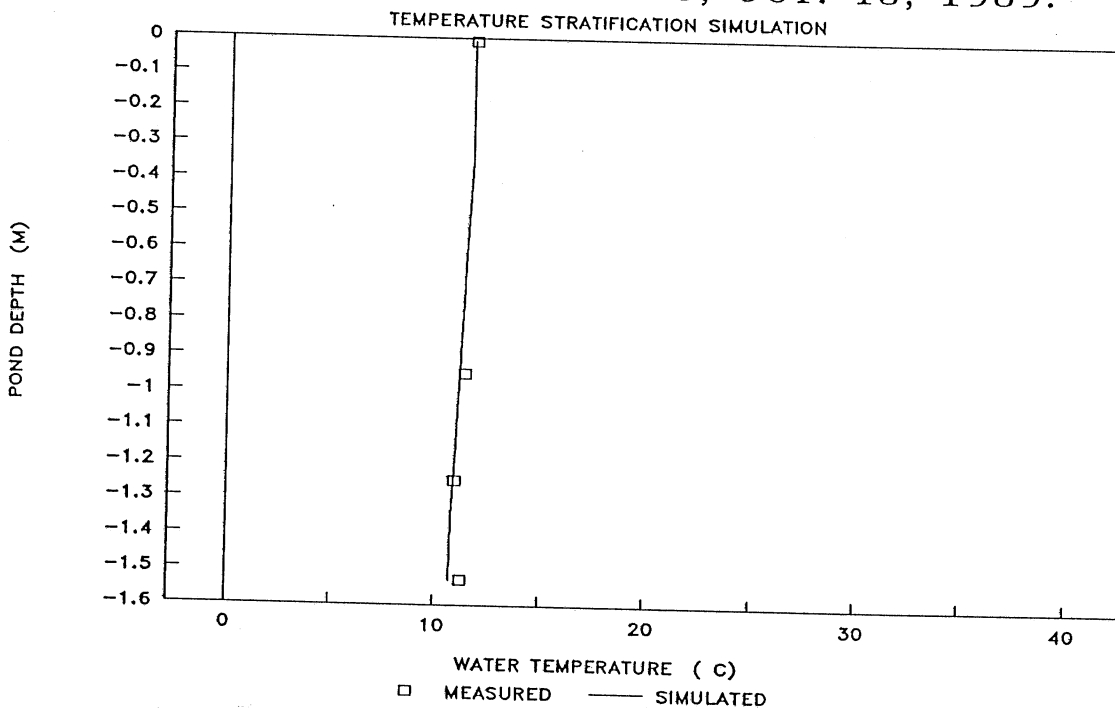


Fig. 8 Measured and simulated water temperatures in pond 3 at 6:00 am, Oct. 13, 1989, timestep = 24 hours



# TEMPERATURE STRATIFICATION SIMULATION

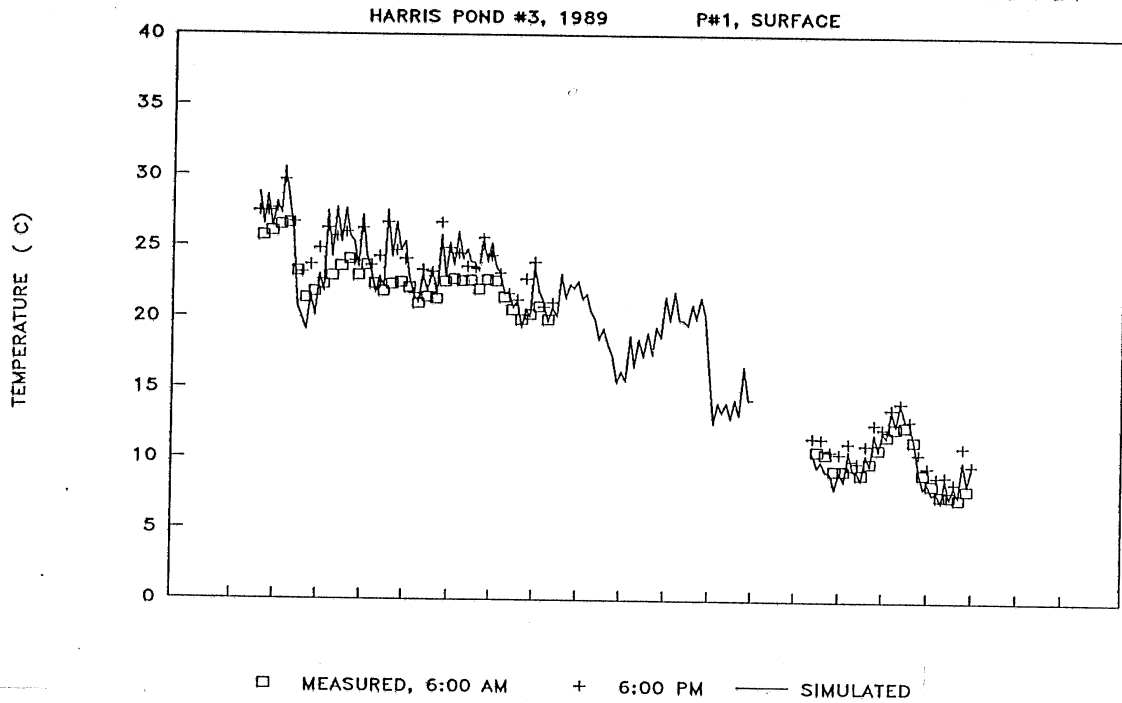


Fig. 9 Measured and simulated water temperatures in pond 3, 1989, timestep = 12 hours, probe #1 (surface)

# TEMPERATURE STRATIFICATION SIMULATION

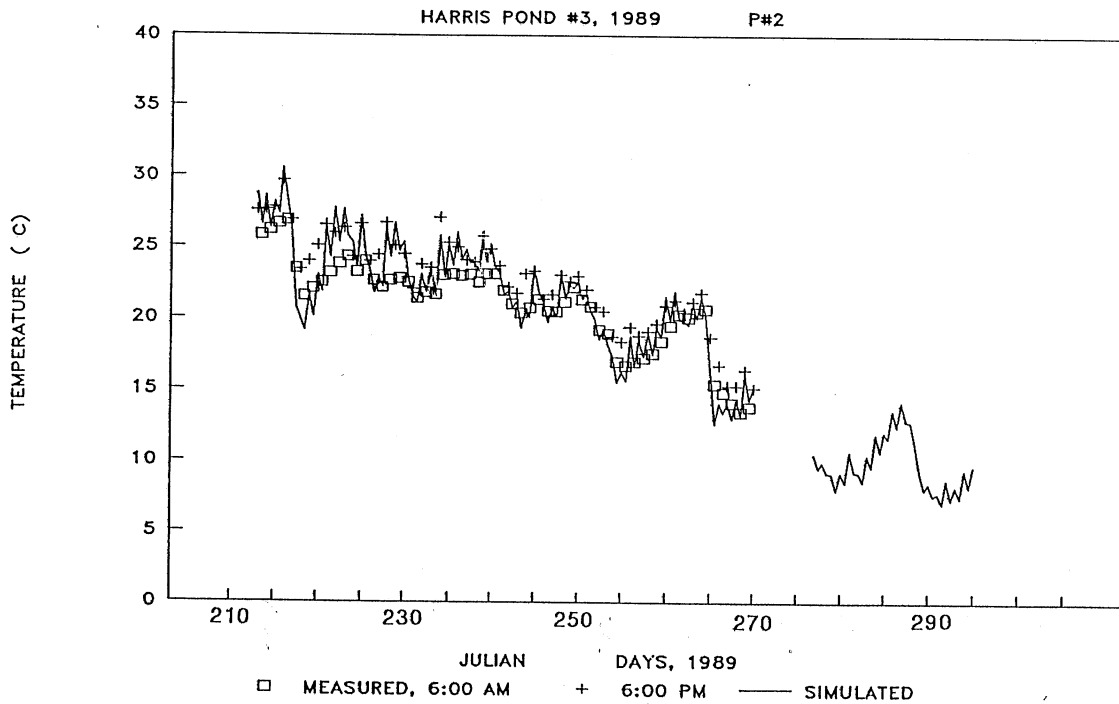


Fig. 10 Measured and simulated water temperatures in pond 3, 1989, timestep = 12 hours, probe #2

# TEMPERATURE STRATIFICATION SIMULATION

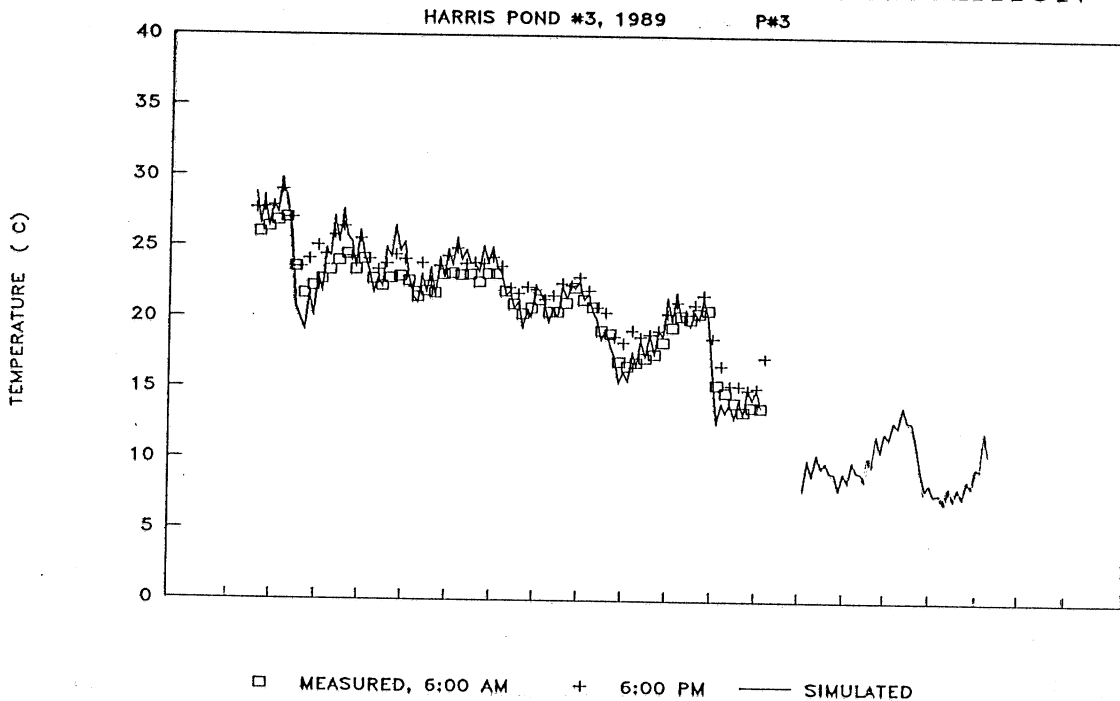


Fig. 11 Measured and simulated water temperatures in pond 3, 1989, timestep = 12 hours, probe #3

# TEMPERATURE STRATIFICATION SIMULATION

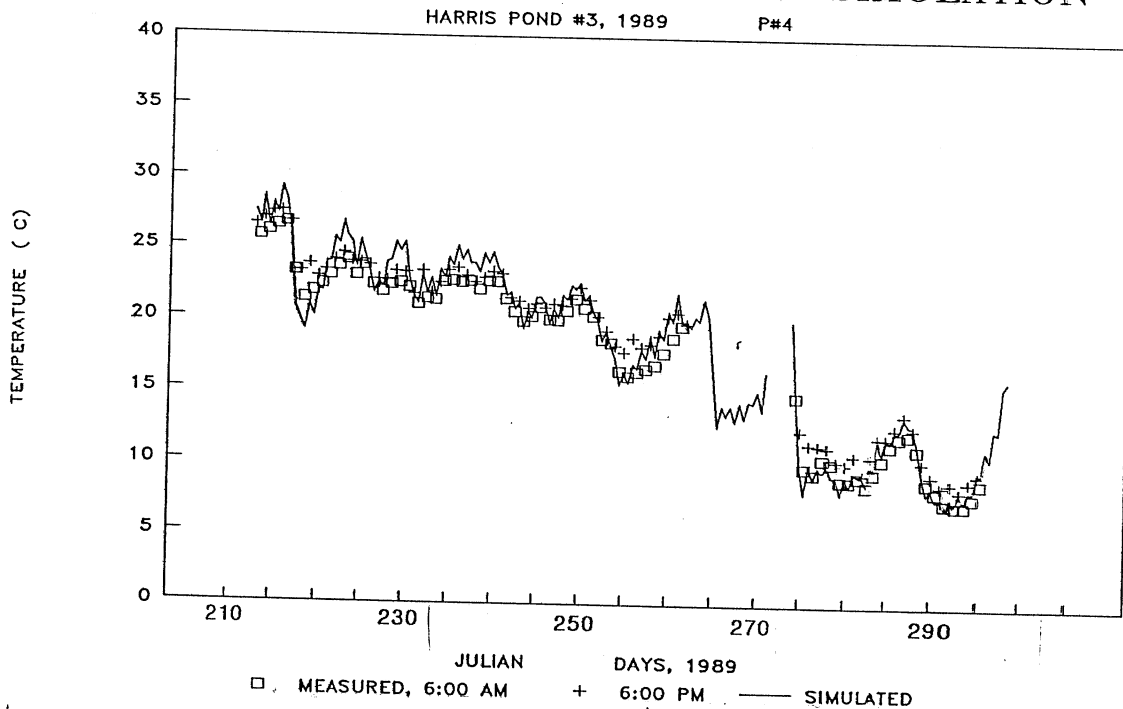


Fig. 12 Measured and simulated water temperatures in pond 3, 1989, timestep = 12 hours, probe #4

# TEMPERATURE STRATIFICATION SIMULATION

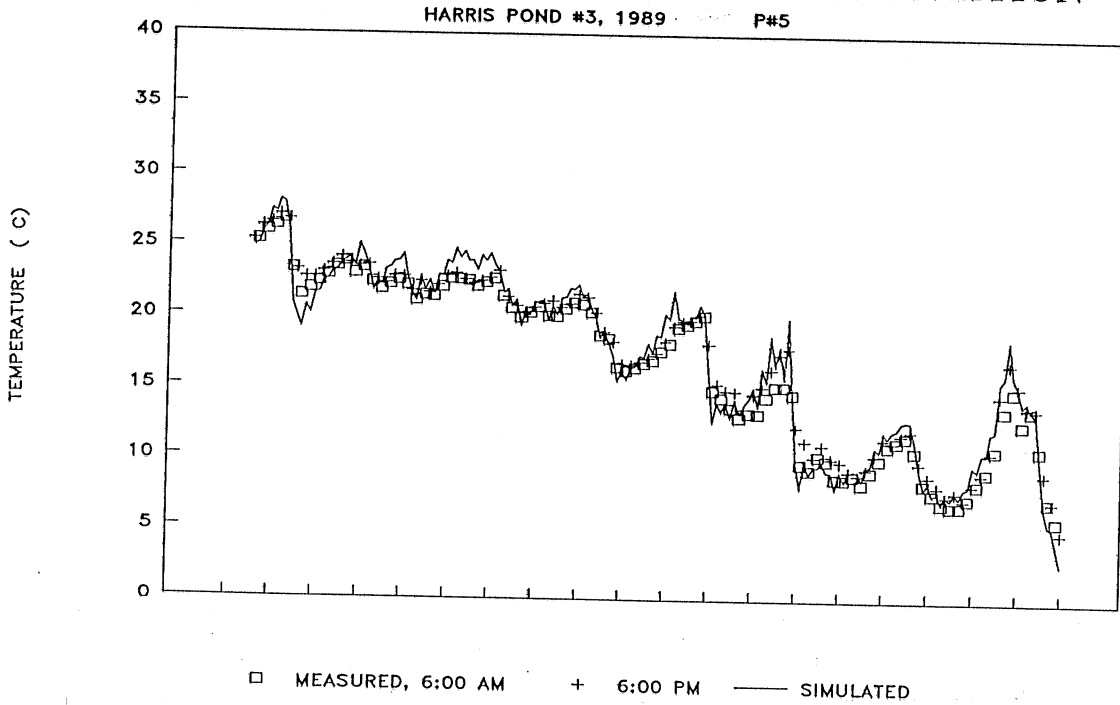


Fig. 13 Measured and simulated water temperatures in pond 3, 1989, timestep = 12 hours, probe #5

# TEMPERATURE STRATIFICATION SIMULATION

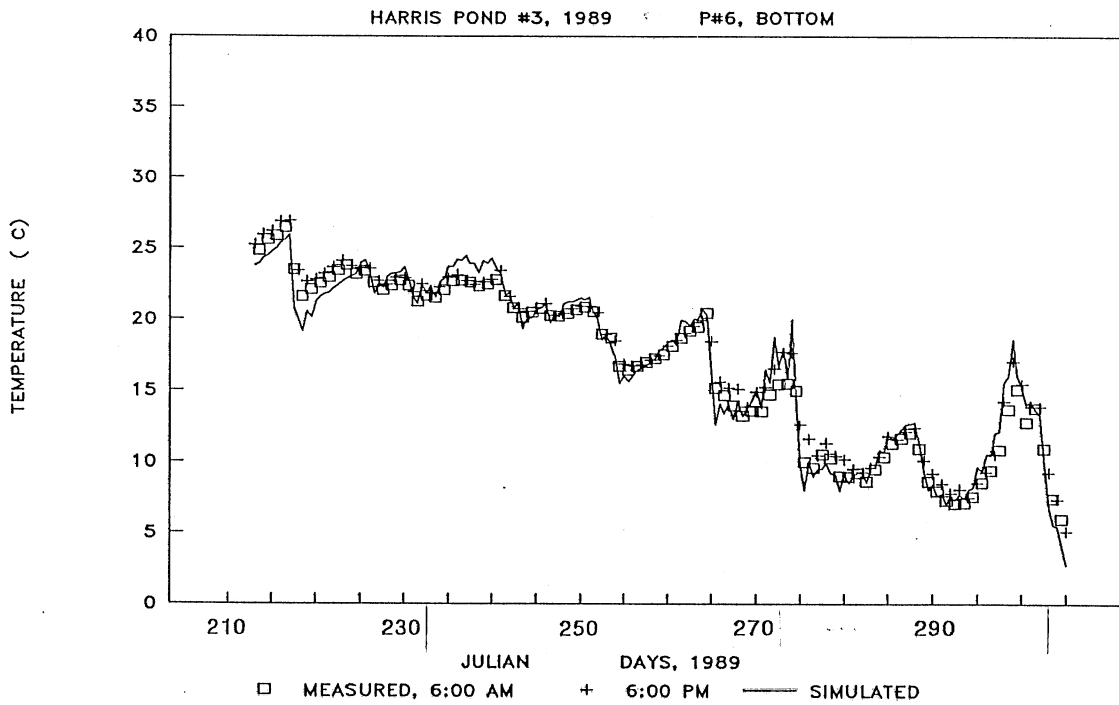


Fig. 14 Measured and simulated water temperatures in pond 3, 1989, timestep = 12 hours, probe #6 (bottom)

# TEMPERATURE STRATIFICATION SIMULATION

HARRIS POND #3, AUG. 4, 1989

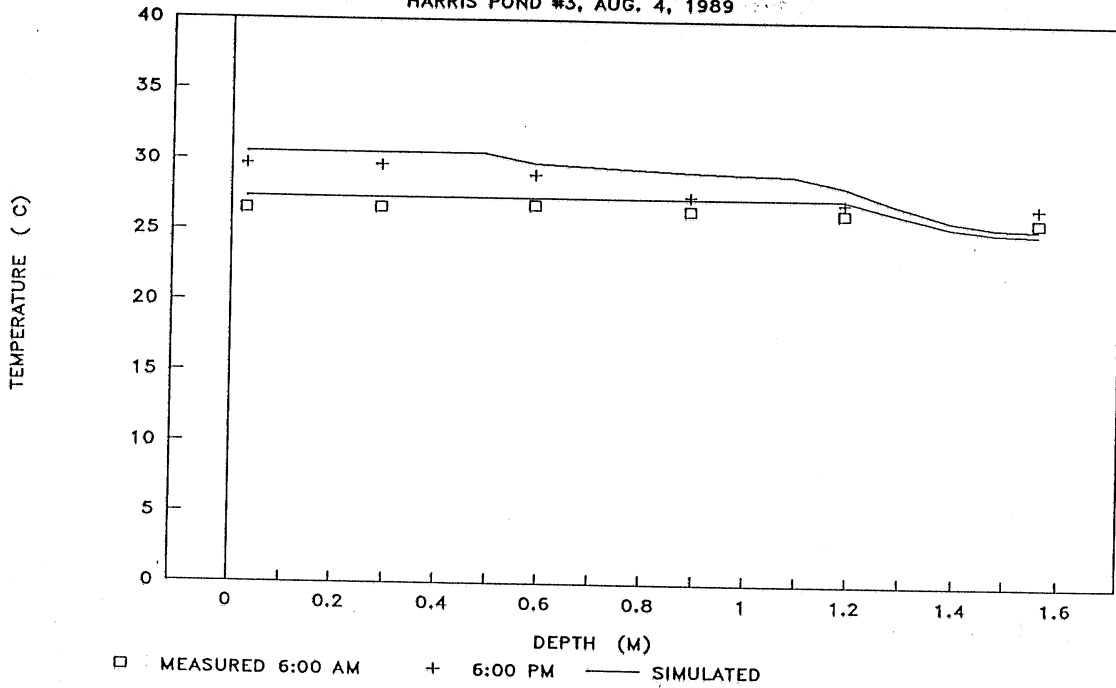


Fig. 15 Measured and simulated diurnal cycle of water temperature stratification, pond 3, Aug. 4, 1989

# TEMPERATURE STRATIFICATION SIMULATION

HARRIS POND #3, AUG. 13, 1989

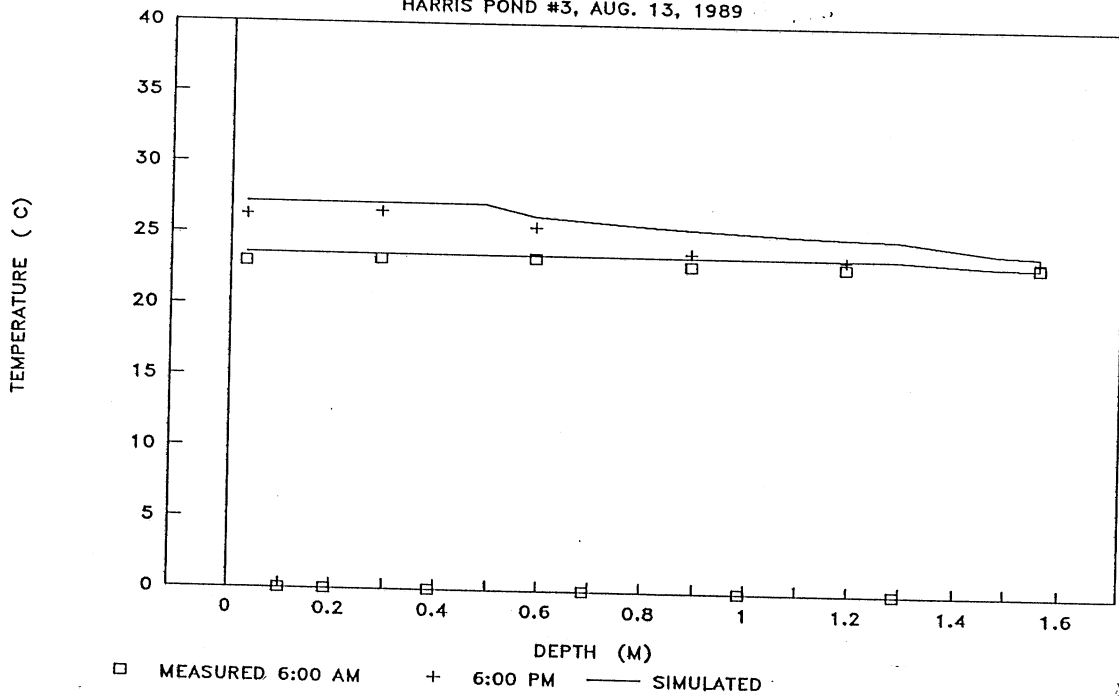


Fig. 16 Measured and simulated diurnal cycle of water temperature stratification, pond 3, Aug. 13, 1989

## TEMPERATURE STRATIFICATION SIMULATION

HARRIS POND #3, AUG. 22, 1989

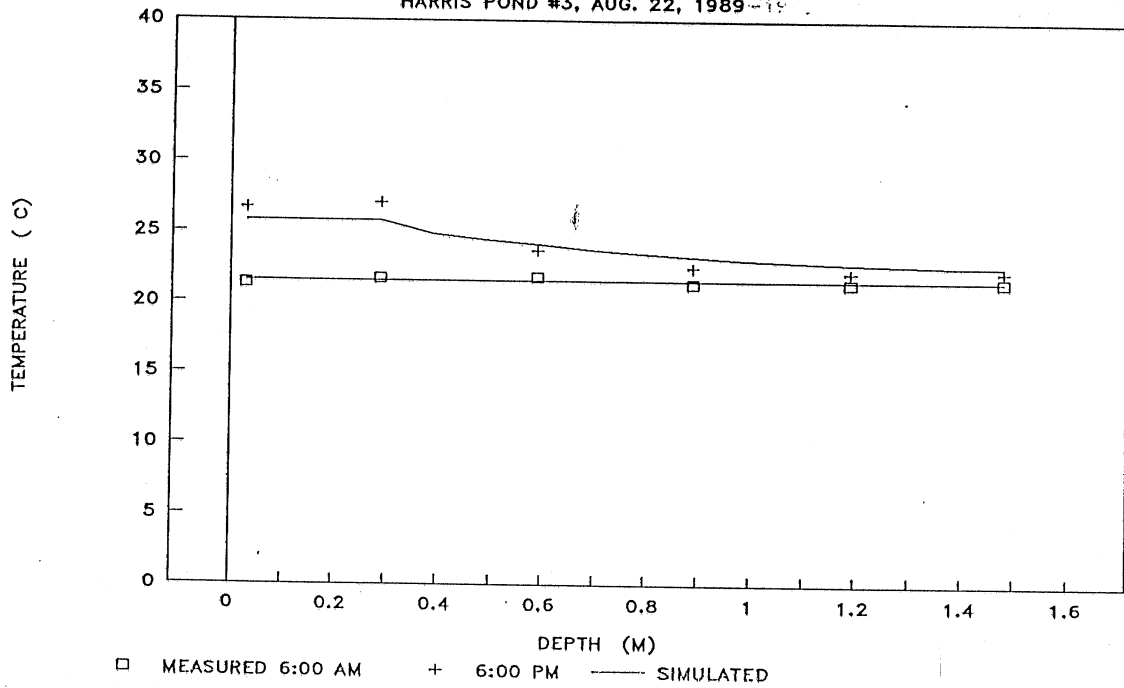


Fig. 17 Measured and simulated diurnal cycle of water temperature stratification, pond 3, Aug. 22, 1989

## TEMPERATURE STRATIFICATION SIMULATION

HARRIS POND #3, SEPT. 2, 1989

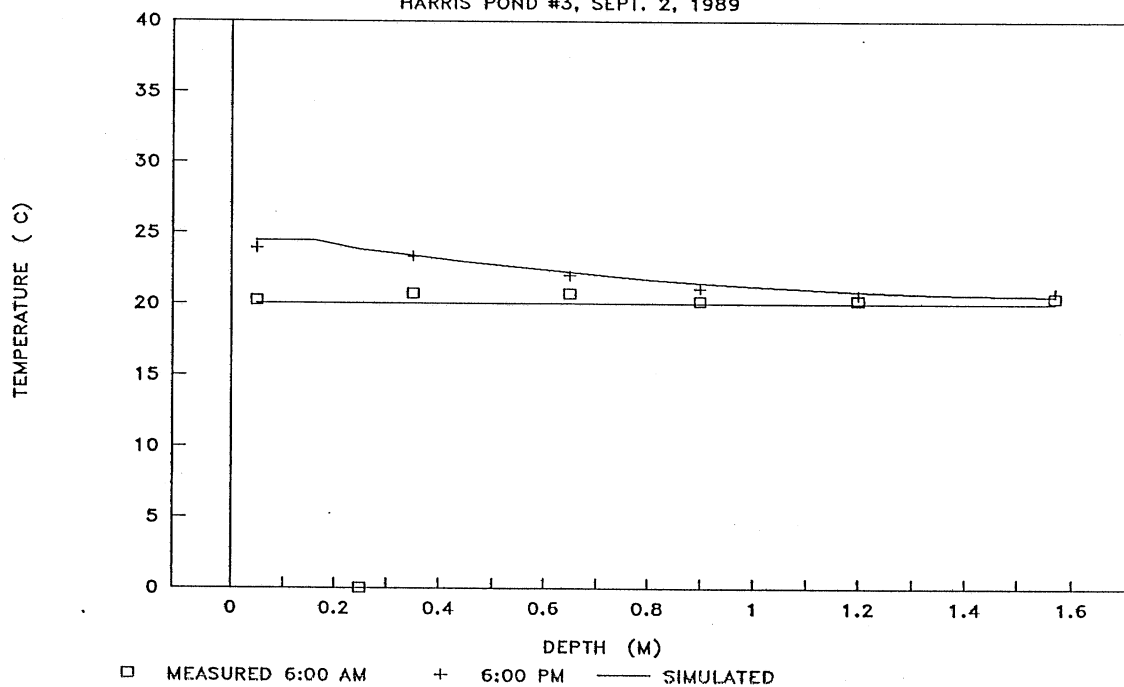


Fig. 18 Measured and simulated diurnal cycle of water temperature stratification, pond 3, Sept. 2, 1989

# TEMPERATURE STRATIFICATION SIMULATION

HARRIS POND #3, SEPT. 25, 1989

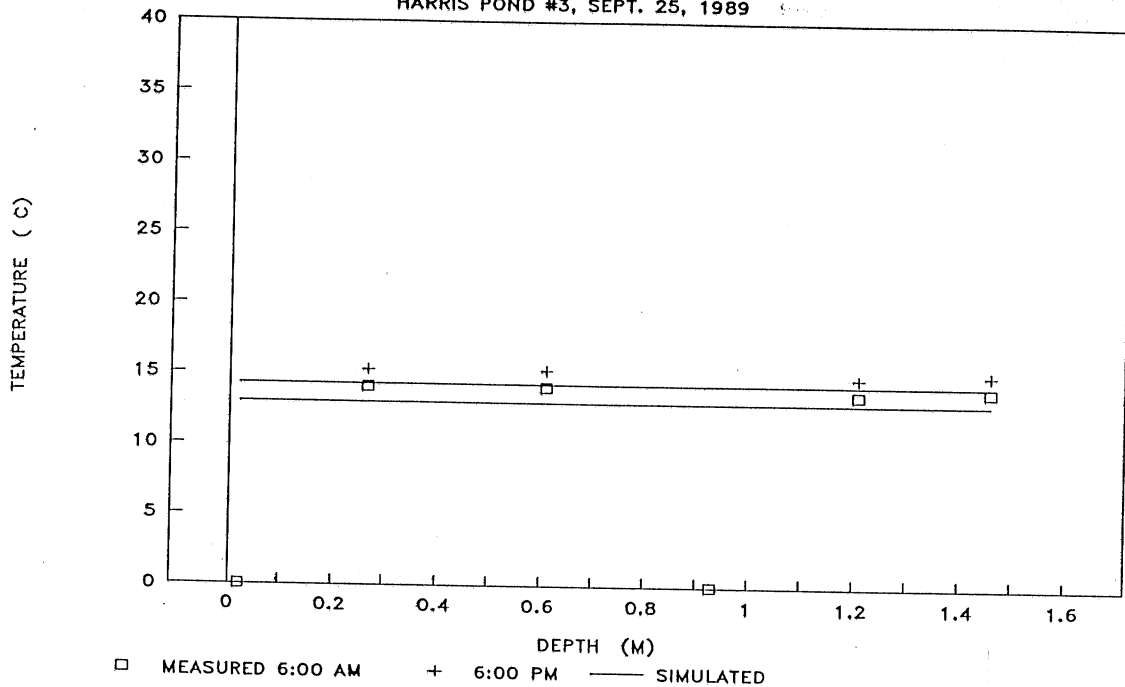


Fig. 19 Measured and simulated diurnal cycle of water temperature stratification, pond 3, Sept. 25, 1989

# TEMPERATURE STRATIFICATION SIMULATION

HARRIS POND #3, OCT. 13, 1989

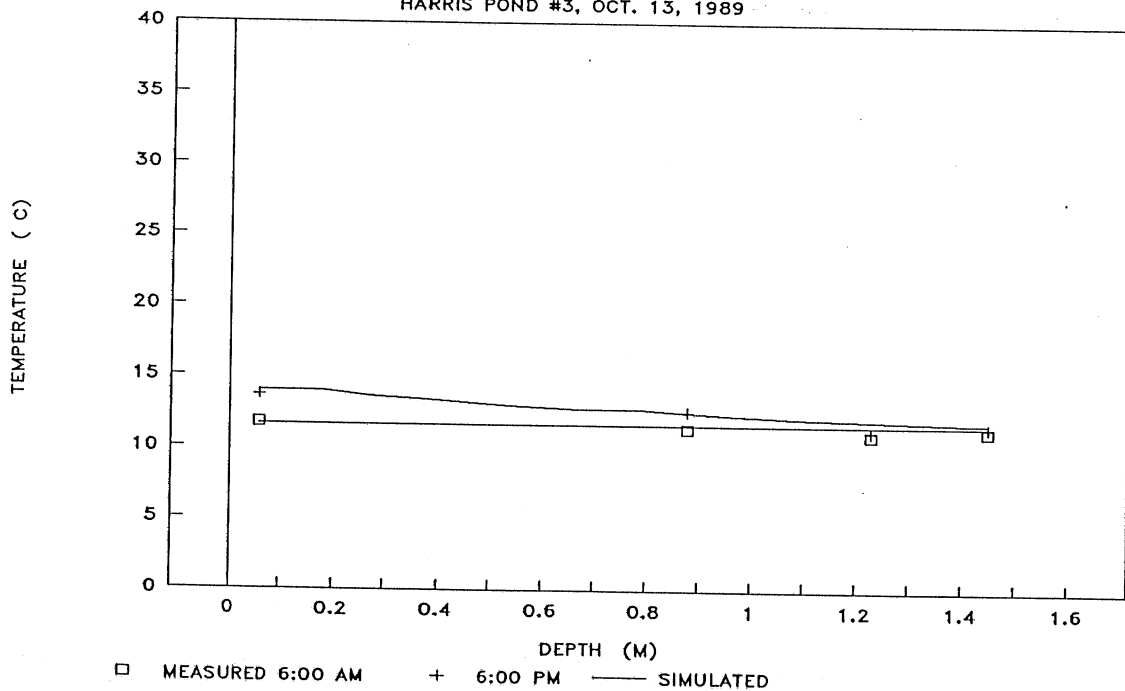


Fig. 20 Measured and simulated diurnal cycle of water temperature stratification, pond 3, Oct. 13, 1989

# TEMPERATURE STRATIFICATION SIMULATION

HARRIS POND #3, OCT. 21, 1989

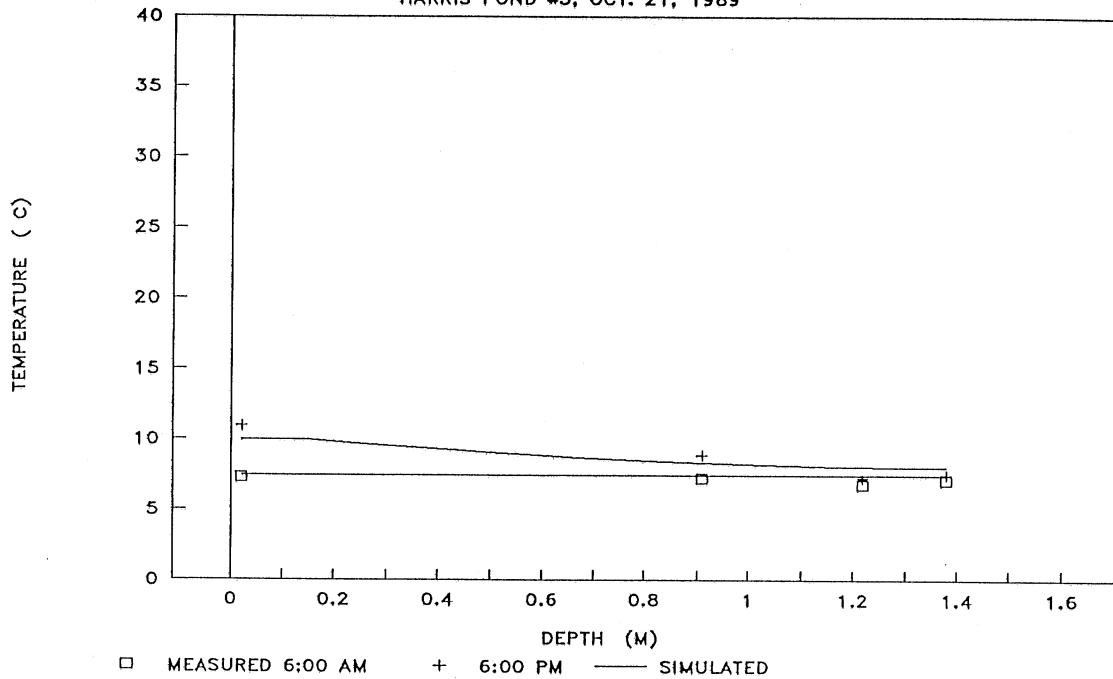


Fig. 21 Measured and simulated diurnal cycle of water temperature stratification, pond 3, Oct. 21, 1989

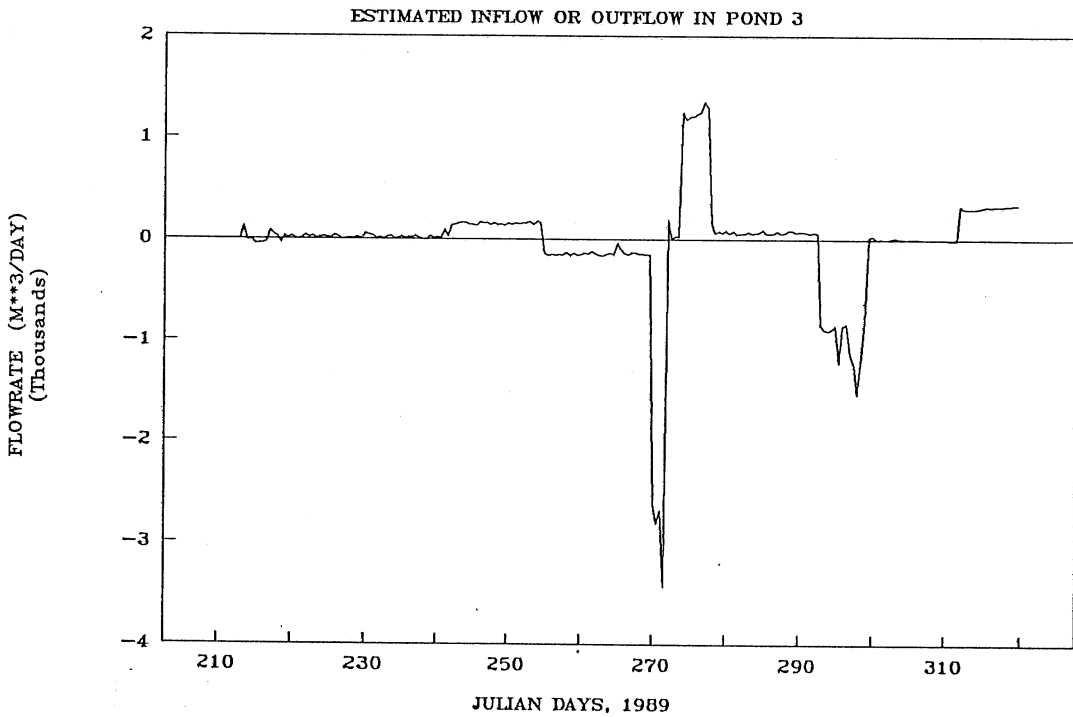
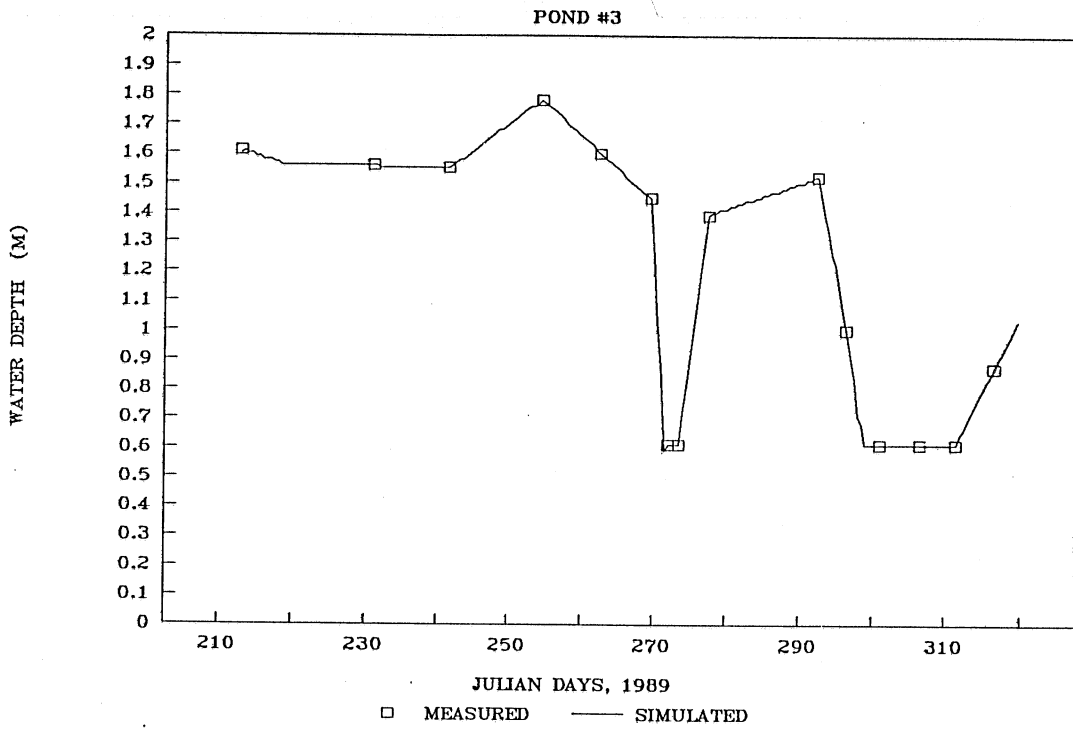


Fig. 22 a) Water depth and b) estimated net flow rate of inflow (positive) and outflow (negative), pond 3, 1989



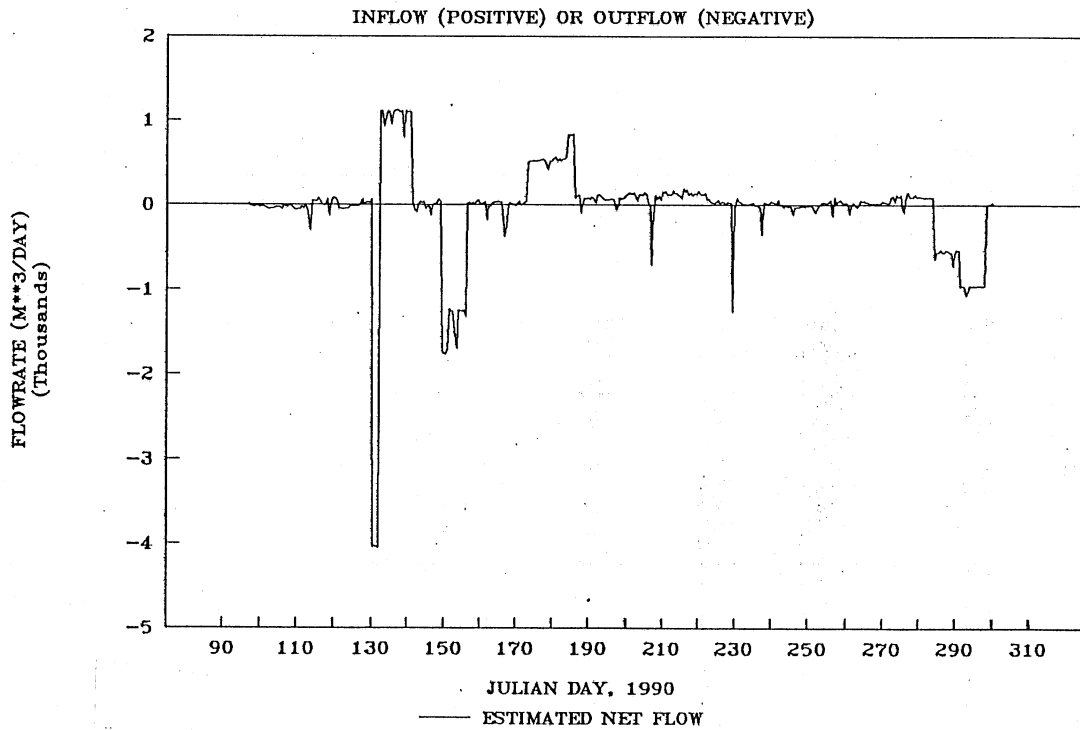
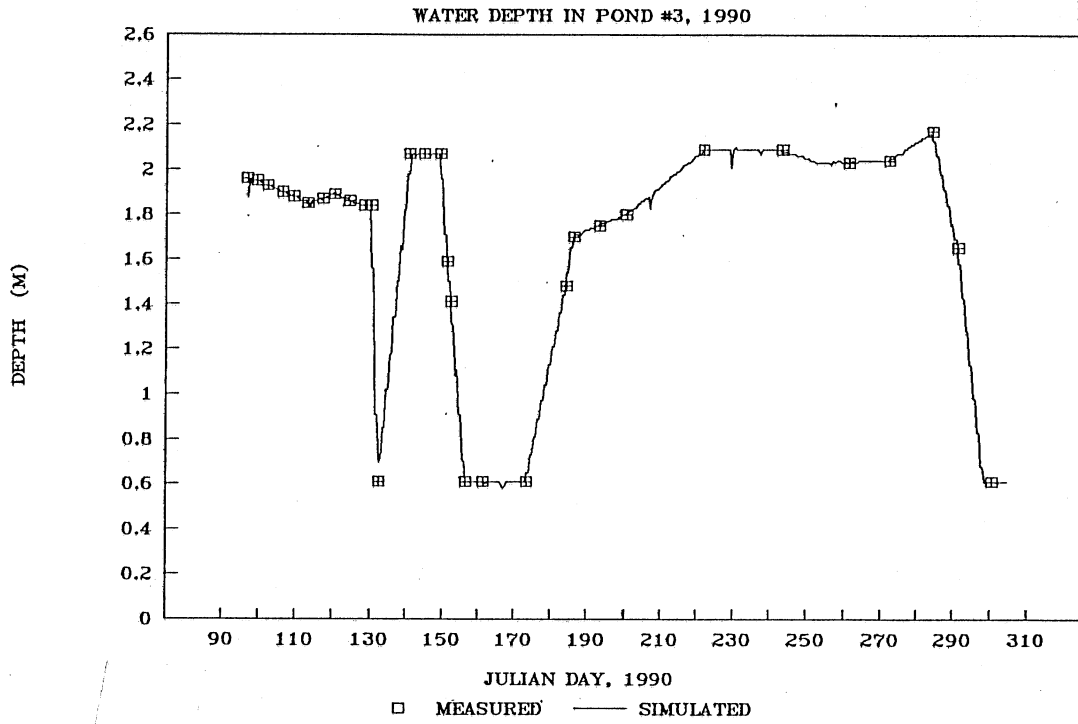


Fig. 23 a) Water depth and b) estimated net flow rate of inflow (positive) and outflow (negative), pond 3, 1990

Table 2 Statistical error analysis (comparison of field data and model simulations)

Pond	Period	Time step	Number of Data points	Mean Temperature		Standard error	Slope of regression	Regression coefficient
		(hr)		Field	Model			
				$\bar{y}$ (°C)	$\bar{x}$ (°C)	$s_e$ (°C)	$s_r$	$r^2$
#1	8/1-11/30/89	12	1566	13.52	13.98	1.33	0.96	0.97
	4/7-10/31/90	12	2337	18.24	18.10	1.36	1.00	0.95
#3	8/1-10/31/89	12	800	19.25	19.23	1.04	1.00	0.96
	4/7-10/31/90	12	1904	19.64	19.42	1.46	1.00	0.94

Regression coefficient is 0.96. The standard error of estimate is 1.04 °C. These statistics indicate good agreement between field data and numerical simulation and the applicability of the program to a pond with a smaller time step than one day.

## 2.6 Model Verification

Following standard practice, the model is verified by rerunning the calibrated model over a different simulation period than that used for calibration. Comparison of the model results for water temperatures to the field data in a second simulation period (Apr. 7 to Oct. 31, 1990) indicates that the calibrated model can simulate other time periods reasonably well as shown in Figs. 24 through 29. Disagreement exists for temperatures measured by the upper probes during draining and filling of pond 3. The pond was drained to 0.61 m at the beginning of June, 1990 and filled back to 1.6 m at the end of that month. During that period, the temperatures measured by the upper probes were air temperatures, not water temperatures, since the probes are exposed to air. During the draining and filling periods pond water depths were measured only every 1 to 3 weeks and water depths on days between measured days were linearly interpolated. This may explain the poorer fit between measurements and simulations during these periods. Analysis of errors between field data and model simulations based on 1904 pairs of water temperature data gave a slope of model to data regression of 1.00, a regression coefficient of 0.94 and a standard error of estimate of 1.46 °C (Table 2).

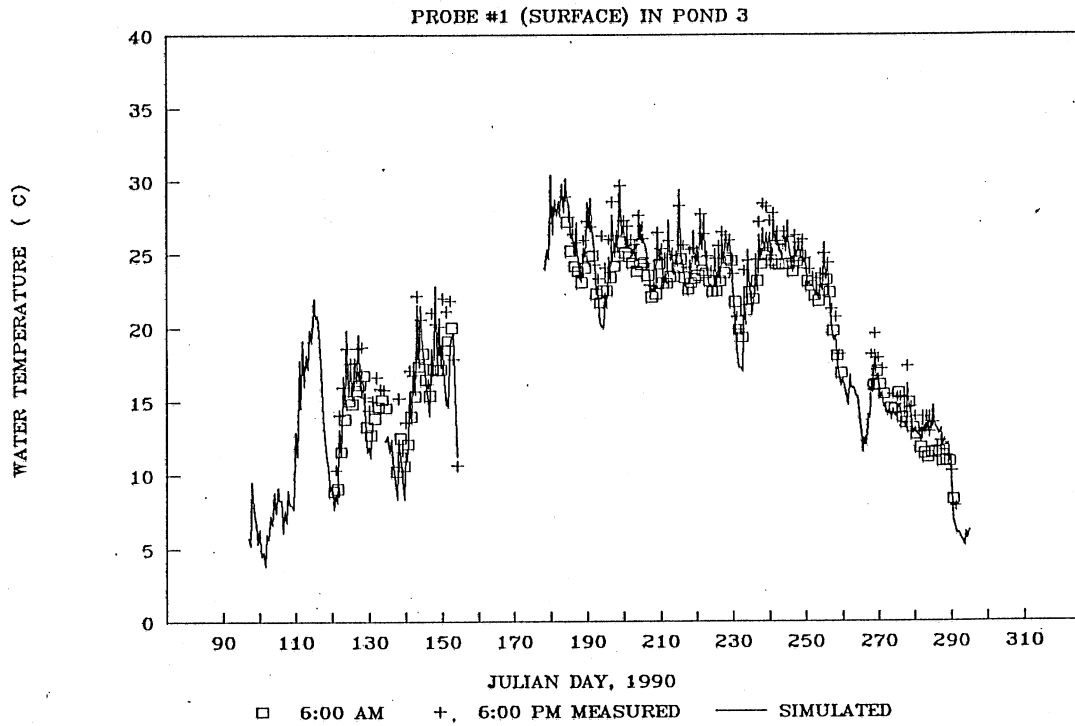


Fig. 24 Measured and simulated water temperatures in pond 3, 1990, timestep = 12 hours, probe #1 (surface)

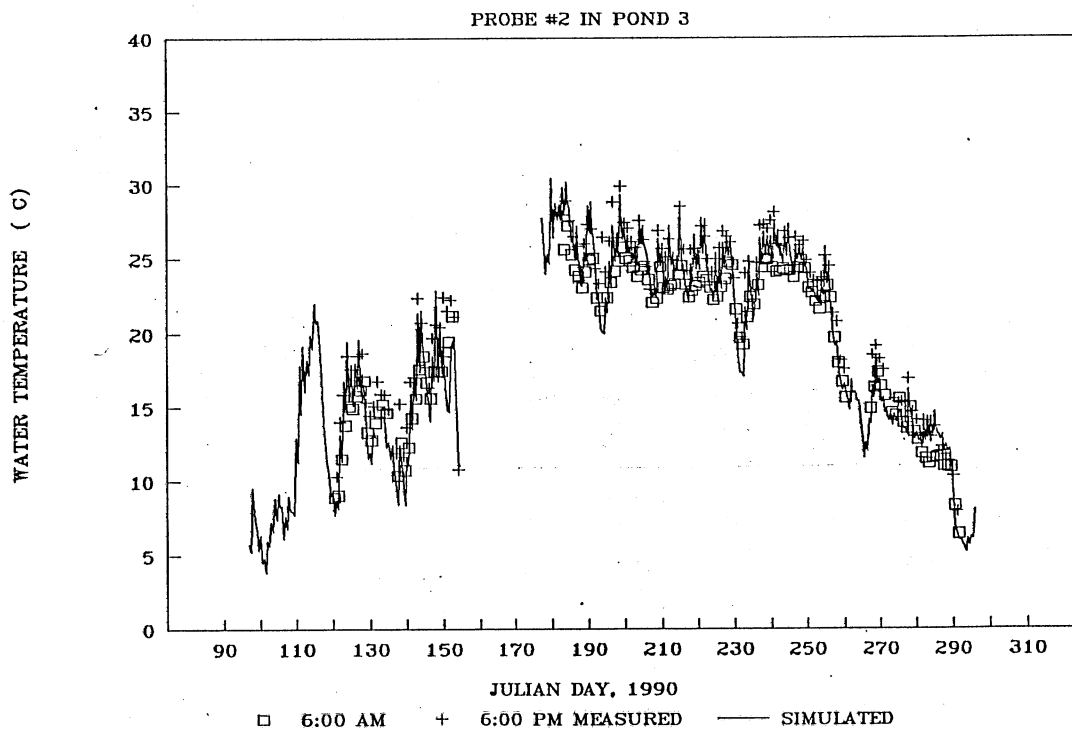


Fig. 25 Measured and simulated water temperatures in pond 3, 1990, timestep = 12 hours, probe #2

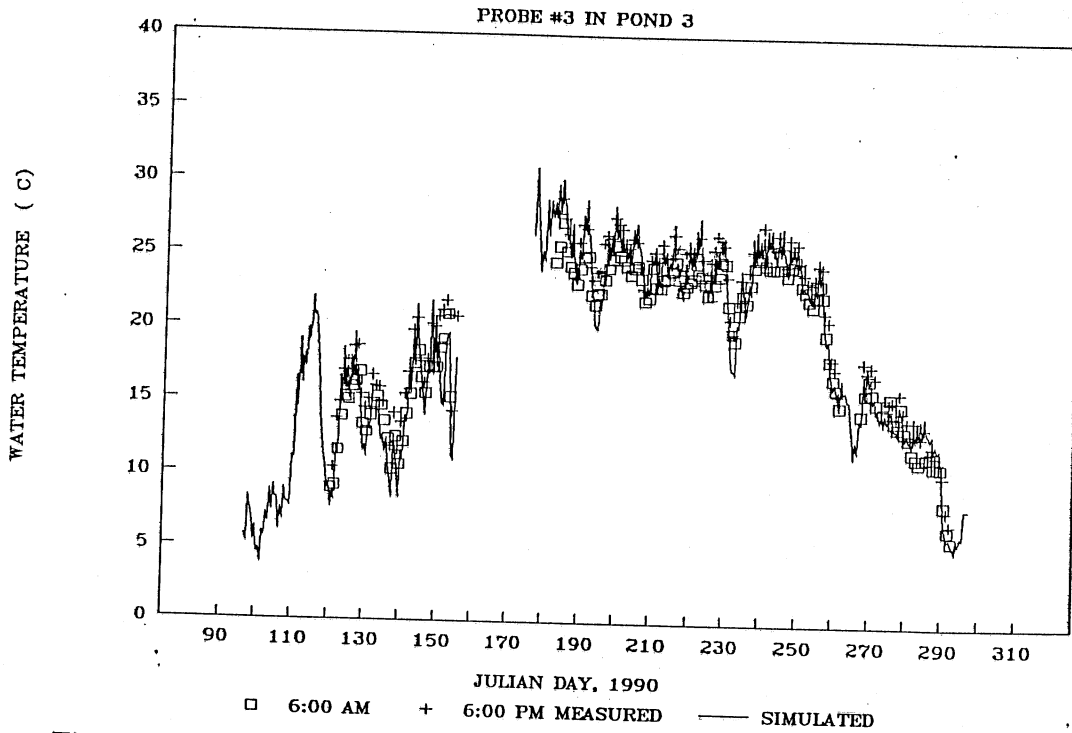


Fig. 26 Measured and simulated water temperatures in pond 3, 1990, timestep = 12 hours, probe #3

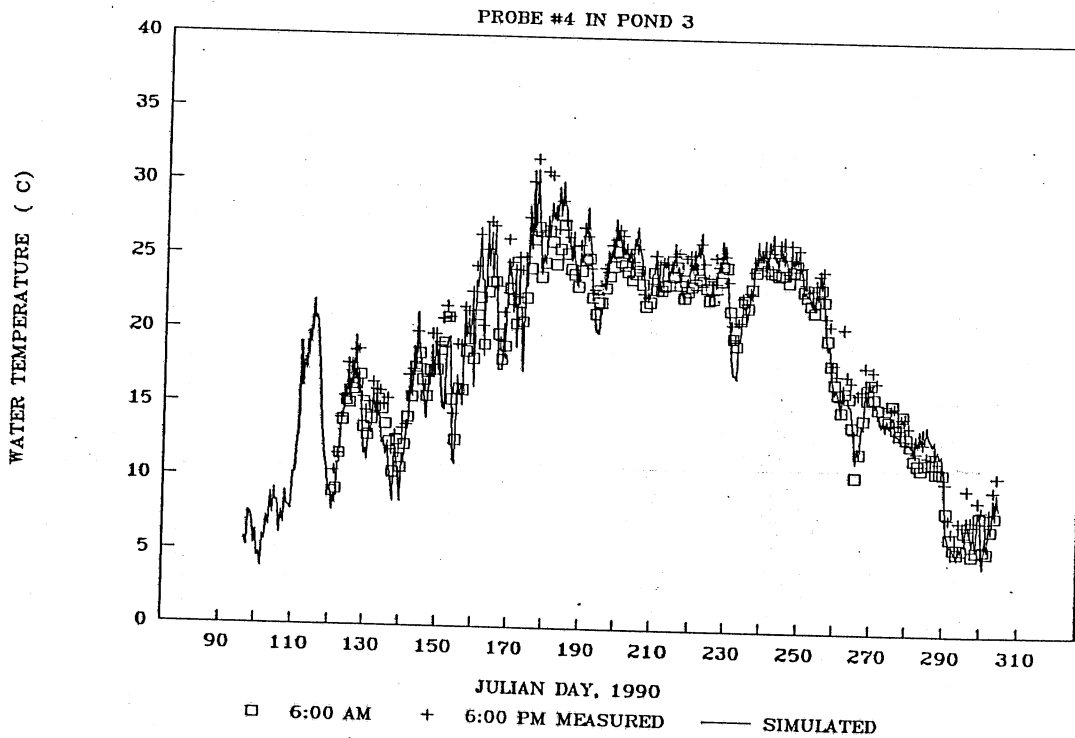


Fig. 27 Measured and simulated water temperatures in pond 3, 1990, timestep = 12 hours, probe #4

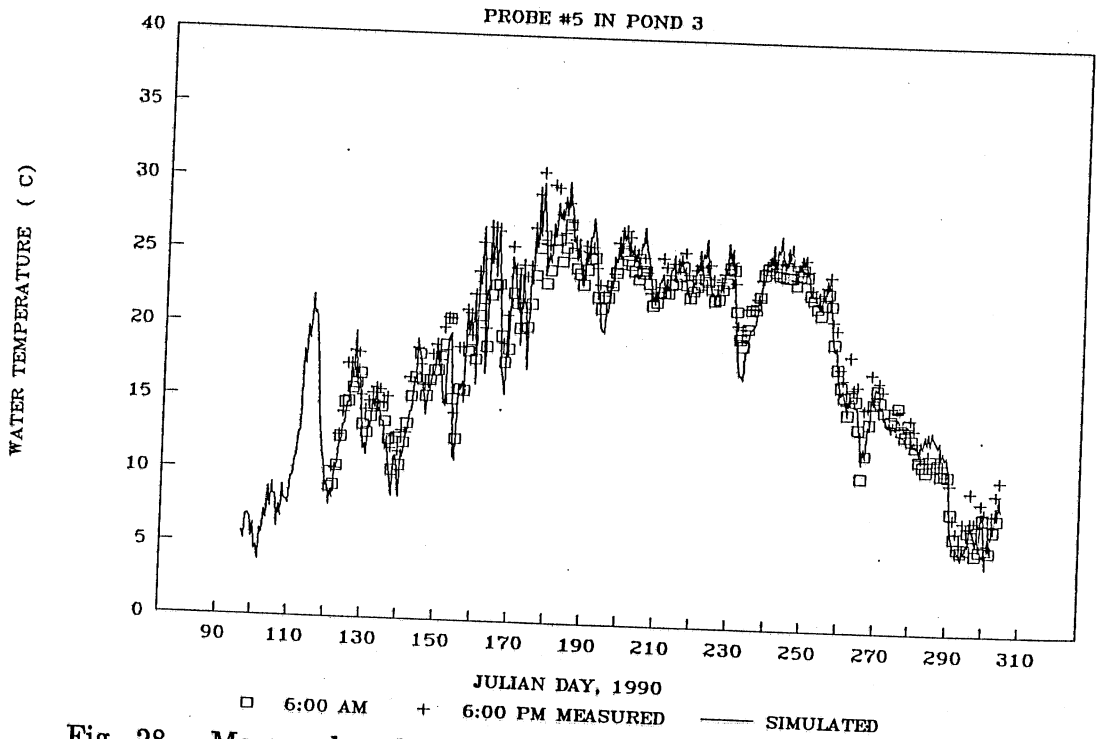


Fig. 28 Measured and simulated water temperatures in pond 3, 1990, timestep = 12 hours, probe #5

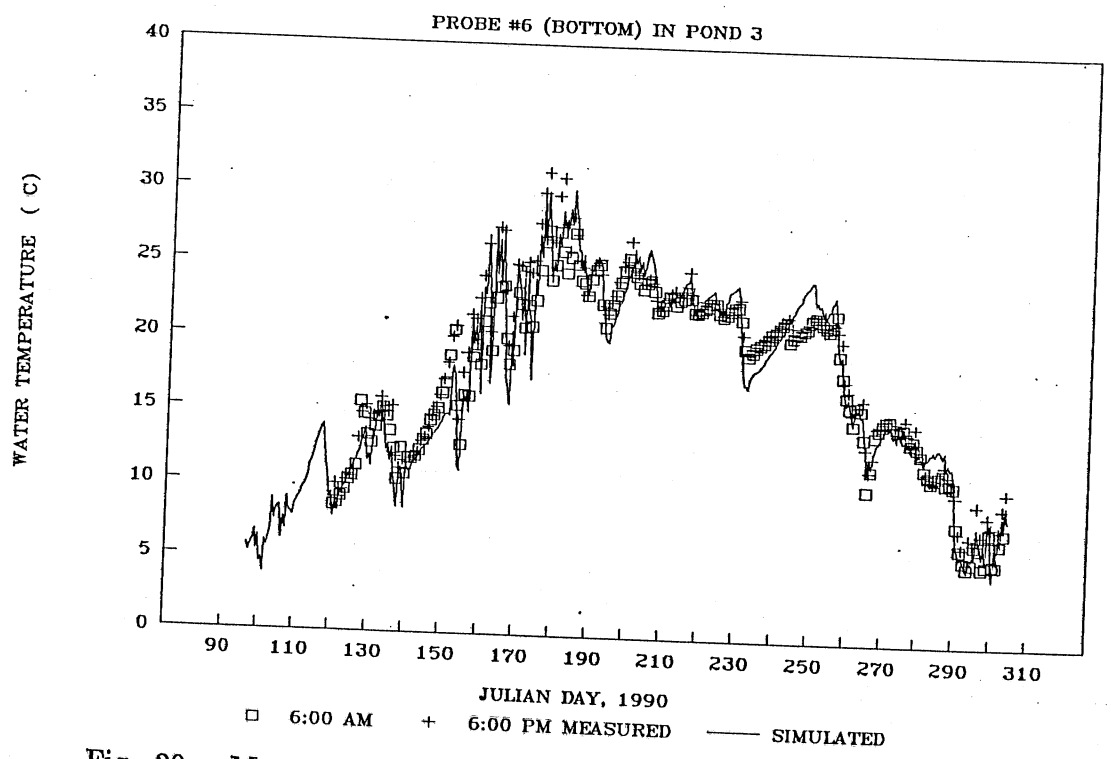


Fig. 29 Measured and simulated water temperatures in pond 3, 1990, timestep = 12 hours, probe #6 (bottom)

### 3. Simulation of Inflow Jet Mixing and Water Transfer

The numerical simulation of water temperature stratification was extended by including wastewater inflow in the form of a vertical water jet, and water transfer between ponds in the form of non-surface inflow and outflow. By doing this the model became applicable also to pond 1 and 2. The extended model was calibrated with 1989 summer temperature data and verified against 1990 summer data for pond 1.

#### 3.1 Jet Entrainment and Mixing

At the Harris wastewater treatment facility wastewater is pumped underground through a 4 inch diameter pipe and discharged vertically at the bottom in the center of pond 1 (Fig. 1). The inflow rate and the inflow water temperature were continuously measured at the pumping station during operation for about 1 year (Luck and Stefan, 1990). The average inflow rate was 185 gallons per minute ( $0.0167 \text{ m}^3/\text{s}$ ). The inflow was intermittent. Typically one of two pumps would kick in at roughly 20 minutes intervals and run for 2-3 minutes. This form of wastewater inflow produces a forced jet which upwells on the surface and a surface spreading flow. Due to differences in densities between the incoming and the ambient pond water the surface spreading flow tends to sink during the summer (Fig. 1). In this section the entrainment by the jet, the spreading and mixing were analyzed to develop a simple jet mixing model.

Fig. 1 illustrates schematically the flow pattern produced by the wastewater discharge in pond 1 during the summer. The jet entrains much ambient water from the bottom portion of the pond. The jet reaches and overshoots the water surface due to shallow water depth (0.6-1.8 m) and high initial momentum. The condition for overshooting is the exceedance of a critical densimetric Froude number for the round jet,  $Fr_c$ , (Stefan and Gu, 1990).

$$Fr_c = 0.087 H^{3/2}/D_j^{3/2} \quad (3.1)$$

in a stratified pond, where  $H$  = total water depth and  $D_j$  = jet diameter. With  $D_j = 0.1016 \text{ m}$  and  $H = 1.8 \text{ m}$  for the wastewater discharge in Harris Pond 1, one obtains

$$Fr_c = 6.5 \quad (3.2)$$

Densimetric Froude number is defined as

$$Fr = \frac{U_j}{\left(\frac{\Delta\rho}{\rho} gD_j\right)^{1/2}} \quad (3.3)$$

in which  $U_j$  = discharge velocity,  $\Delta\rho = (\rho_o - \rho_j)$  = density difference between jet and ambient pond water at the discharge. A typical inflow temperature is 17 °C in late summer when the pond temperature is approximately 10 °C. For the pond temperature difference of 7 °C, the density difference is about 0.9 kg/m<sup>3</sup>. With  $U_j = 1.44$  m/s (discharge flow rate  $Q_j = 0.0167$  m<sup>3</sup>/s) from field measurements, Fr is estimated as

$$Fr = 48 \quad (3.4)$$

Since this value is much larger than  $Fr_c$  the discharge jet will emerge on the water surface. Jet emergence on the water surface was indeed observed in the field. Following impingement and radial spreading on the water surface, the much diluted inflow sinks (plunges) into the pond (Fig. 1). A horizontal intruding-spreading interflow is formed in the layer where buoyancy is neutral, i.e. where inflow density is identical to ambient water density (equilibrium layer). This discharge configuration is termed stable because the discharged water is not recirculated into the buoyant jet near the jet discharge (Lee, 1980). Based on theoretical and experimental studies of an axisymmetric (round) turbulent buoyant jet discharged vertically into a stagnant shallow water body, Lee (1980) indicated that there would be no recirculation if the jet densimetric Froude number Fr (Eqn. 3.3) is less than the value

$$Fr_s = 4.6 \frac{H}{D_j} \quad (3.5)$$

with  $H = 1.8$  m and  $D_j = 0.1016$ , for the wastewater discharge in Harris pond 1

$$Fr_s = 82 \quad (3.6)$$

The jet flow in pond 1 satisfies the stability criterion.

If Fr is greater than  $Fr_s$  due to either shallow water (H) or low buoyancy ( $\Delta\rho$ ) or high initial momentum ( $U_j$ ), an unstable discharge configuration is formed. In this situation, recirculation cells are set up near the jet discharge, leading to re-entrainment into the discharge. It was also suggested by Lee (1980) that in deep water and stable discharge



conditions, the spreading layer thickness on the surface was about one tenth of the total depth (0.1H). Therefore the depth over which jet entrainment contributes to dilution of the jet is estimated to be on the order of 0.9H.

A simplified model for jet entrainment in the nearfield and mixing in the farfield is formulated for incorporation into the pond temperature stratification simulation model. The entrainment rate of ambient water by the vertical jet is determined from the jet flow rate as a function of distance from the orifice (Albertson et al, 1948)

$$\frac{Q}{Q_j} = 1 + 1.0133C_2\frac{z}{D_j} + 1.9735C_2^2\left(\frac{z}{D_j}\right)^2 \quad (3.7)$$

in which  $Q$  = volume flux at height  $z$  above the efflux,  $Q_j$  = jet discharge,  $C_2$  = coefficient, in the range from 0.081 to 0.111. The total entrainment by the jet over height 0.9H is estimated as

$$Q_e = Q_t - Q_j \quad (3.8)$$

or

$$Q_e = Q_j \left[ 1.0133C_2\frac{0.9H}{D_j} + 1.9735C_2^2\left(\frac{0.9H}{D_j}\right)^2 \right] \quad (3.9)$$

Entrainment from an individual horizontal water layer of thickness  $\Delta z$  is

$$q = \frac{dQ_e}{dx} \Delta z \quad (3.10)$$

or in numerical form

$$q_i = Q(z_i + \frac{1}{2}\Delta z_i) - Q(z_i - \frac{1}{2}\Delta z_i), \quad i = 1, 2, \dots, I \quad (3.11)$$

where  $I$  = total number of layers contributing to entrainment. It is assumed that there is no entrainment into the plunging-intruding-spreading flow beyond the jet region (nearfield). Flow rate and temperature of the interflow are therefore approximated, respectively, as

$$Q_p = Q_t \quad (3.12)$$

and

$$T_p = \frac{\sum_{i=1}^I (q_i T_i) + T_j Q_j}{Q_e + Q_j} \quad (3.13)$$

A density-temperature function  $\rho(T)$  (Gu and Stefan, 1988) is used to determine the depth of the interflow layer by neutral buoyancy. If information on suspended and dissolved solids is available, the density increment due to total solids should be taken into account although the effect of organic solids on the water density might not be significant.

The volume of each layer in the pond is modified in each timestep by subtracting the water entrained from the layer and adding the interflow to the equilibrium layer. The temperature in the equilibrium layer is modified using temperature of the incoming water weighted by its volume over a computational timestep (typically 12 hours).

### 3.2 Water Transfer

The water balance in the Harris ponds can be evaluated by the following equation

$$\Delta S = I - O + P - E \pm G \quad (3.14)$$

where  $\Delta S$  = change in storage volume,  $O$  = outflow volume,  $I$  = inflow volume,  $P$  = volume of rainfall,  $E$  = volume of evaporation, and  $G$  = groundwater or seepage volume.

Stages in each pond were intermittently measured (Luck and Stefan, 1990). The change in pond storage,  $\Delta S$ , is then estimated from the depth-volume function. Wastewater inflows to pond 1 were recorded at the pumping station. These records included the duration of each pump run (two pumps operated intermittently), flow rate, and temperature of the pumped wastewater inflow from which the inflow volume,  $I$ , is calculated. Rainfall (precipitation) data was available from the weather station. The groundwater or seepage,  $G$ , is neglected in this study because of the lining of the ponds. Outflow,  $O$ , was not directly measured, but was estimated using Eq. 3.14. Evaporation was calculated in the water temperature model. According to the operational procedure, inflow to pond 2 is equal to outflow from pond 1, and similarly inflow to pond 3 is the same as outflow from pond 2.

Modifications to the program were made to deal with sub-surface inflows, and outflows since the original model was developed for surface outflows and surface inflows only. The additional sub-surface inflows and outflows were incorporated through the LAKE specific subroutine and subroutines WDEPTH and ADVECT. Flow rates and water quality parameters of outflows or inflows are specified through the LAKE specific subroutine. The elevation of the layer which receives the inflowing water is determined by the density of the inflow water and the density of ambient pond water. Calculation of sub-surface inflows is made in subroutine ADVECT by calling subroutine CONSMAS. Subroutine WDEPTH is modified to deal with sub-surface outflows.

In summary the numerical simulation with this simple water transfer model accomplishes the following: 1) determines the layer from which water is taken out or to which water is added, 2) calculates the volume of withdrawal or addition for each layer in the pond and 3) computes the final temperatures in each layer using temperatures after mixing with inflowing water. Outflow does not change the temperature in a layer, only its volume. Outflow water quality is determined by pond water quality.

#### 4. Simulation of Stratification Dynamics with Jet Mixing and Water Transfer

In the overall pond system, effluent water quality from pond 3 is of greatest concern since it has impact on water quality in the streams into which pond water is discharged. The importance of pond 3 has been considered in section 2 where a simulation model for stratification dynamics has been developed, calibrated and verified against data. With the addition of jet mixing and water transfer to this model, the pond system can be simulated as it was practically operated starting with pond 1, transiting with pond 2 and ending with pond 3. This simulation procedure takes account of the unique property of pond 1 in jet dynamics and mixing processes and characteristics of water transfer between ponds. Field measurements showed that water quality characteristics in pond 1 and pond 2 are similar but pond 3 has clearer water and weaker stratification.

Numerically simulated water temperatures in pond 1 in the open water period of 1989 and 1990 are presented to demonstrate the applicability of the extended model to a general pond system. The main season for pond or lake water quality problems is summer. The periods from Aug. 1 to Nov. 30, 1989 and from Apr 7 to Oct. 31, 1990 were selected for the simulation of pond 1. Data were available for both these periods.

The water budget simulation was performed by taking account of change in storage, rainfall, evaporation and water transfer, inflow and outflow. As shown in Figs. 30 and 31, precipitation events were followed by inflow peaks with lags of one day to two days which in turn were followed by outflow peaks. Two sudden drops in storage change at the beginning and end of November, 1989, respectively, are due to the filling of pond 3 with water from ponds 2 and 1 following the fall discharge of pond 3. Shown in Figs. 32 and 33 are total water balances for 1989 and 1990, respectively. There is more storage change in 1989 than in 1990. Fig. 34 and Fig. 35 illustrate that inflow and outflow are similar percentages of the total water budget and that amounts of rainfall and evaporation are of similar magnitude.

Entrainment of ambient water by the vertical water jet is a function of the total pond water depth as described in Eq. 3.7 and shown in Figs. 36 to 39. Calculated results show that the ratio of entrainment,  $Q_e$ , to the inflow,  $Q_j$ , is in the range of 4 to 9 for 1989 and 6 to 10 for 1990. The temperature in the intruding-spreading layer depends on both inflow and ambient water temperature. Temperature in the spreading water is mainly determined by the ambient water temperature, which is between the injected water temperature and ambient temperature but much closer to the latter (Fig. 40). If entrainment is small due to shallow depth, inflow temperature

WATER BALANCE FOR HARRIS POND 1

34

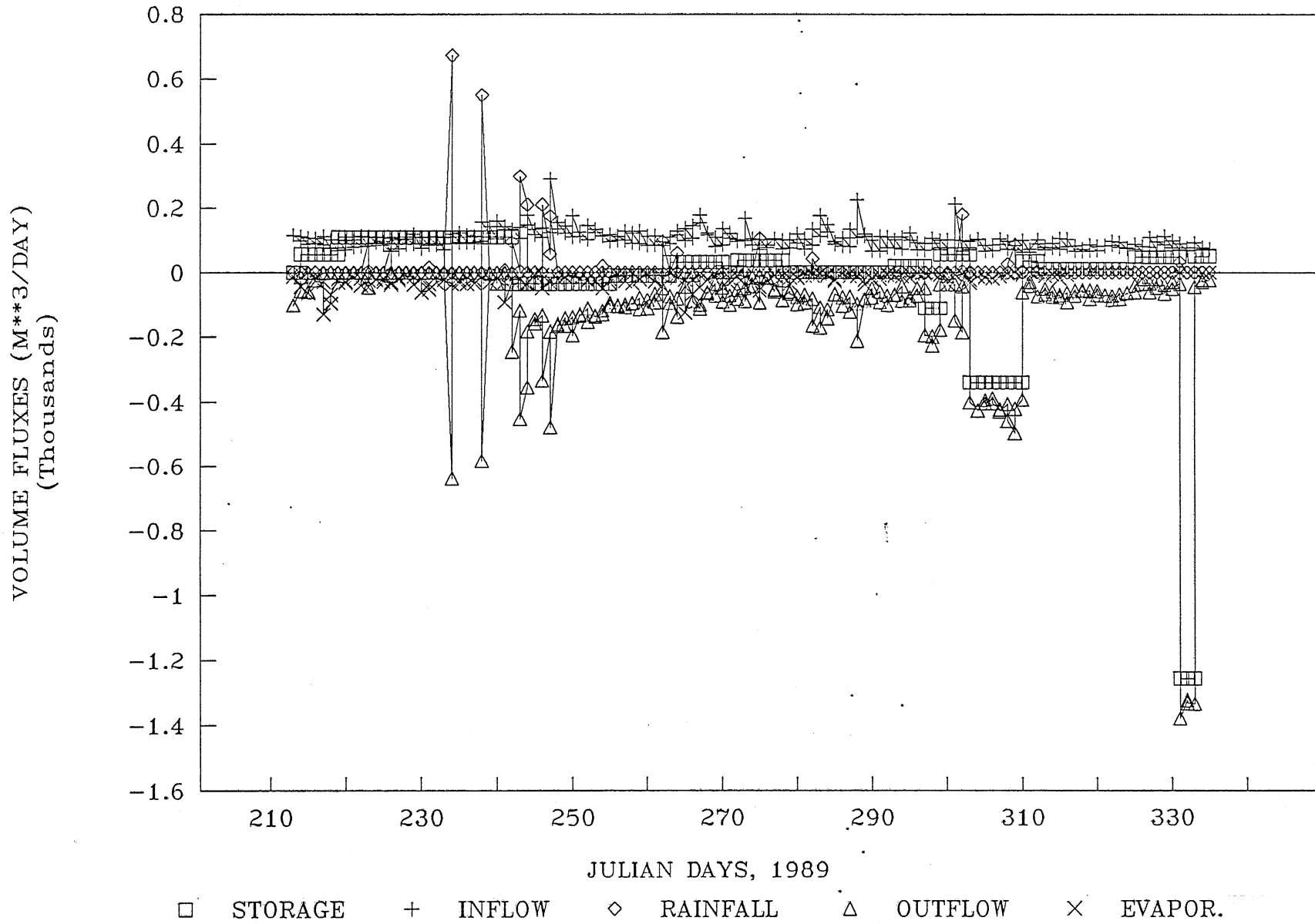


Fig. 30 Variation of inflow, outflow, rainfall, evaporation and storage with time, pond 1, Aug. 1 - Nov. 30, 1989

VOLUME FLUXES (M\*\*3/DAY)  
(Thousands)

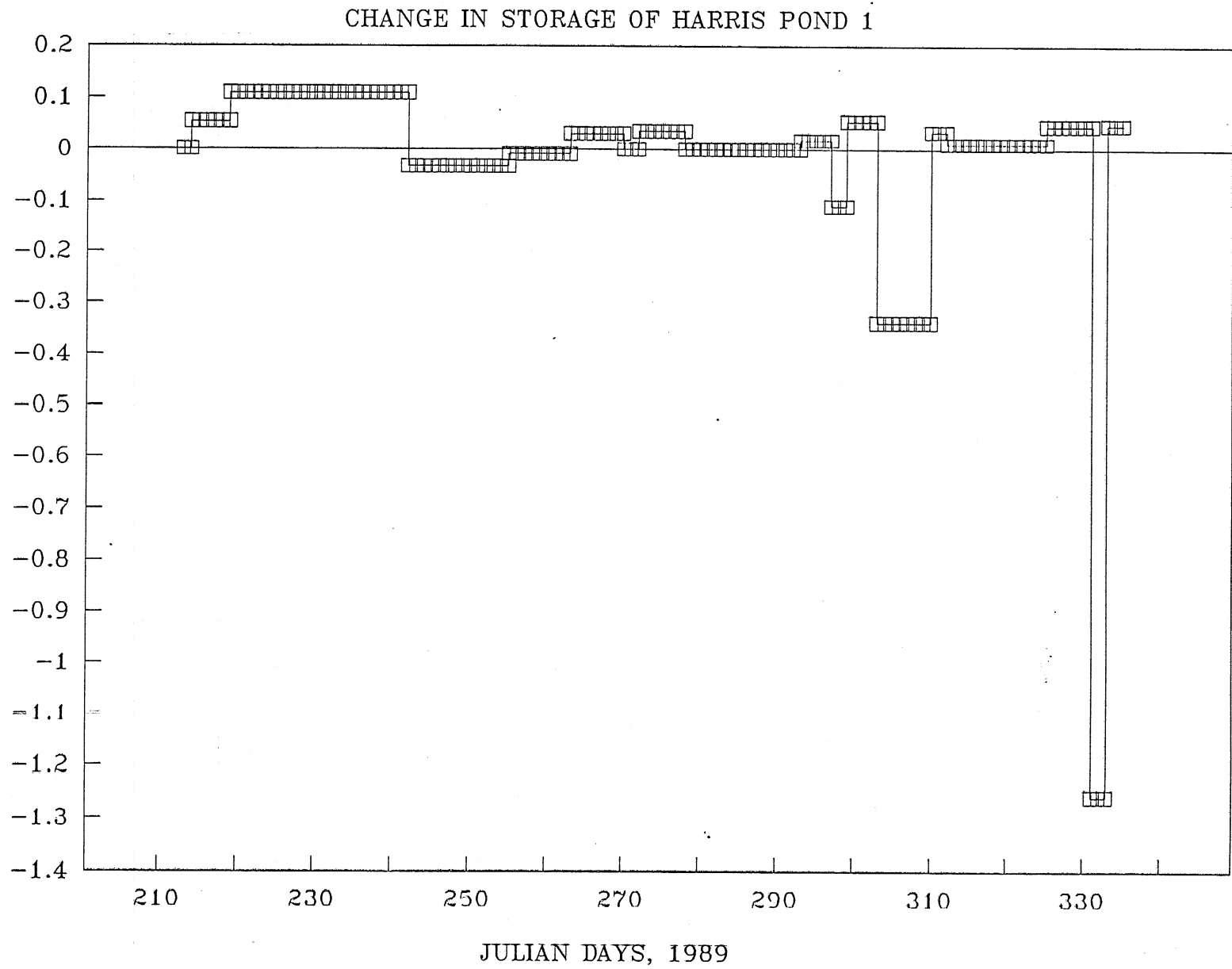


Fig. 30 (Cont'd) Variation of inflow, outflow, rainfall, evaporation and storage with time, pond 1, Aug. 1 - Nov. 30, 1989

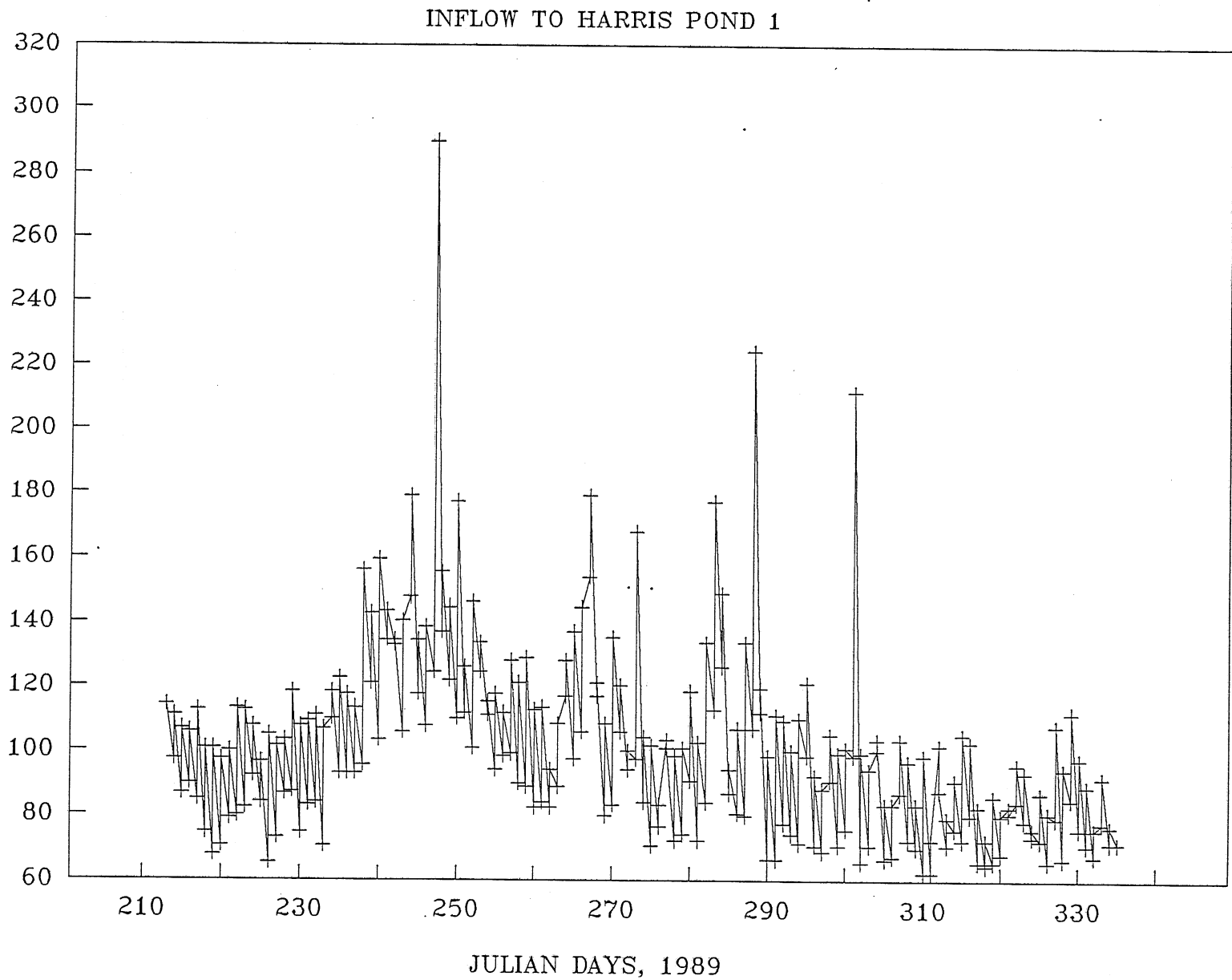


Fig. 30 (Cont'd) Variation of inflow, outflow, rainfall, evaporation and storage with time, pond 1, Aug. 1 - Nov. 30, 1989

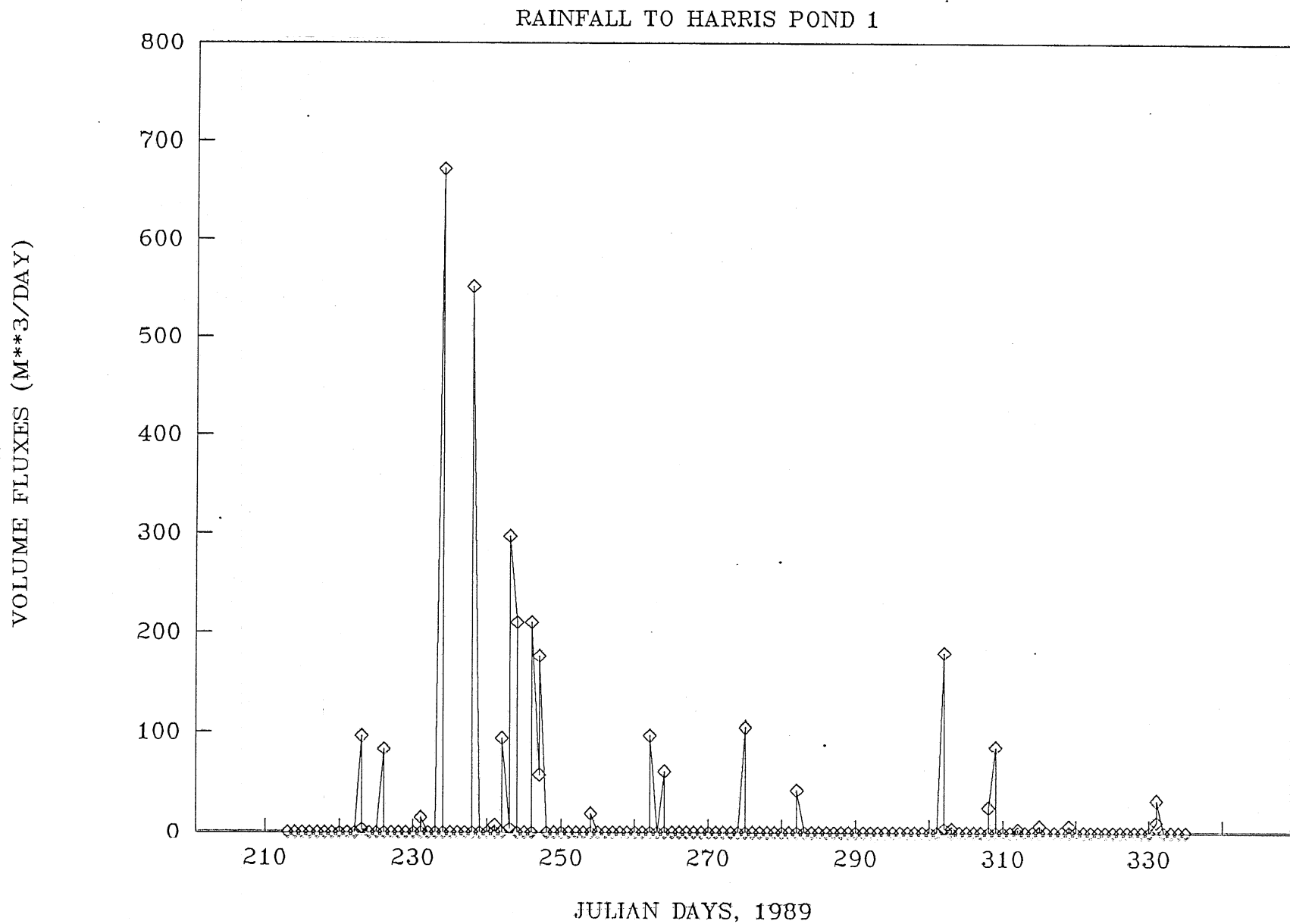


Fig. 30 (Cont'd) Variation of inflow, outflow, rainfall, evaporation and storage with time, pond 1, Aug. 1 - Nov. 30, 1989

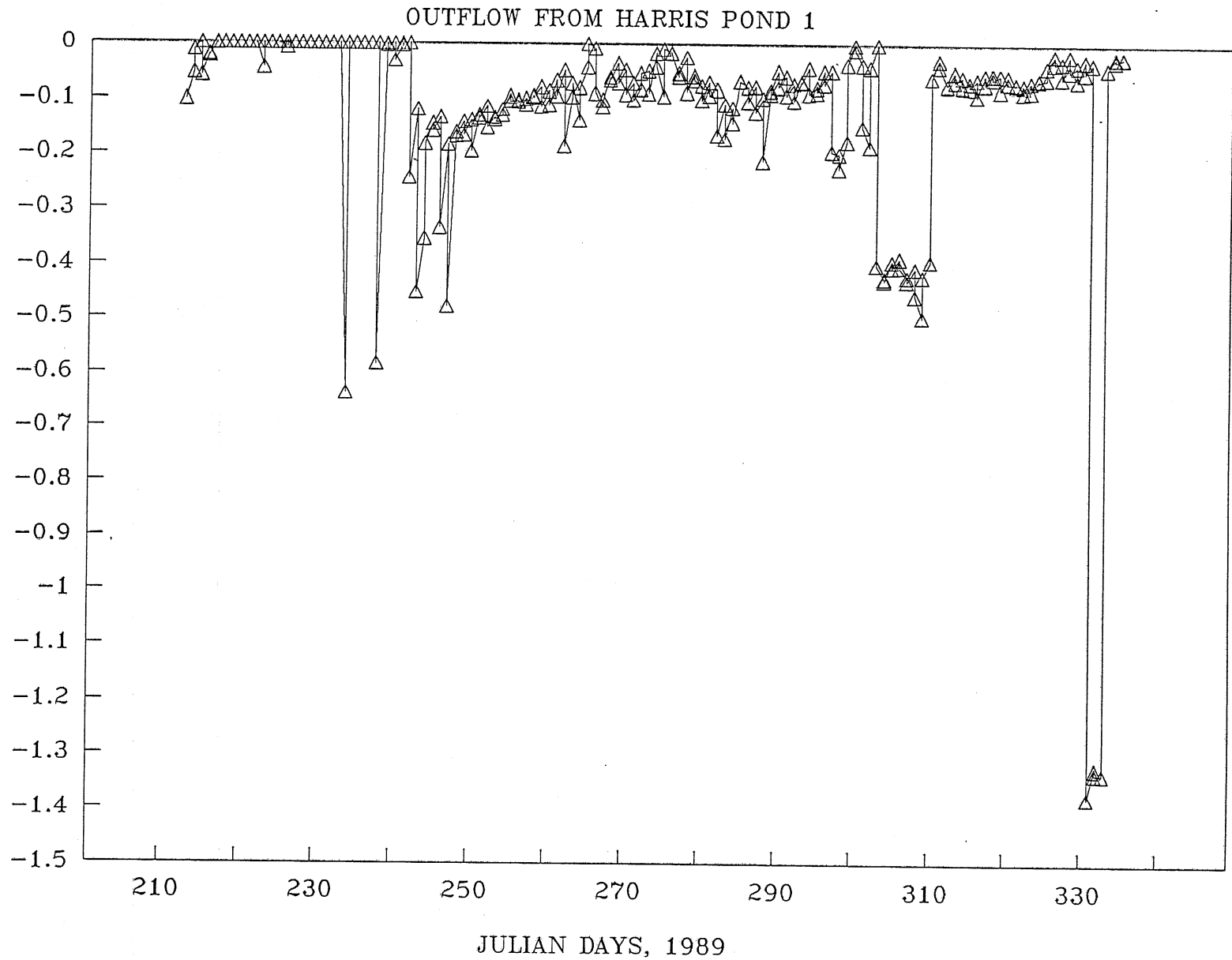
VOLUME FLUXES (M\*\*3/DAY)  
(Thousands)

Fig. 30 (Cont'd) Variation of inflow, outflow, rainfall, evaporation and storage with time, pond 1, Aug. 1 - Nov. 30, 1989



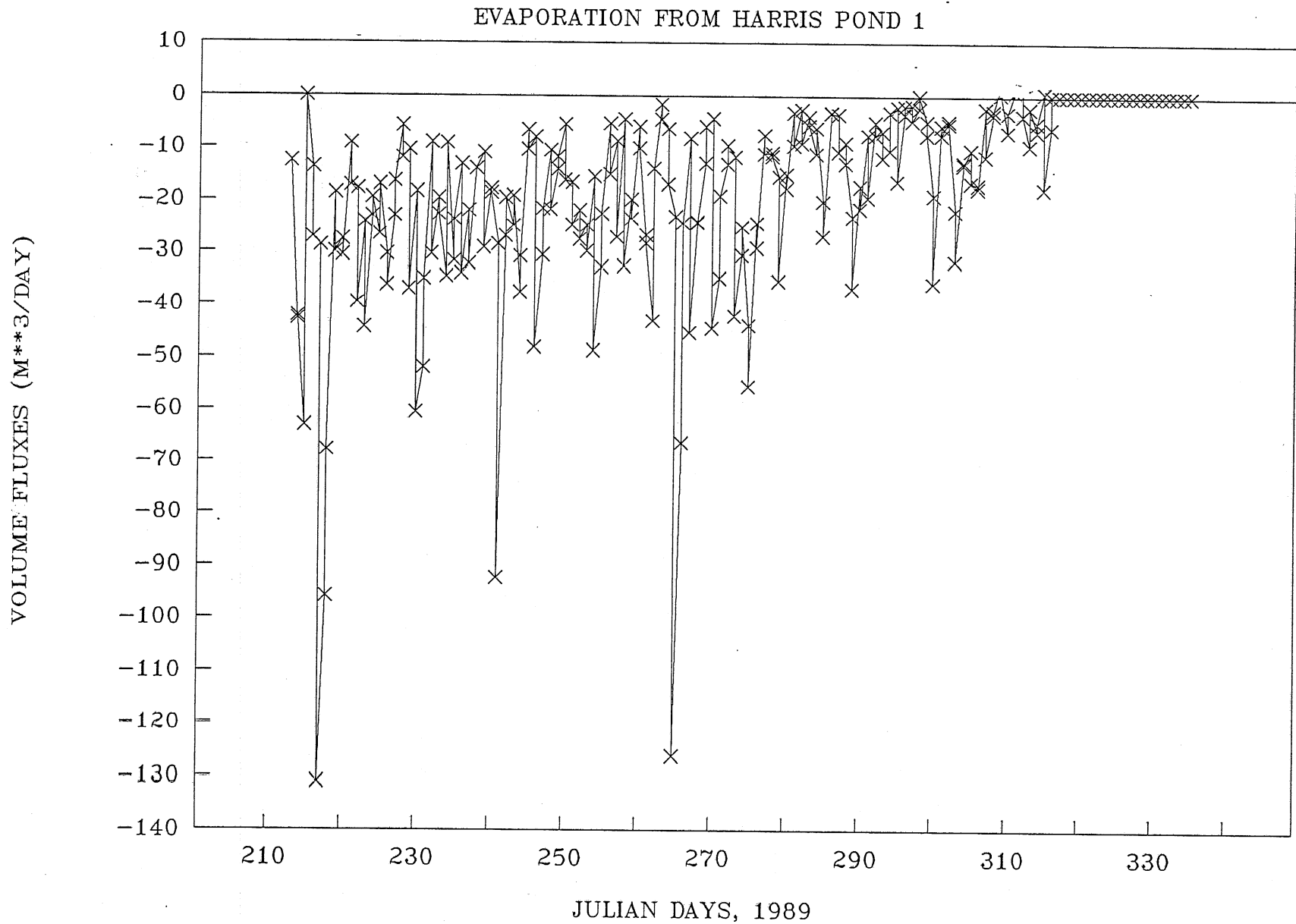


Fig. 30 (Cont'd) Variation of inflow, outflow, rainfall, evaporation and storage with time, pond 1, Aug. 1 - Nov. 30, 1989

WATER BALANCE: POND 1, 4/7 - 10/31/1990

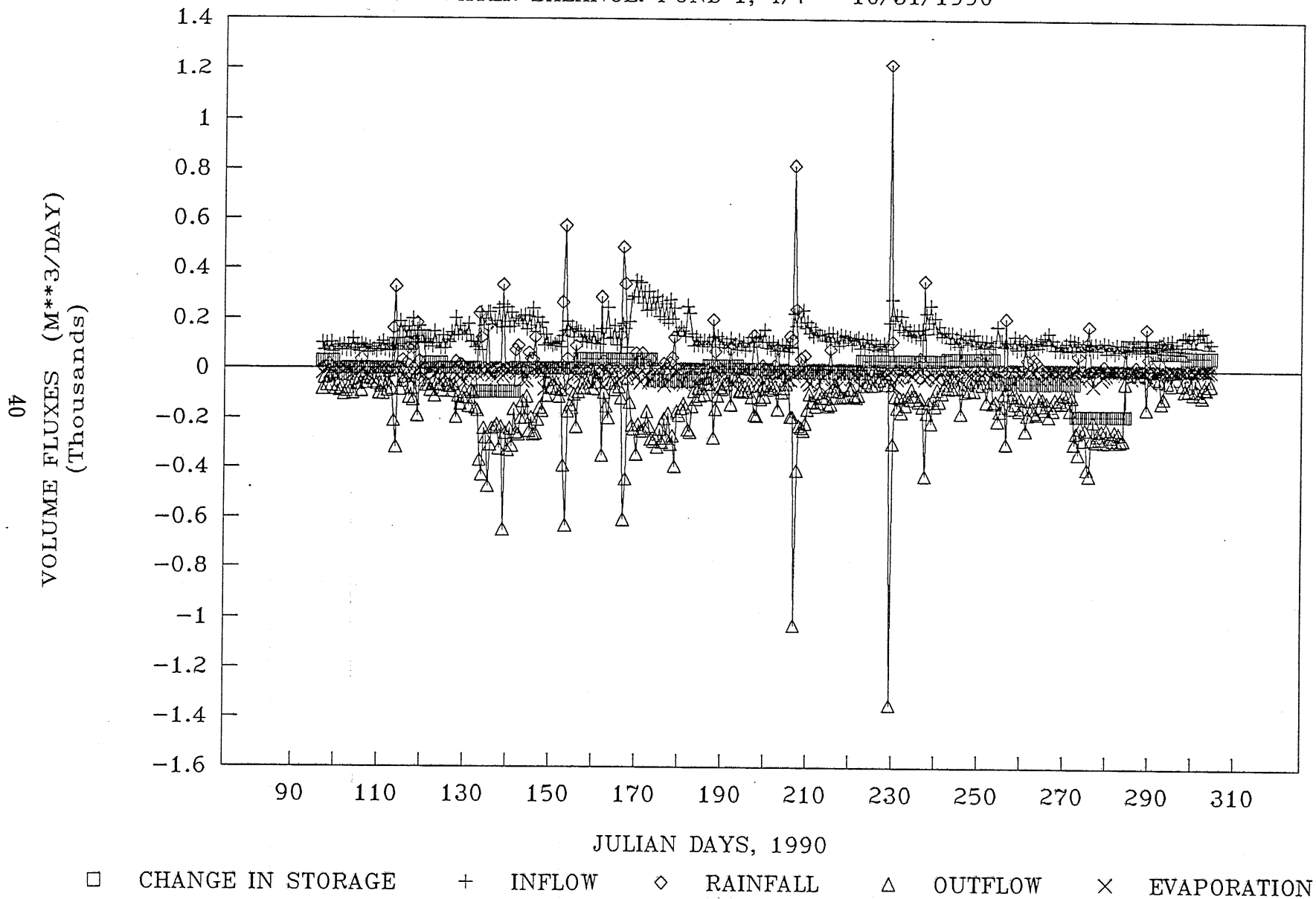


Fig. 31 Variation of inflow, outflow, rainfall, evaporation and storage with time, pond 1, April, 7 - Oct. 31, 1990

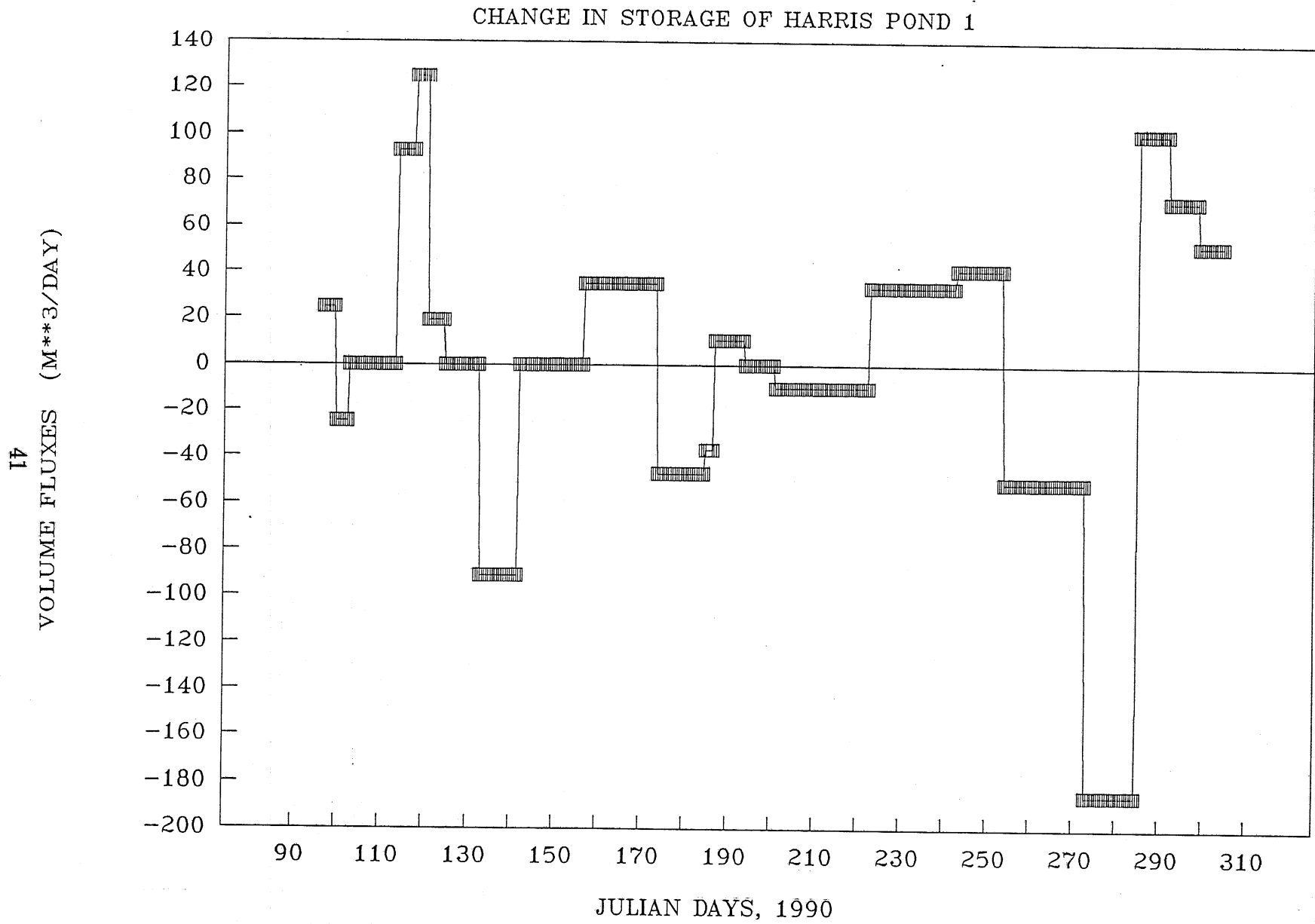


Fig. 31 (Cont'd) Variation of inflow, outflow, rainfall, evaporation and storage with time, pond 1, April, 7 - Oct. 31, 1990

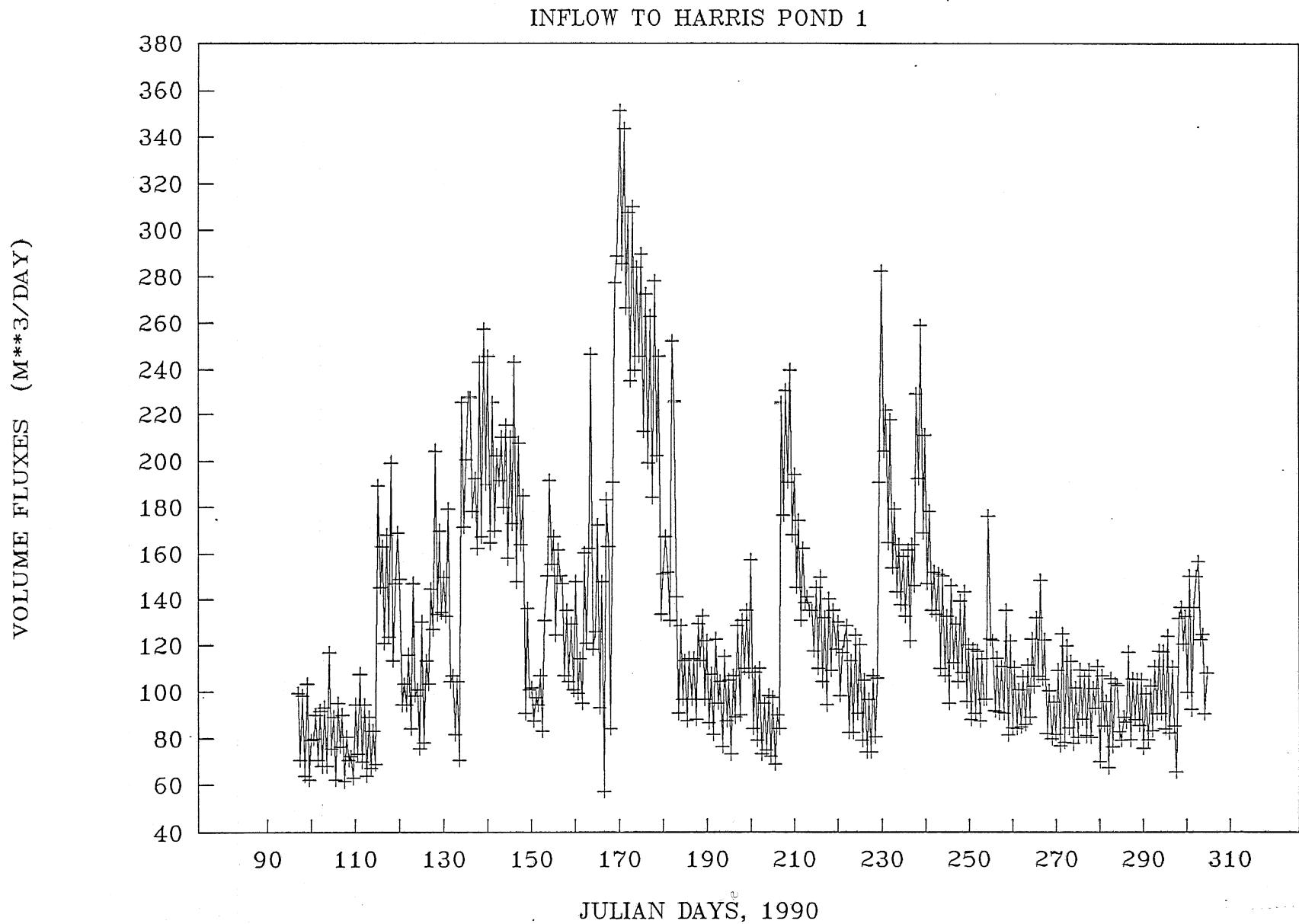


Fig. 31 (Cont'd) Variation of inflow, outflow, rainfall, evaporation and storage with time, pond 1, April, 7 - Oct. 31, 1990

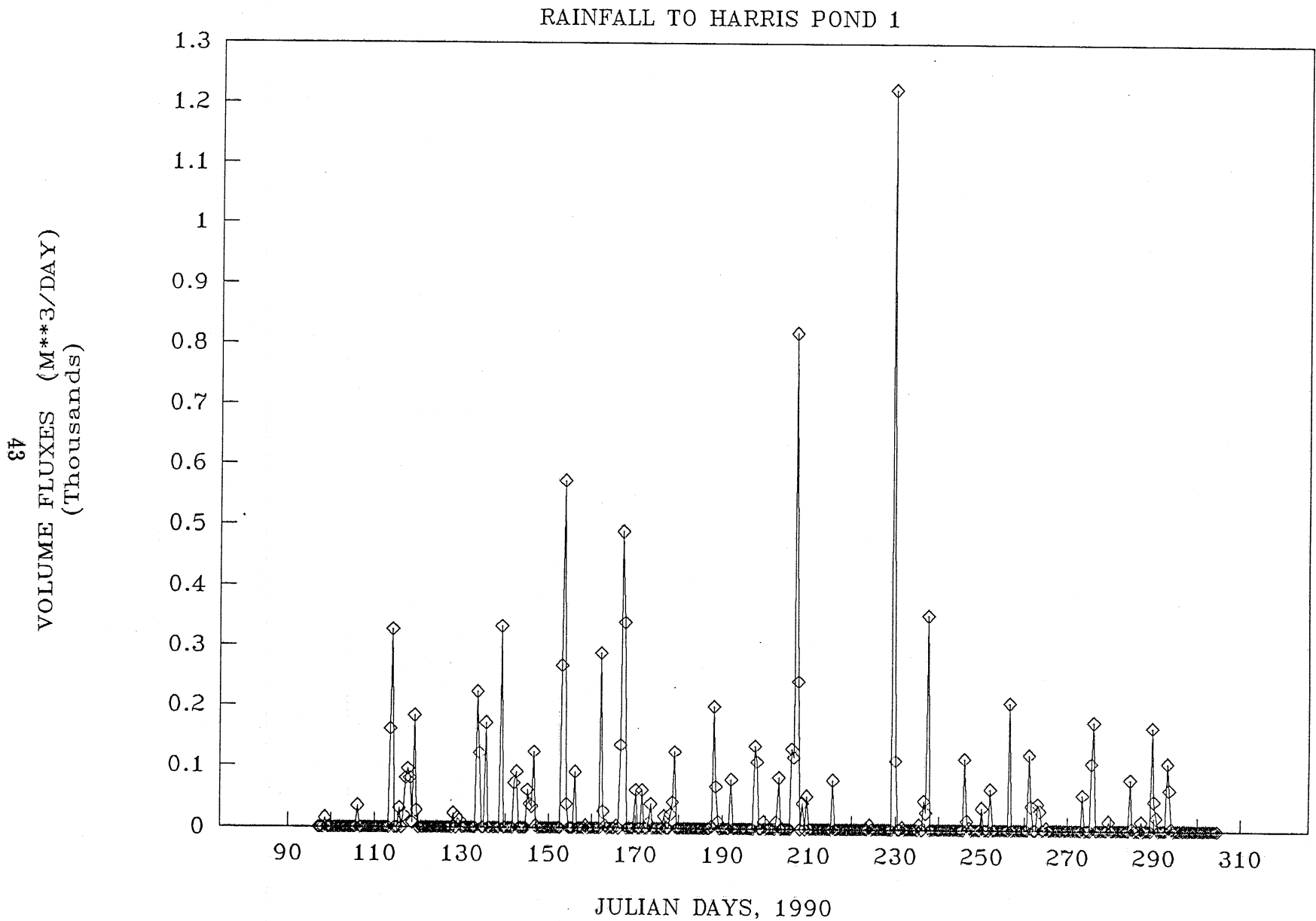


Fig. 31 (Cont'd) Variation of inflow, outflow, rainfall, evaporation and storage with time, pond 1, April, 7 - Oct. 31, 1990

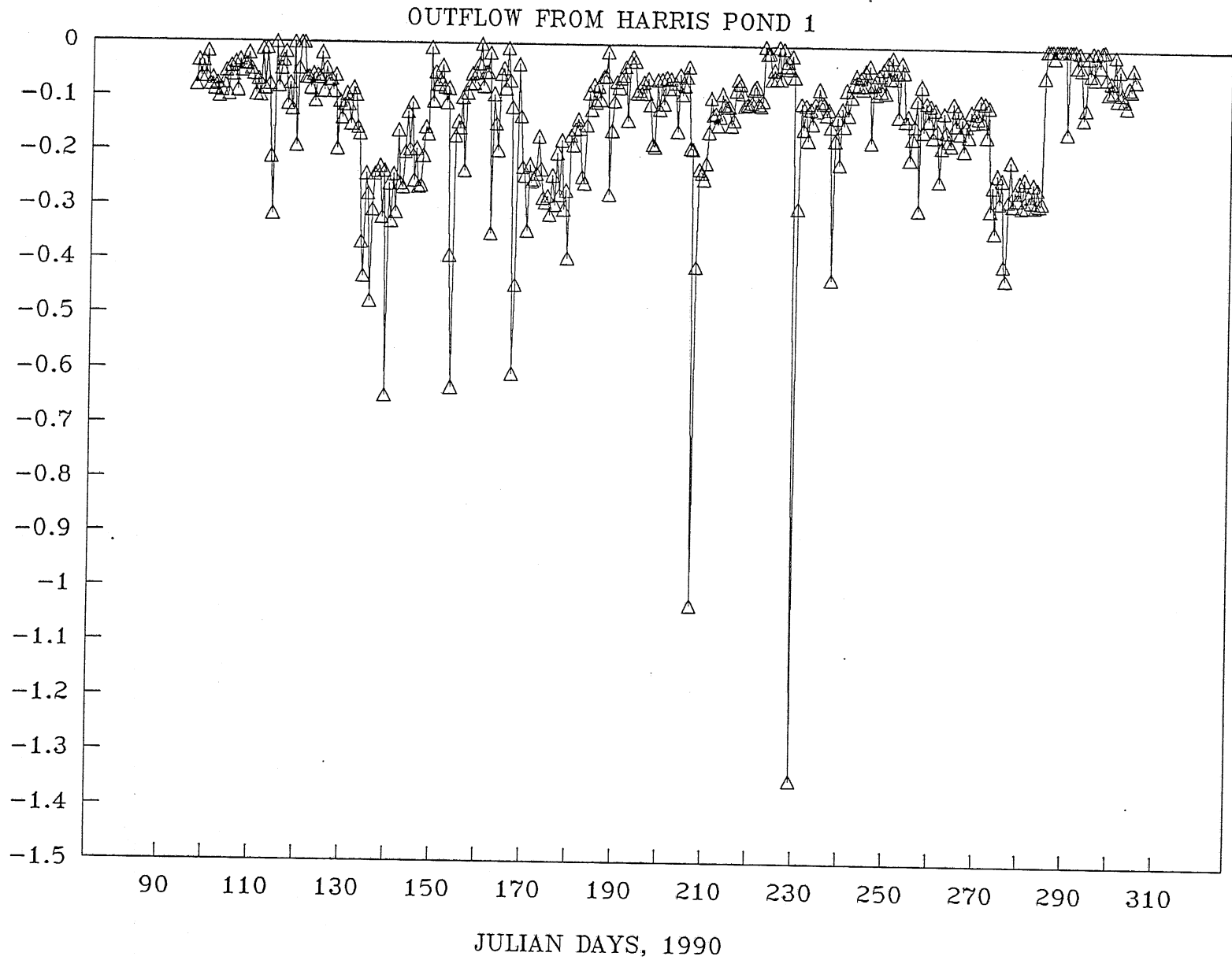
VOLUME FLUXES (M\*\*3/DAY)  
(Thousands)

Fig. 31 (Cont'd) Variation of inflow, outflow, rainfall, evaporation and storage with time, pond 1, April, 7 - Oct. 31, 1990

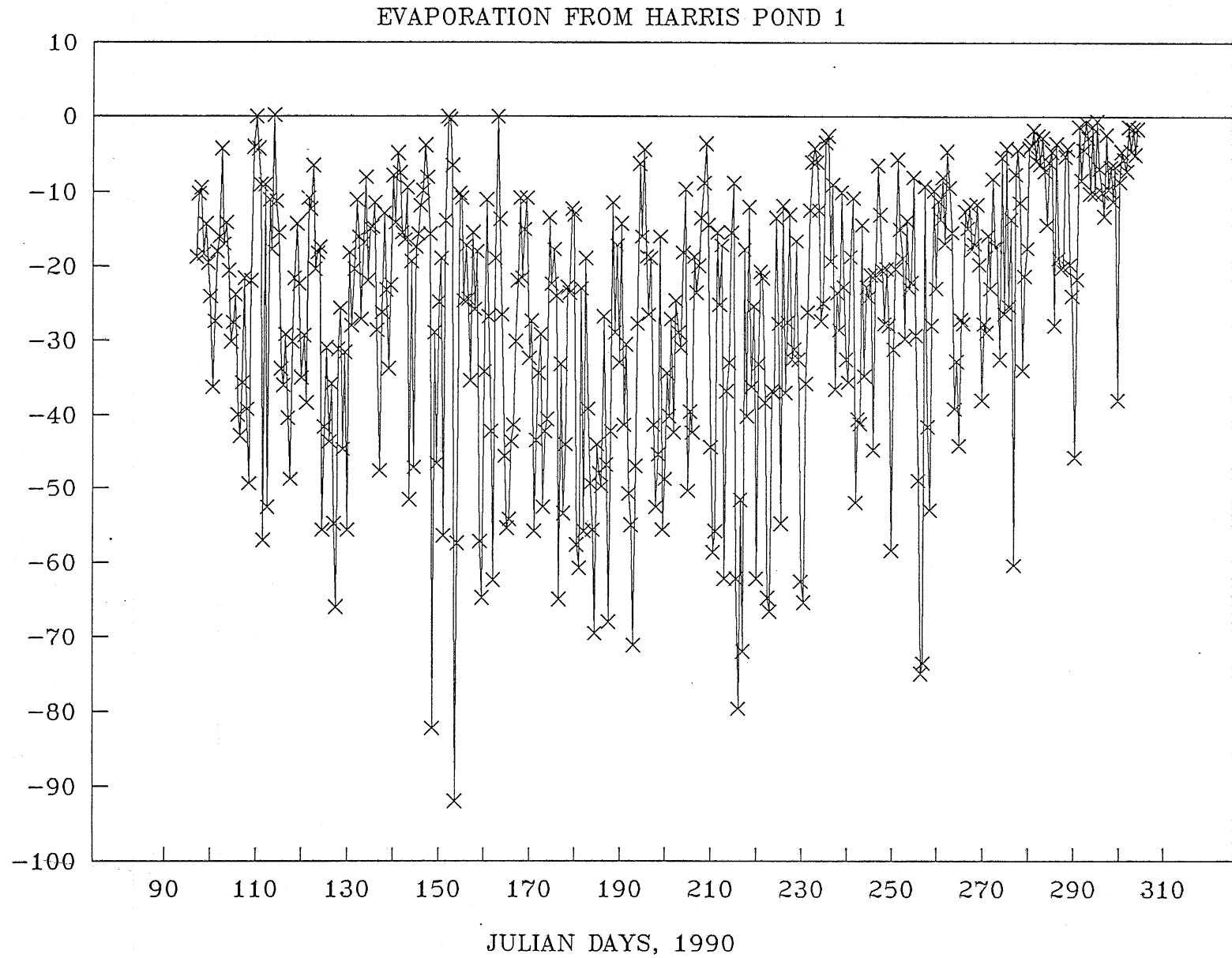


Fig. 31 (Cont'd) Variation of inflow, outflow, rainfall, evaporation and storage with time, pond 1, April, 7 - Oct. 31, 1990

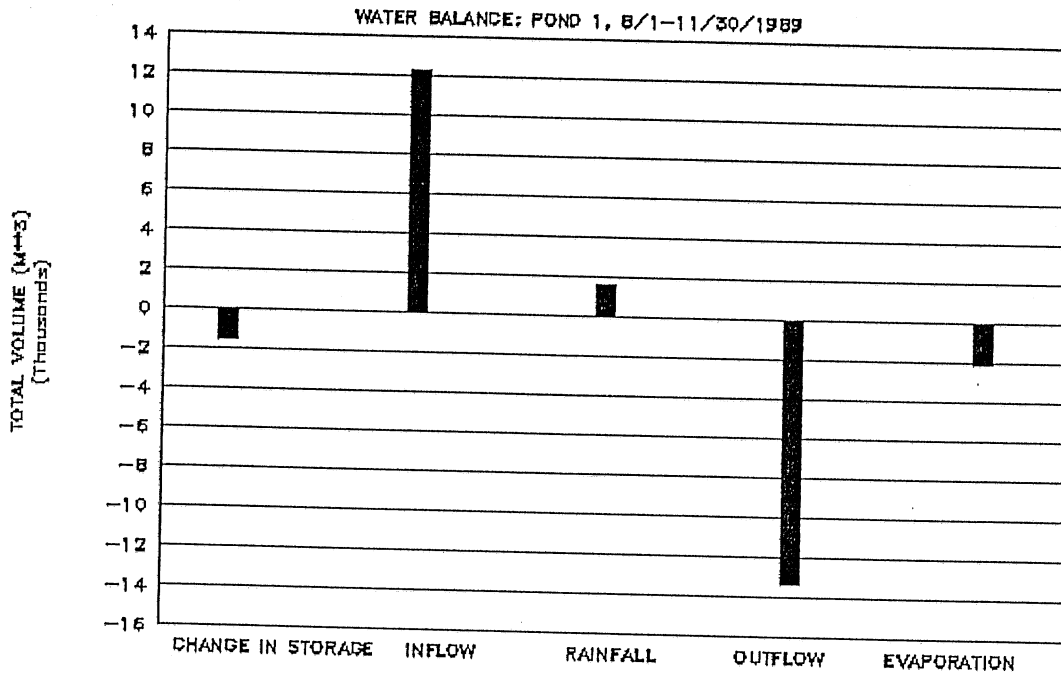


Fig. 32 Total volumes of inflow, outflow, rainfall, evaporation and change in storage, Aug. 1 - Nov. 30, 1989

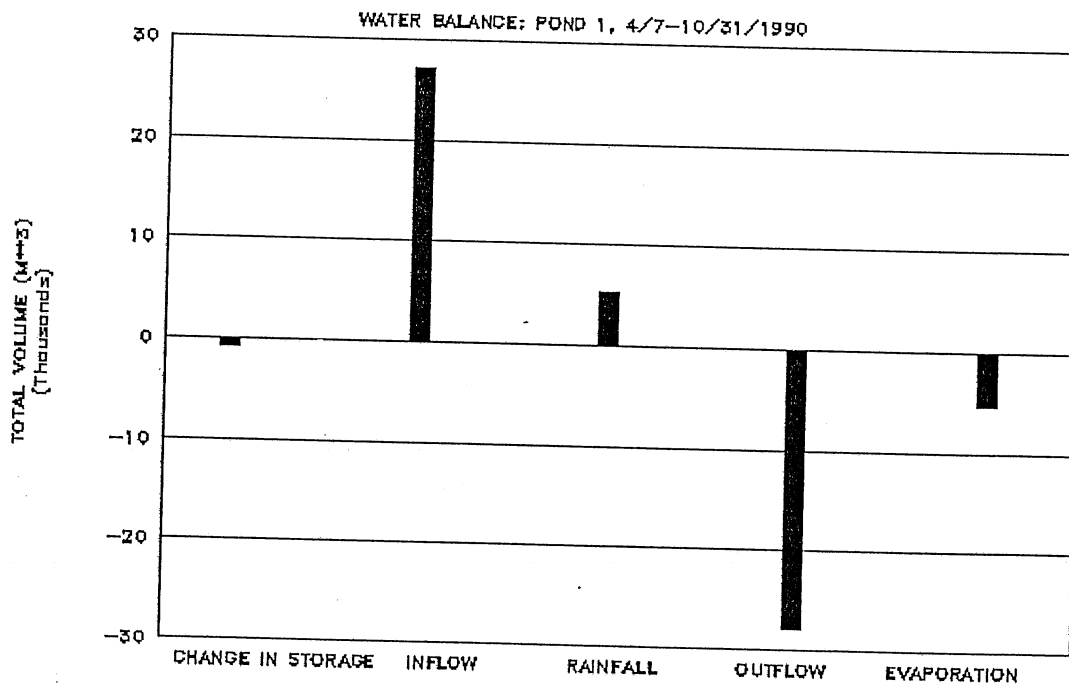
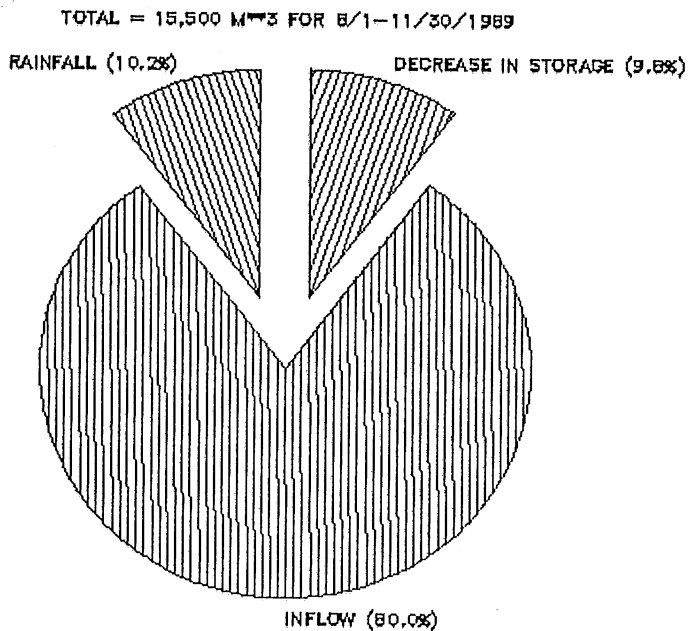


Fig. 33 Total volumes of inflow, outflow, rainfall, evaporation and change in storage, April 7 - Oct. 31, 1990



### INFLOWS TO POND 1 AND CHANGE IN STORAGE



### OUTFLOWS FROM POND 1

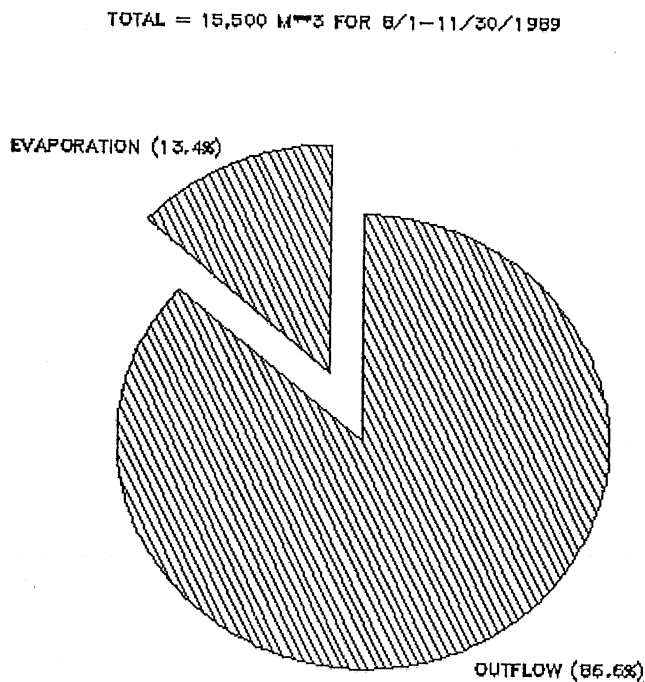
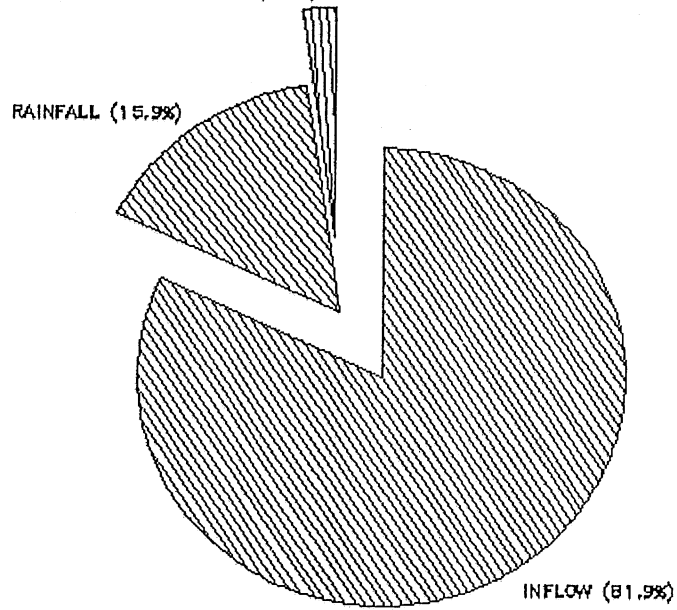


Fig. 34 Water balance for pond 1, Aug. 1 - Nov. 30, 1989

### INFLOWS TO POND 1 AND CHANGE IN STORAGE

TOTAL = 33,282 M<sup>3</sup> FOR 4/7-10/31/1990  
DECREASE IN STORAGE (2.1%)



### OUTFLOWS FROM POND 1

TOTAL = 33,282 M<sup>3</sup> FOR 4/7-10/31/1990

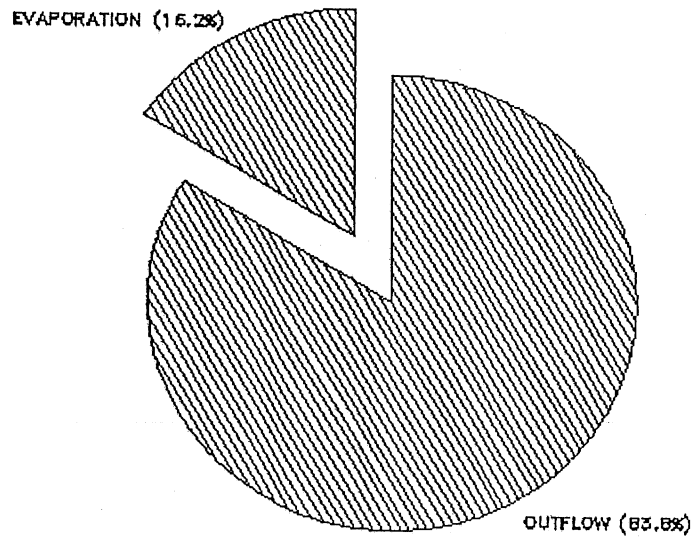


Fig. 35 Water balance for pond 1, April 7, - Oct. 31, 1990

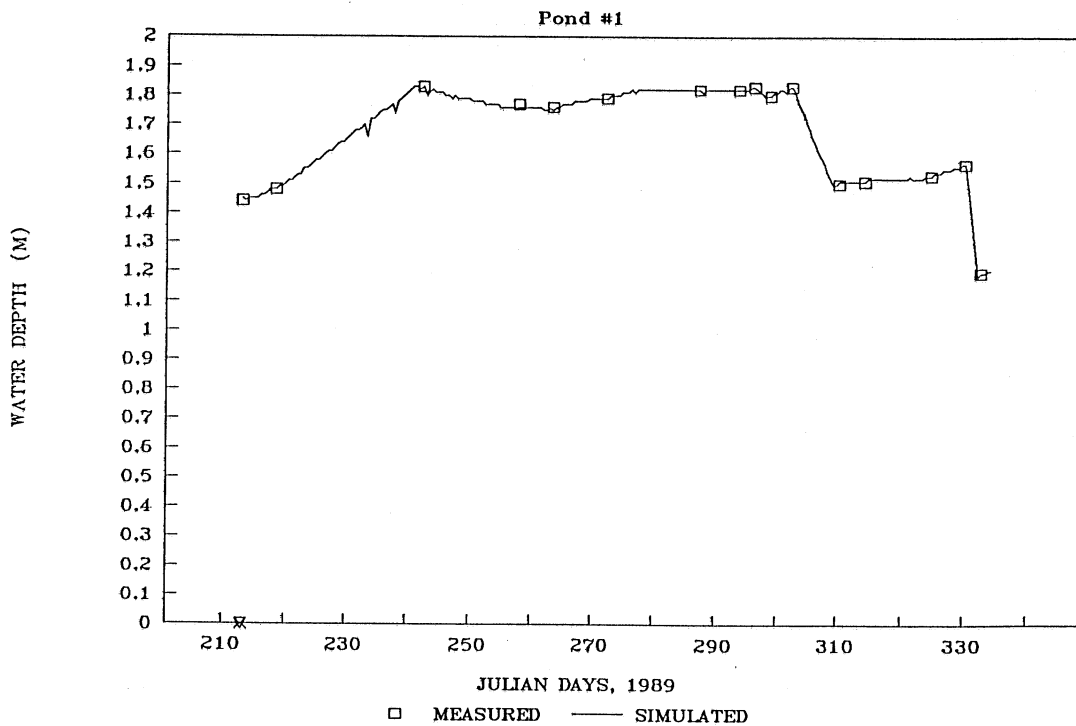


Fig. 36 Measured and calculated water depth, pond 1, Aug. 1–Nov. 30, 1989

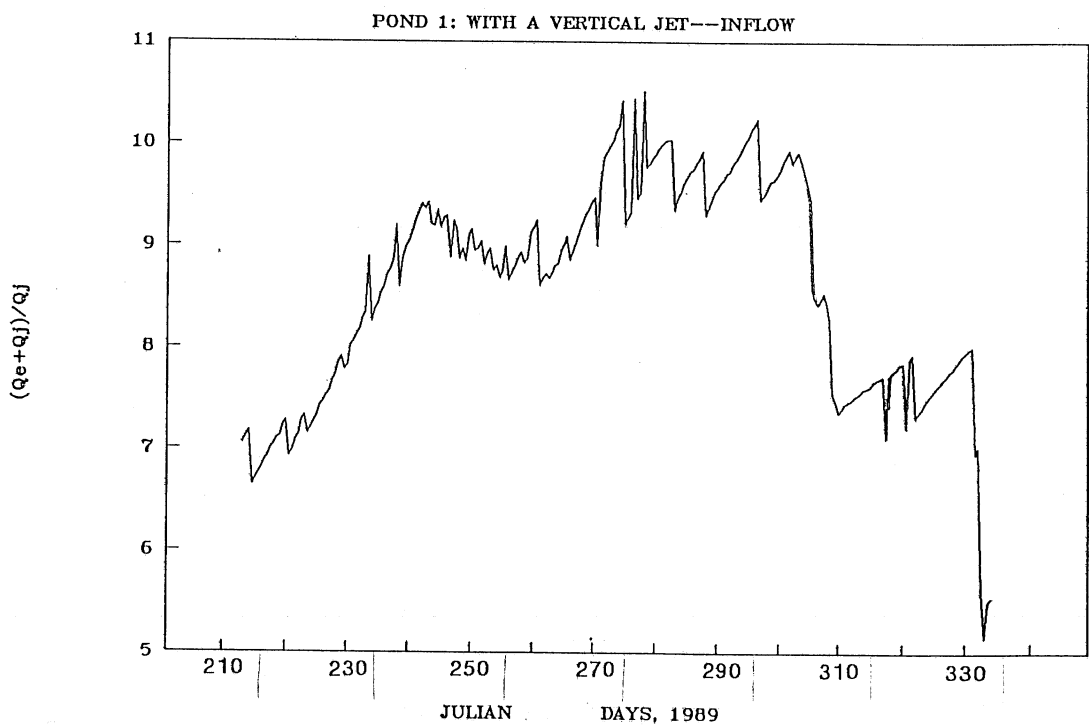


Fig. 37 Calculated flowrate of entrainment by inflow jet in pond 1, 1989

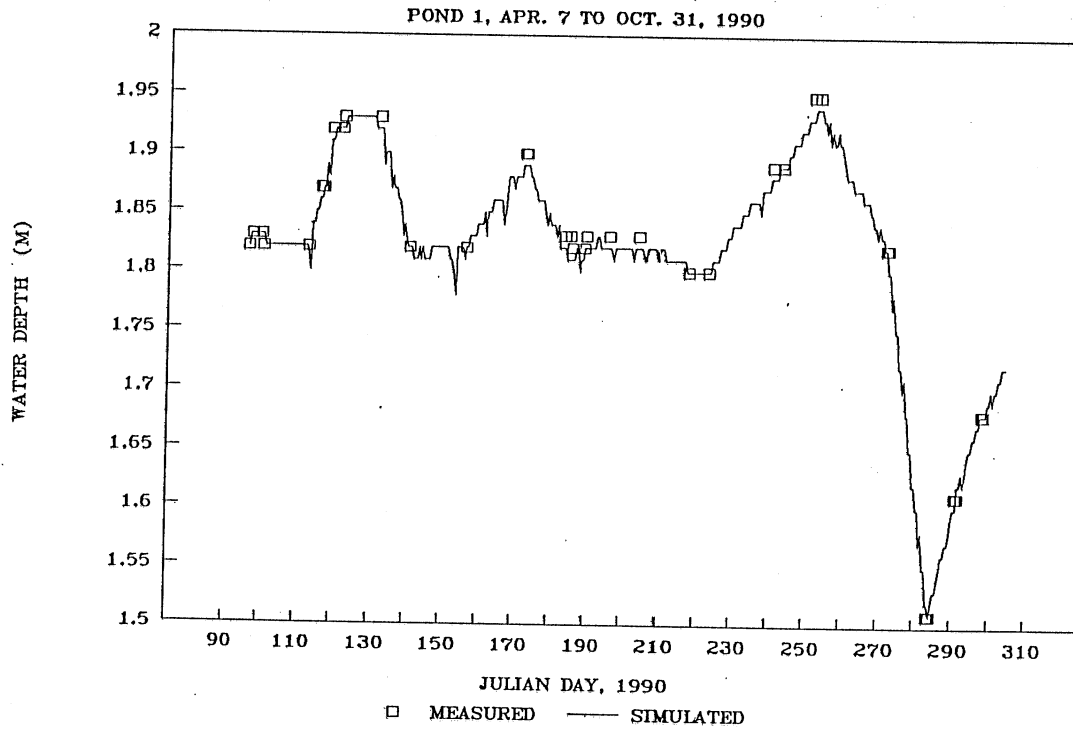


Fig. 38 Measured and calculated water depth, pond 1, April 7–Oct. 31, 1990

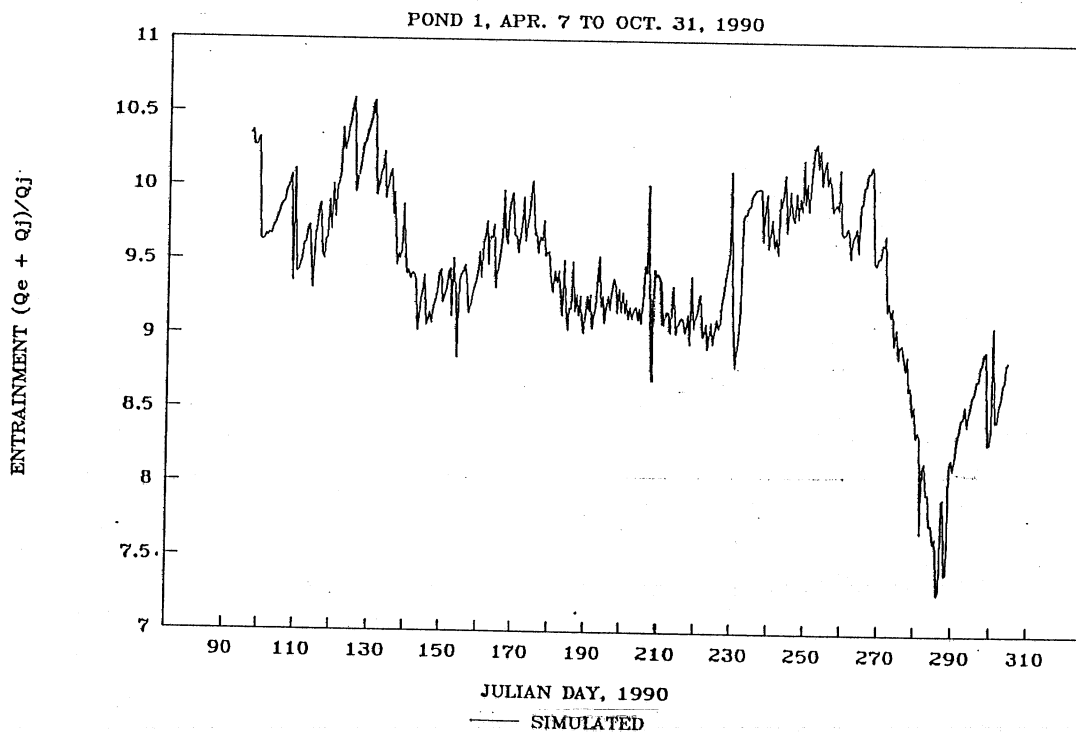


Fig. 39 Calculated flowrate of entrainment by inflow jet in pond 1, 1990

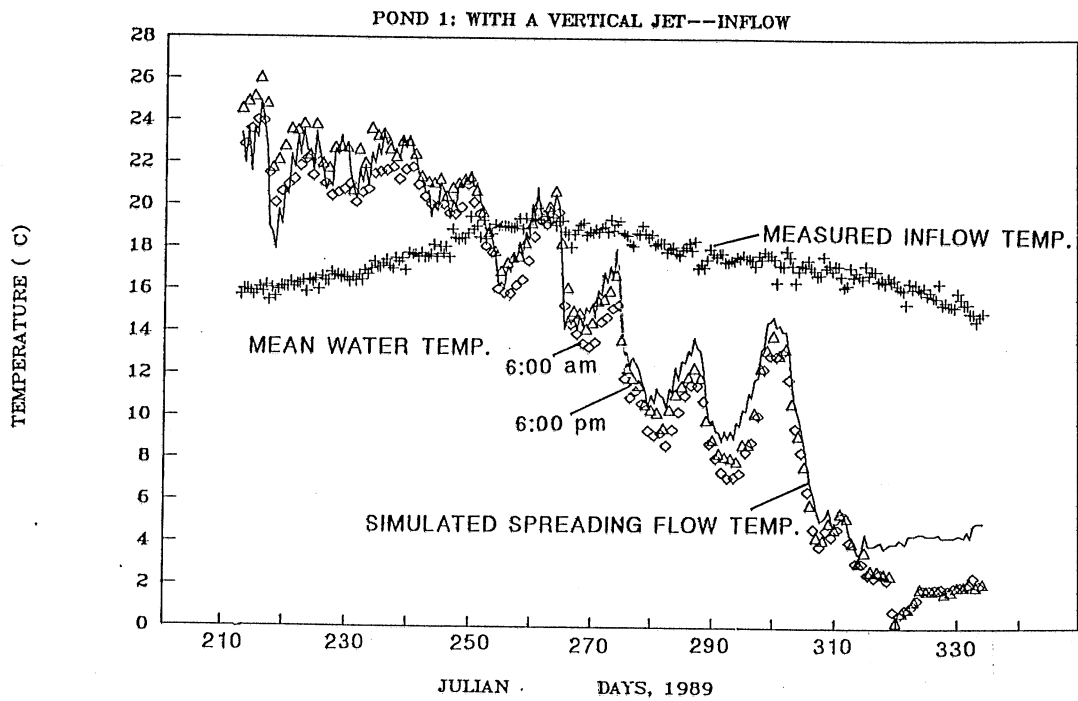


Fig. 40 Measured inflow temperature and simulated spreading flow temperature, pond 1, 1989

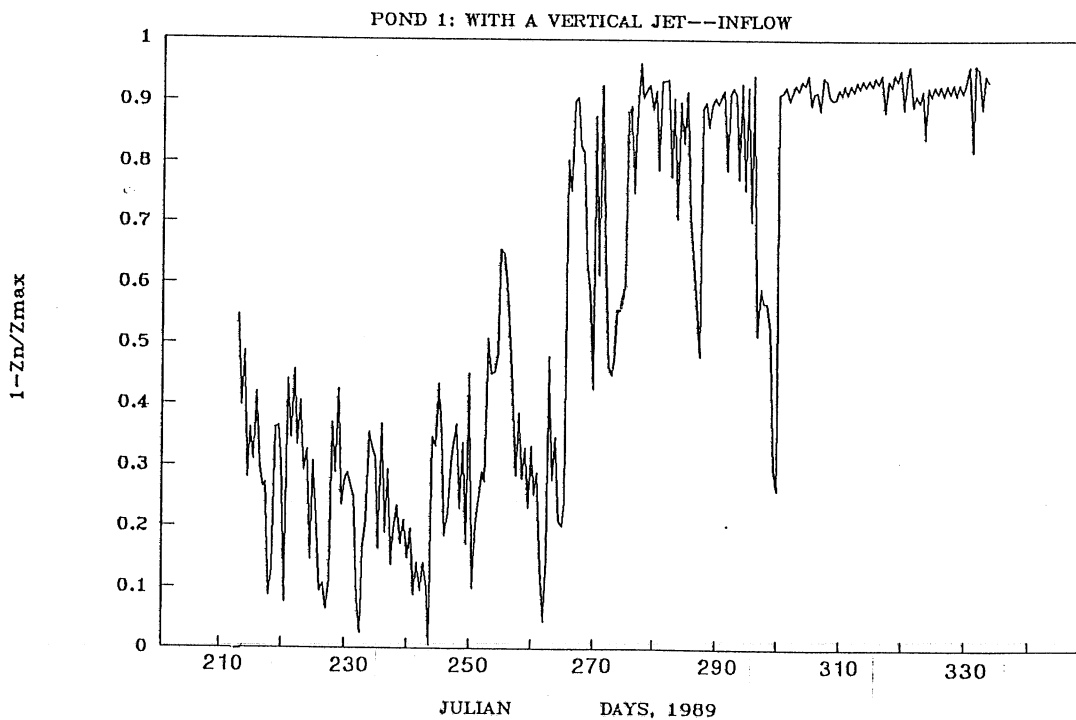


Fig. 41 Calculated depth of intruding interflow (equilibrium layer), pond 1, 1989

is of importance. Figs. 41 and 43 show the locations where the interflow intrudes and spreads, i.e. the equilibrium layer. It can be seen (in Fig. 40 and 42) that the inflow spreads closer to the bottom when the injected water is heavier (colder) than ambient water. The role of vertical jet entrainment and mixing in the temperature stratification simulation of pond 1 can be seen in the comparison of temperature-depth profiles simulated with and without the jet model (see Figs. 44 and 45).

Numerically predicted temperatures in the pond including jet mixing and water transfer are presented in the form of time series and compared to measured temperatures for probes placed at different depths in the pond. Probes #1 to #6 were located at 0.04, 0.20, 0.40, 0.60, 0.80, 1.00 m depth, respectively. Probe #7 is fixed at the pond bottom. Results shown in Figs. 46 to 57 suggested that the computed and measured water temperatures in the pond agree reasonably well. Statistical results from error analysis of field data and modeled water temperatures are given in Table 2. Poorer agreement is achieved with weaker stratification; upper (top) layer temperatures are underestimated and lower (bottom) temperatures overestimated. This may be related to insufficient information on concentration of solids and algae and hence light attenuation in the pond. Pond 1 has high solid concentrations which contribute to high light attenuation resulting in strong stratification. Values of attenuation coefficients are from 3 to 11 ( $\text{m}^{-1}$ ) for pond 1, in contrast within a range of 1.5 to 3.5 ( $\text{m}^{-1}$ ) for pond 3. Better results for pond 3 than pond 1 were obtained in the model calibration and verification. In the numerical prediction, a constant attenuation coefficient for the whole simulation period is used and effects of time variable solids and algae concentrations have not been simulated. An improvement may occur after the model is extended to include chemical and biological components.

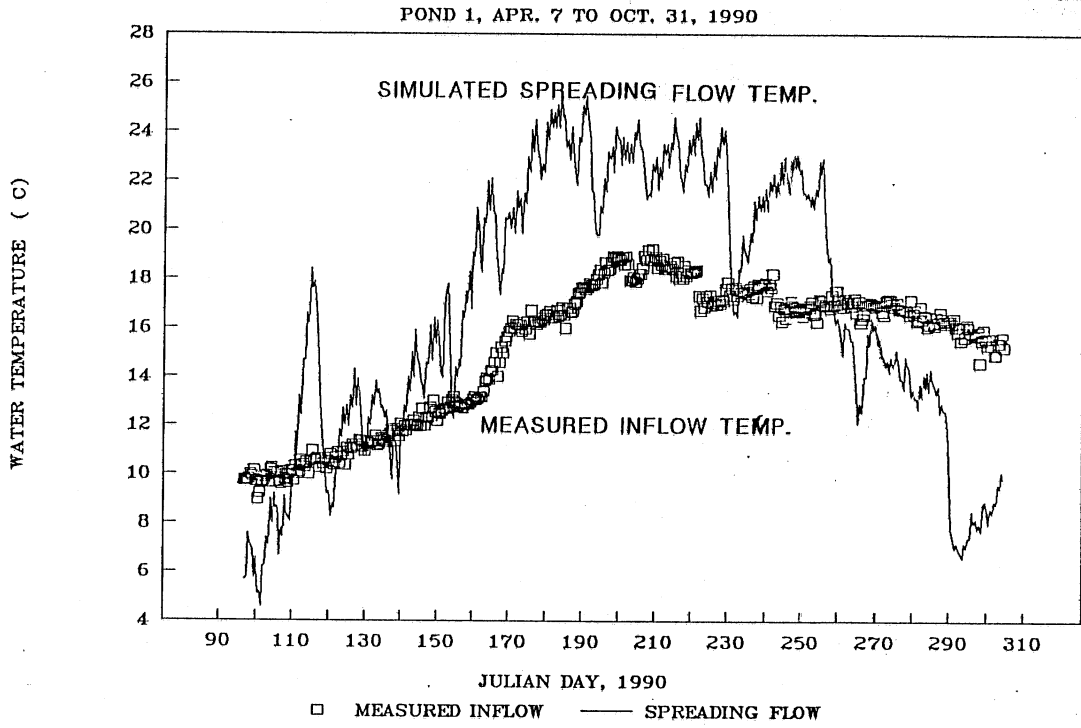


Fig. 42 Measured inflow temperature and simulated spreading flow temperature, pond 1, 1990

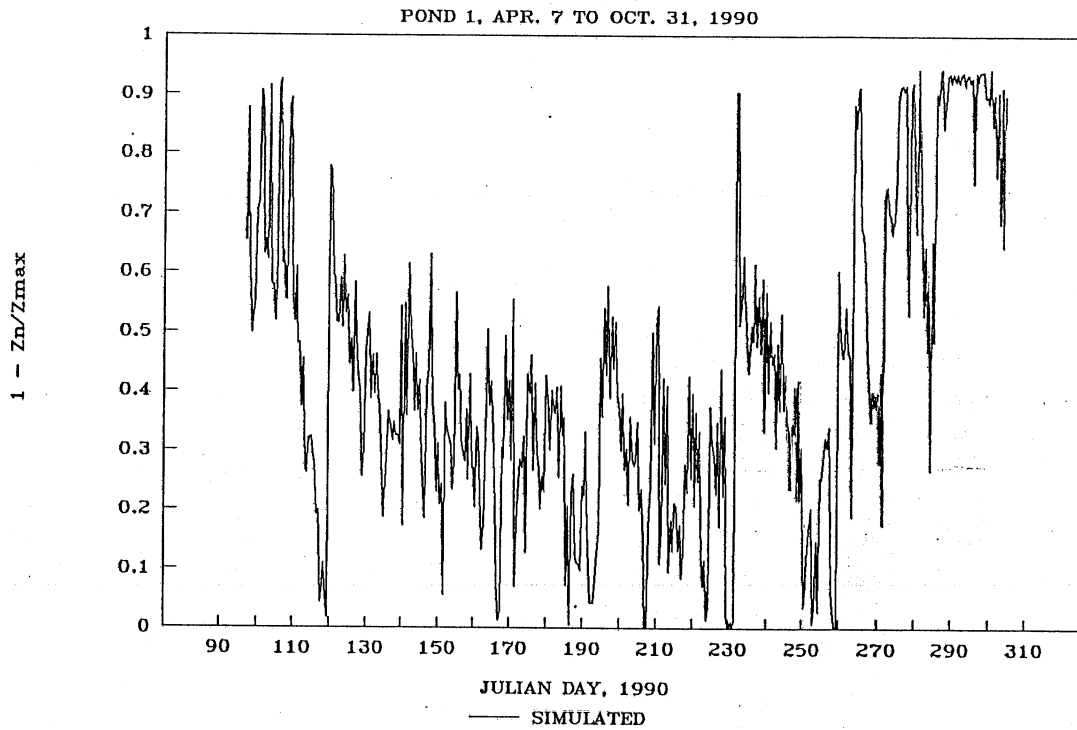


Fig. 43 Calculated depth of intruding interflow (equilibrium layer), pond 1, 1990

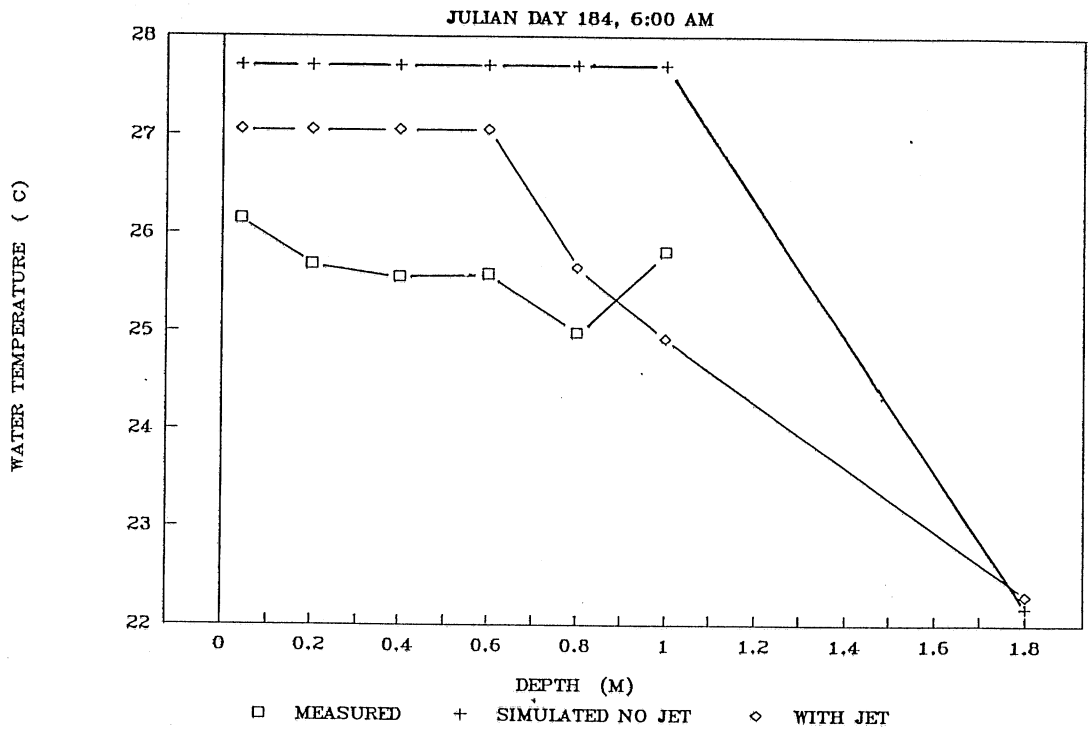


Fig. 44 Comparison of water temperature profiles simulated with jet and without jet, pond 1, 6:00 pm, July 3, 1990

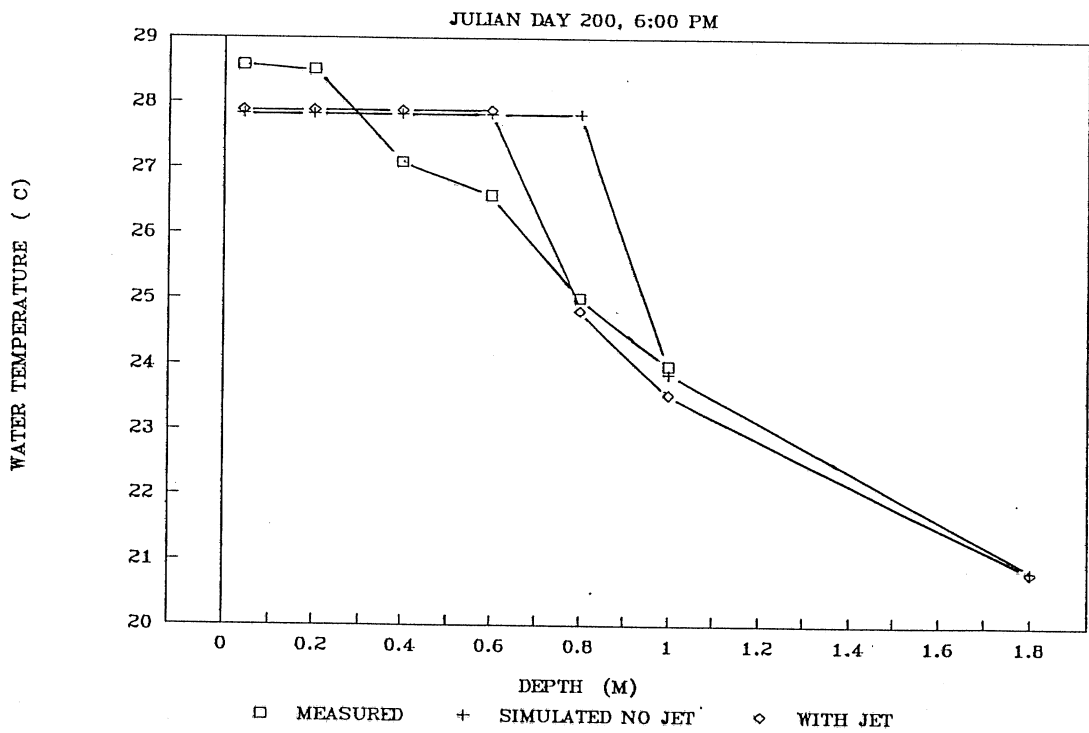


Fig. 45 Comparison of temperature-depth profiles simulated with jet and without jet, pond 1, 6:00 pm, Aug. 29, 1990



# TEMPERATURE STRATIFICATION SIMULATION

HARRIS POND #1, 1989: PROBE #1, SURFACE

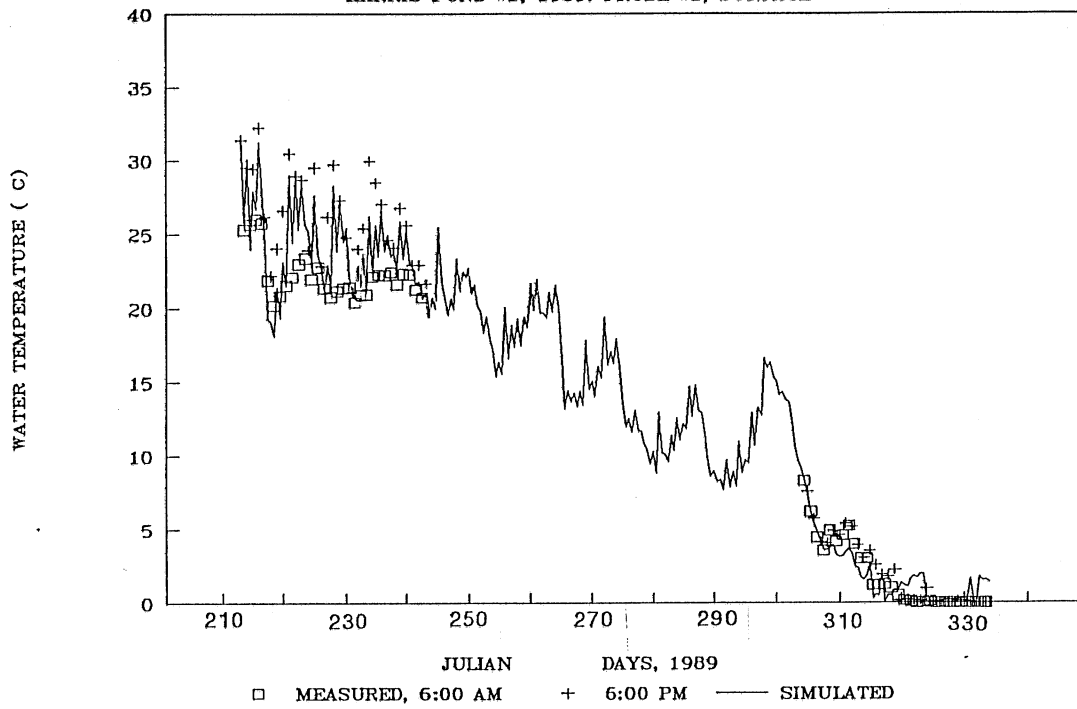
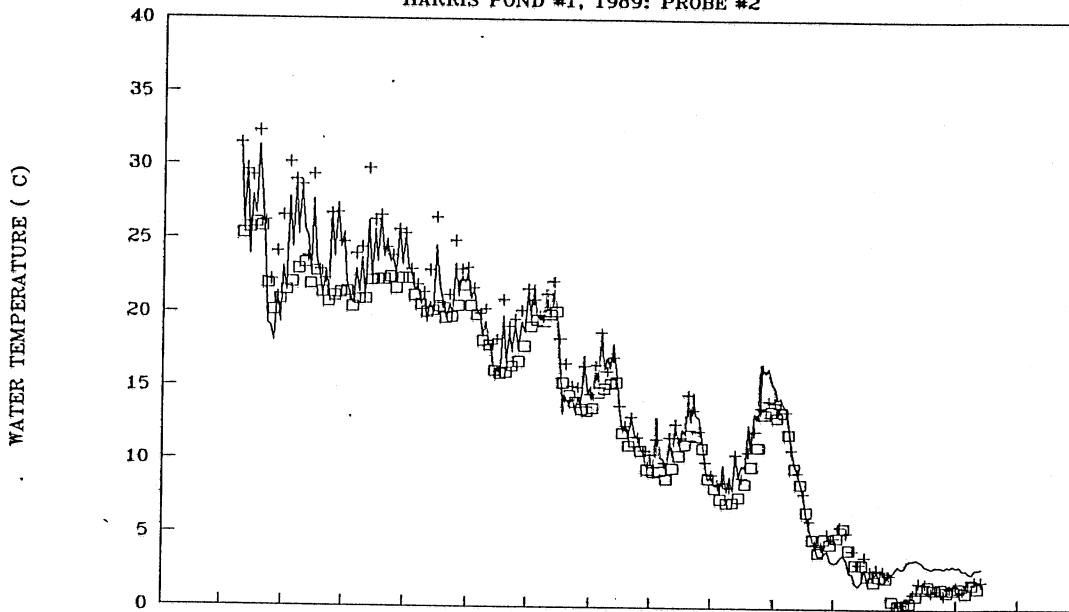


Fig. 46 Measured and simulated water temperatures in pond 1, 1989 timestep = 12 hours, probe #1

# TEMPERATURE STRATIFICATION SIMULATION

HARRIS POND #1, 1989: PROBE #2

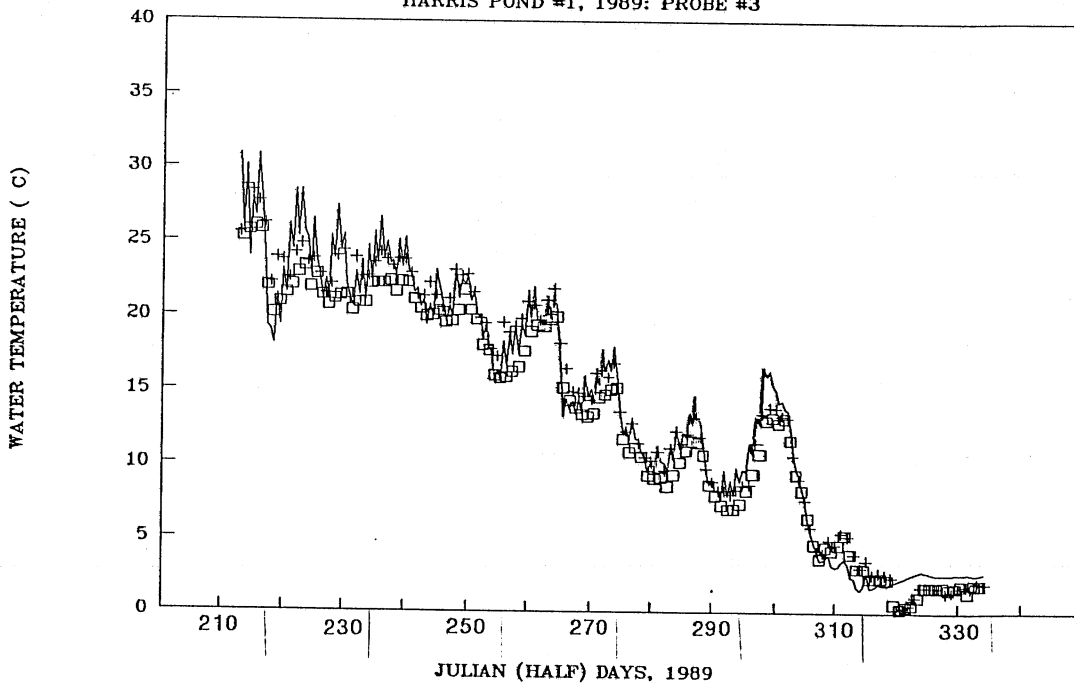


□ MEASURED, 6:00 AM + 6:00 PM — SIMULATED

Fig. 47 Measured and simulated water temperatures in pond 1, 1989 timestep = 12 hours, probe #2

# TEMPERATURE STRATIFICATION SIMULATION

HARRIS POND #1, 1989: PROBE #3

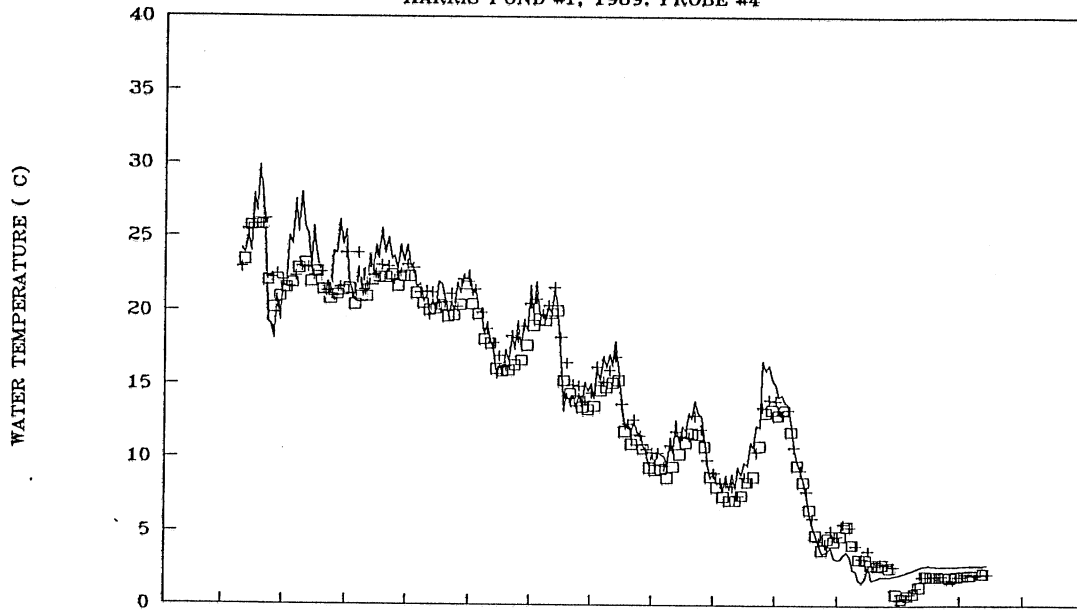


□ MEASURED, 6:00 AM + 6:00 PM — SIMULATED

Fig. 48 Measured and simulated water temperatures in pond 1, 1989 timestep = 12 hours, probe #3

# TEMPERATURE STRATIFICATION SIMULATION

HARRIS POND #1, 1989; PROBE #4

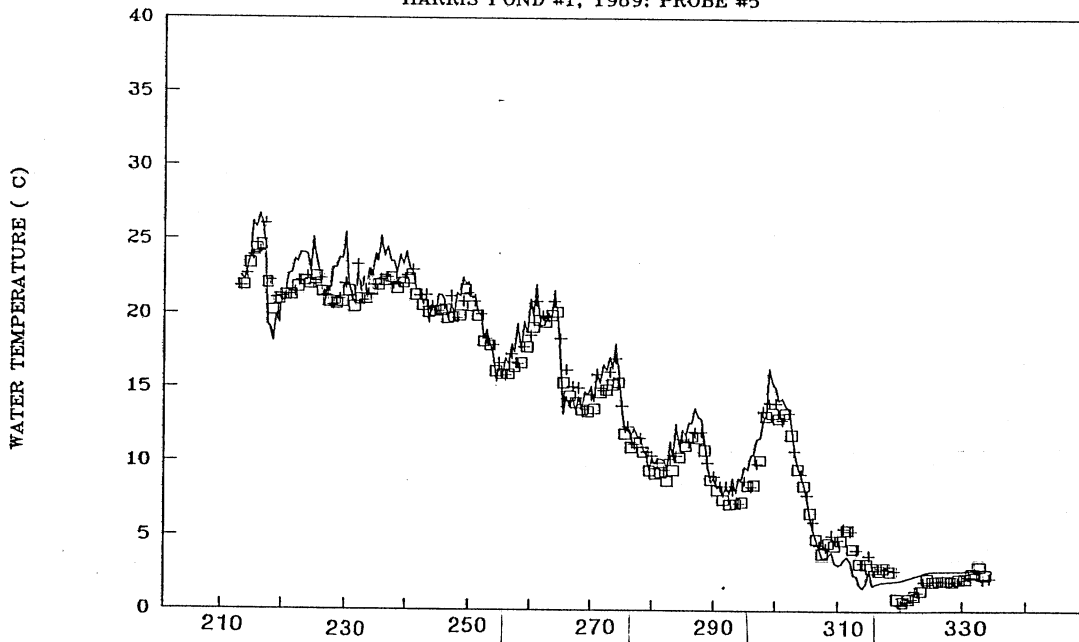


□ MEASURED, 6:00 AM + 6:00 PM — SIMULATED

Fig. 49 Measured and simulated water temperatures in pond 1, 1989 timestep = 12 hours, probe #4

# TEMPERATURE STRATIFICATION SIMULATION

HARRIS POND #1, 1989; PROBE #5



□ MEASURED, 6:00 AM + 6:00 PM — SIMULATED

Fig. 50 Measured and simulated water temperatures in pond 1, 1989 timestep = 12 hours, probe #5

# TEMPERATURE STRATIFICATION SIMULATION

HARRIS POND #1, 1989: PROBE #6

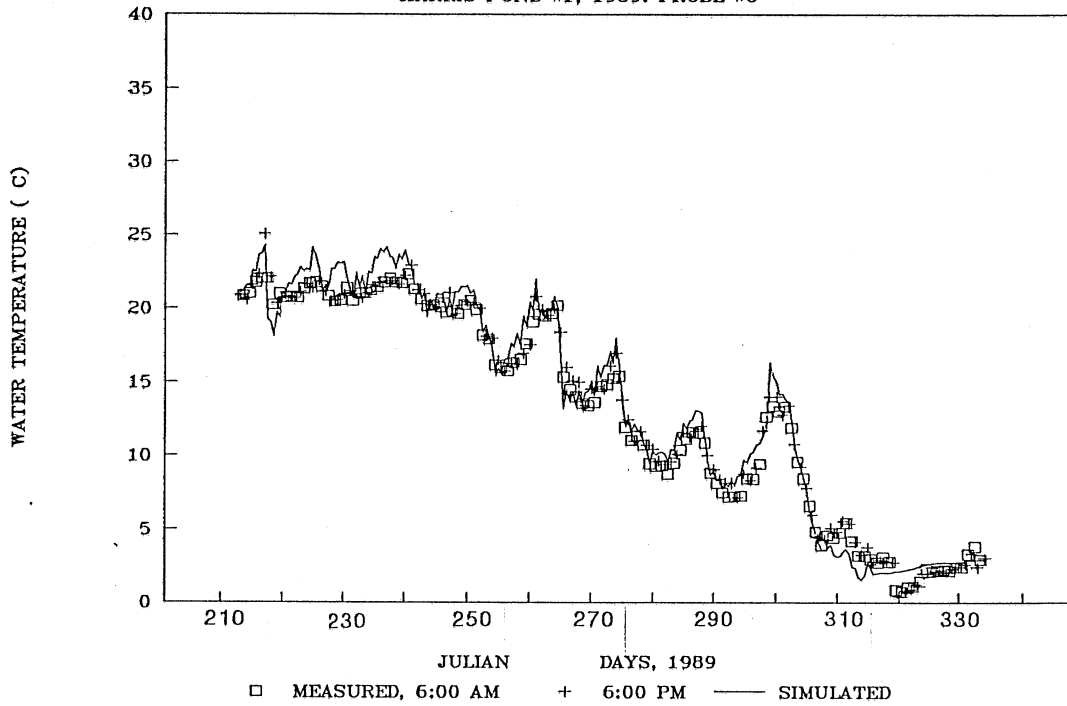


Fig. 51 Measured and simulated water temperatures in pond 1, 1989 timestep = 12 hours, probe #6

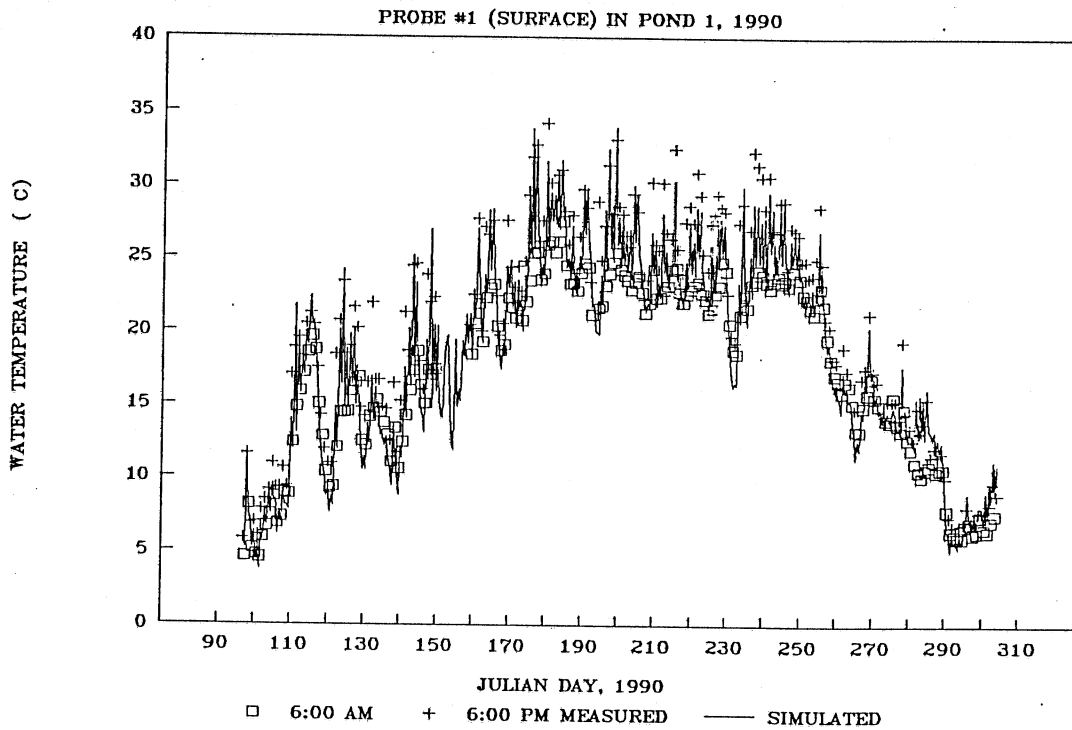


Fig. 52 Measured and simulated water temperatures in pond 1, 1990 timestep = 12 hours, probe #1

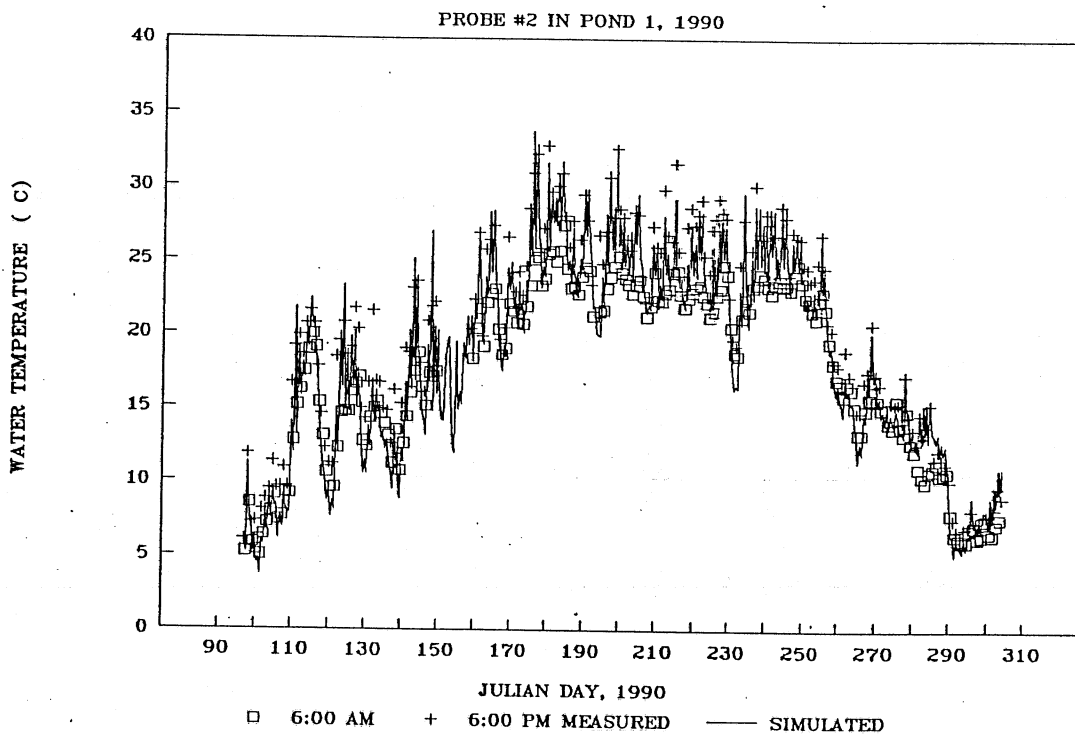


Fig. 53 Measured and simulated water temperatures in pond 1, 1990 timestep = 12 hours, probe #2

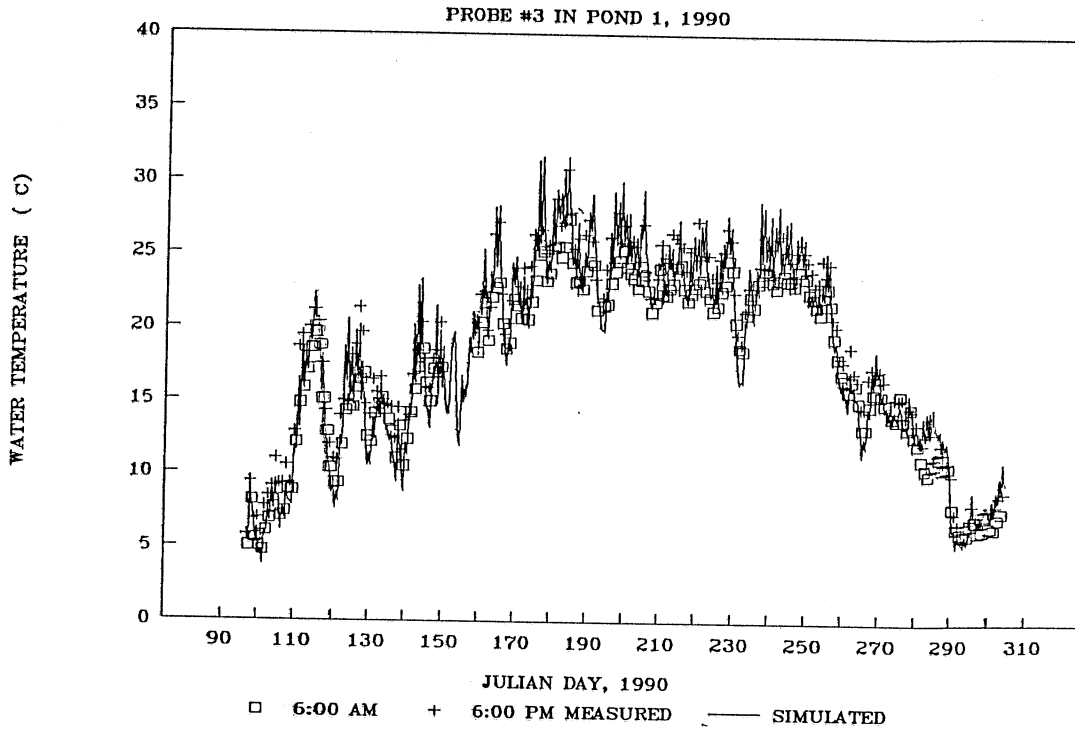


Fig. 54 Measured and simulated water temperatures in pond 1, 1990 timestep = 12 hours, probe #3

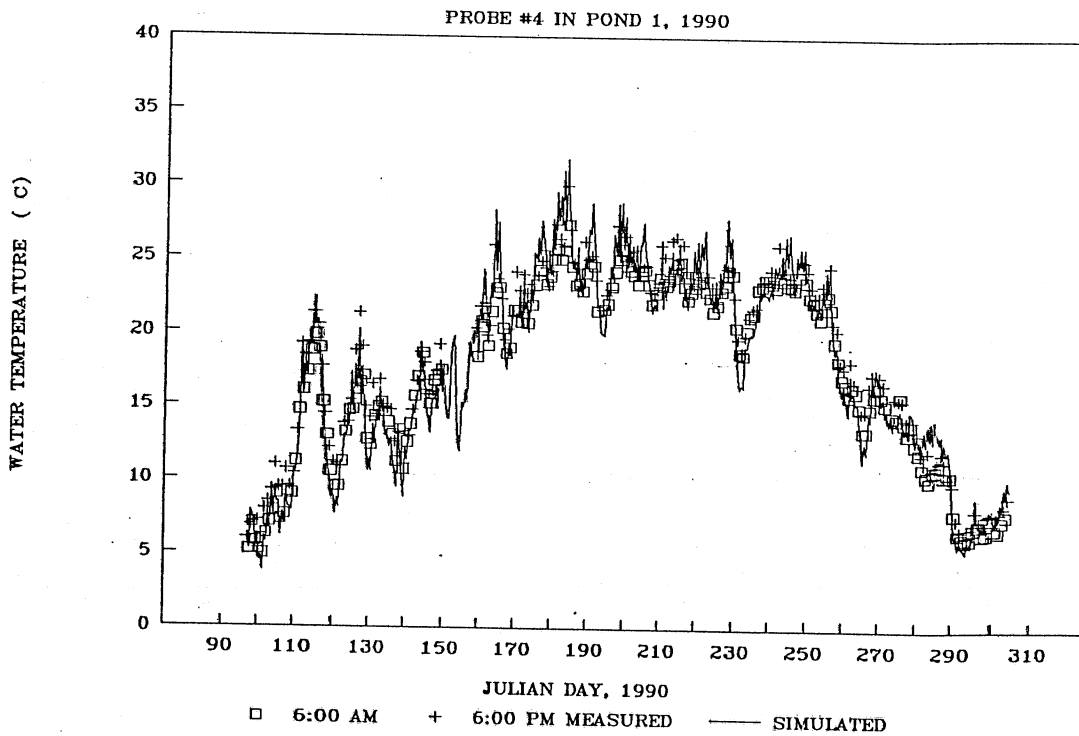


Fig. 55 Measured and simulated water temperatures in pond 1, 1990 timestep = 12 hours, probe #4

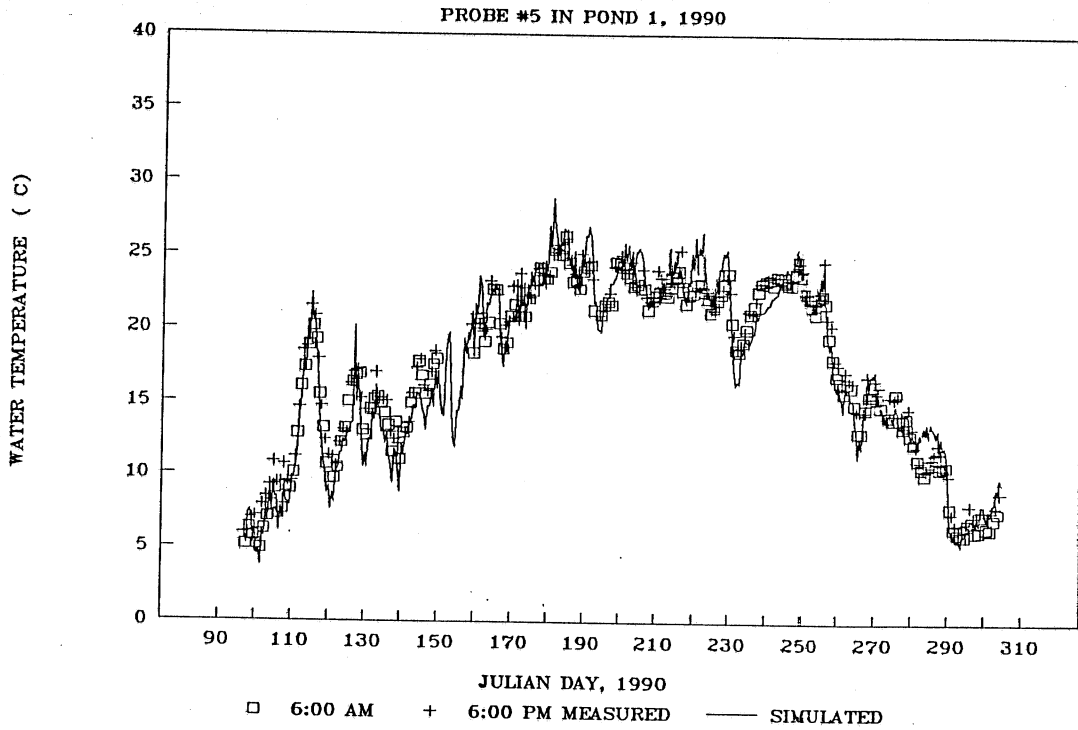


Fig. 56 Measured and simulated water temperatures in pond 1, 1990 timestep = 12 hours, probe #5

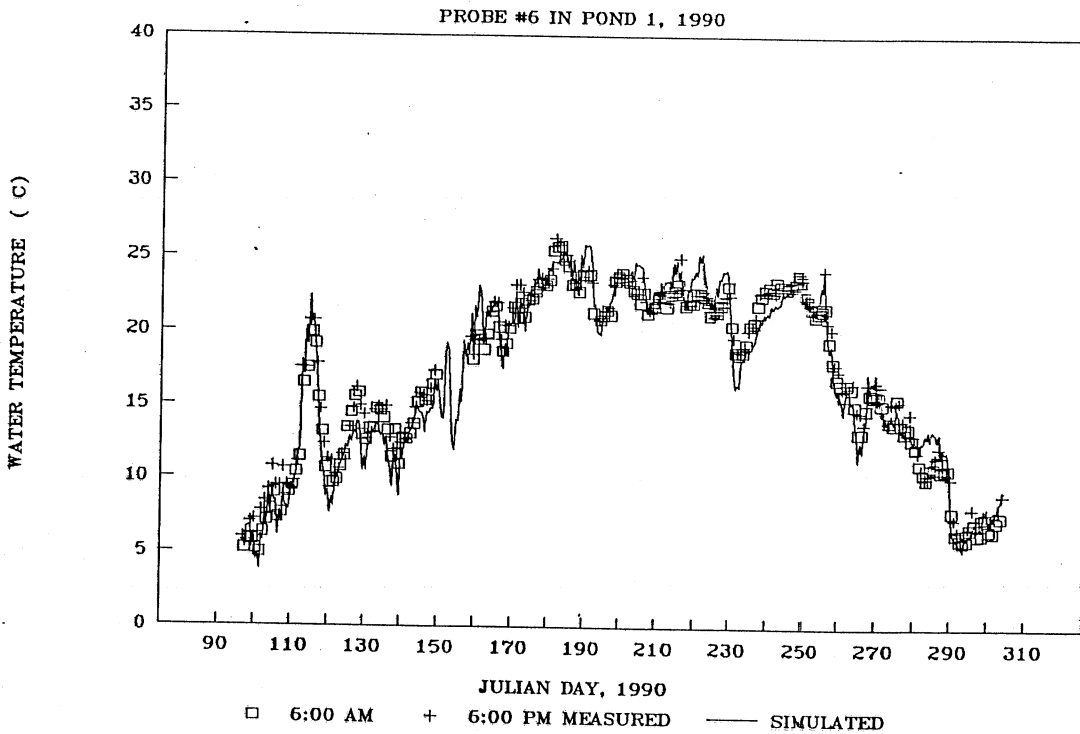


Fig. 57 Measured and simulated water temperatures in pond 1, 1990 timestep = 12 hours, probe #6

## 5. Evaluation of Stratification and Mixing Dynamics

Pond water temperatures measured with six probes distributed from the water surface to the pond bottom were presented by Luck and Stefan (1990) in the form of temperature versus time (days). Luck and Stefan (1990) also plotted the composite weather and pond water temperature profiles which showed the stratification dynamics. It can be seen that solar radiation causes daytime heating of the surface layers and contributes mainly to the stratification in the pond. A completely or partially mixed state is brought about by nighttime cooling. Air temperature also is a factor affecting heat exchange through the surface and pond temperatures. More mixing occurs during periods of stronger winds.

The simulated pond water temperatures are shown in Figs. 58 through 78 in the same form as the field data (Luck and Stefan, 1990), but only the surface, mid-depth and bottom temperatures are presented. This is enough to illustrate the stratification and mixing of a pond. Based on the thermal structure of the ponds over months as described by the variation of temperature distributions with time, the ponds can be characterized by three types of stratification processes: I) completely mixed during consecutive day and night, II) stratified during the day and mixed during the night and III) continuously stratified during several days and nights.

A classification based on these measured and simulated processes of stratification and mixing dynamics is listed in Table 3. The number of days for which each type of stratification and/or mixing was observed or simulated is given in Table 3. Each type of stratification may appear several times in a month. The total number of days for each of type stratification, measured (m) and simulated (s), are compared for an overall evaluation of simulations of dynamic stratification processes (Table 3).

An error is defined as the number of days in a year for each type of measured stratification process minus the simulated one. The relative error is the normalized absolute error with respect to field measurements. As listed in Table 3, the maximum absolute error is nine days and the minimum error is 0. The relative error reaches its maximum at 63% and minimum at 0%. The relative errors for type I, II and III, respectively, are averaged for pond 1 and pond 3, 1989 and 1990.

The numerical model simulated the mixing process during days and nights (type I) well and with only 2% underprediction. The process of day stratification and night mixing (type II) was simulated with an error of 17% (underprediction). The model overpredicted the process of stratification during days and nights with -25% error. This result may be improved by reexamining the effects of wind and night cooling on mixing.



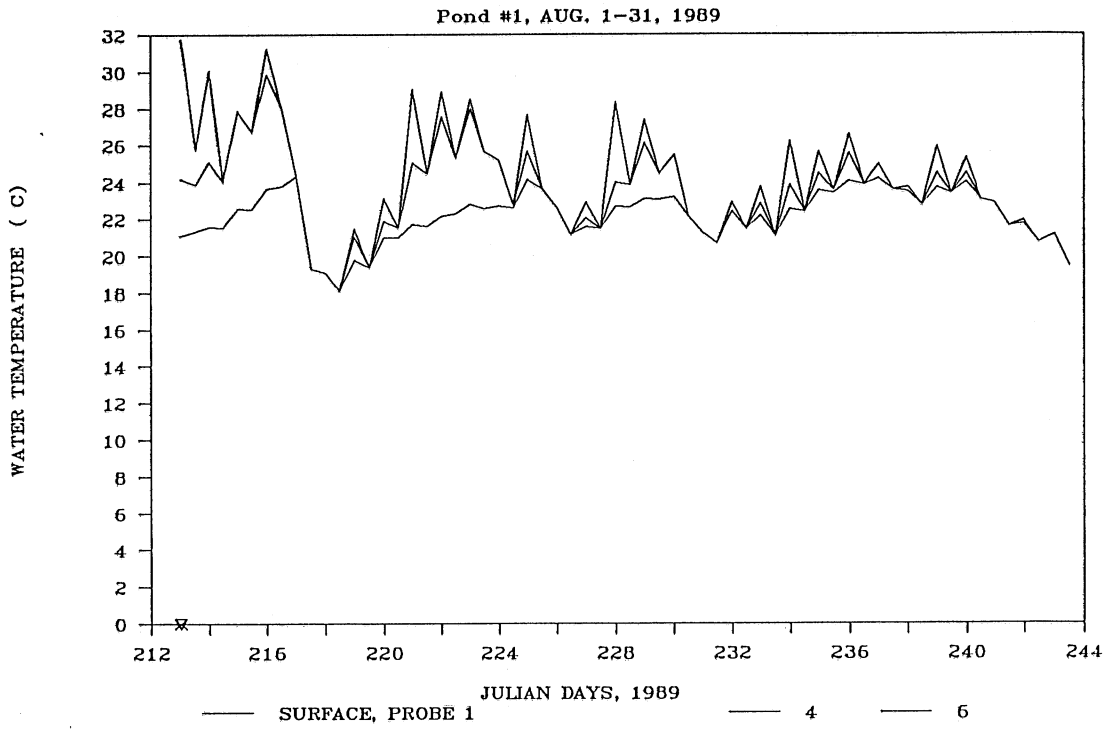


Fig. 58 Simulated water temperatures, pond 1, August, 1989

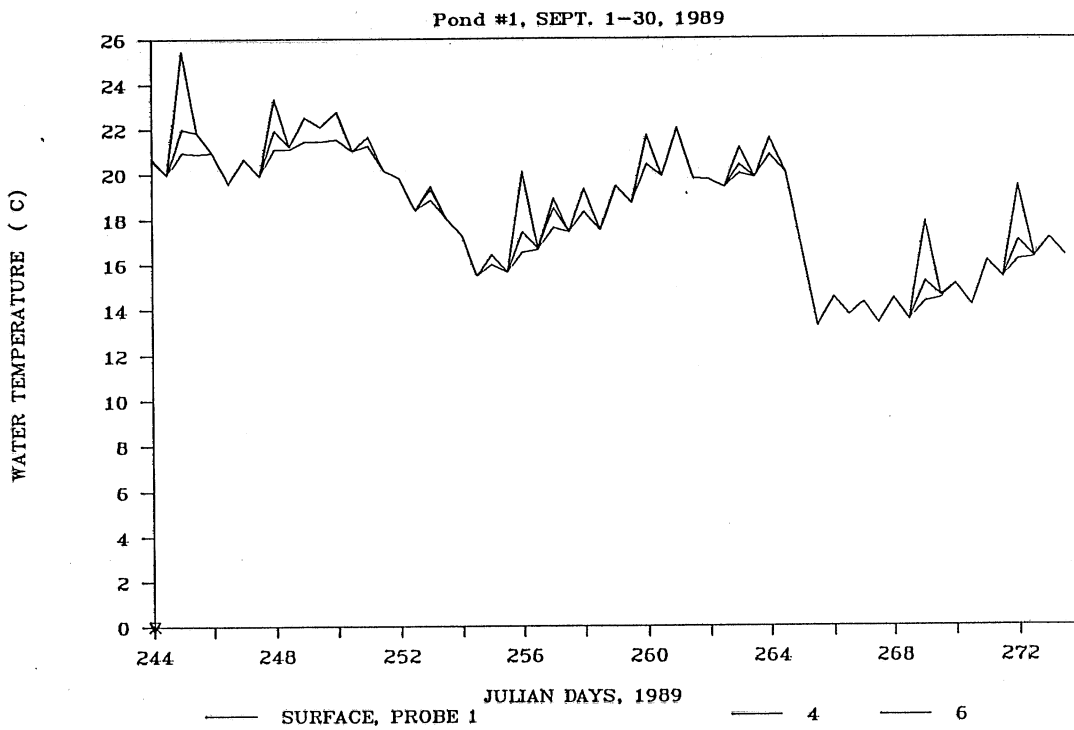


Fig. 59 Simulated water temperatures, pond 1, September, 1989

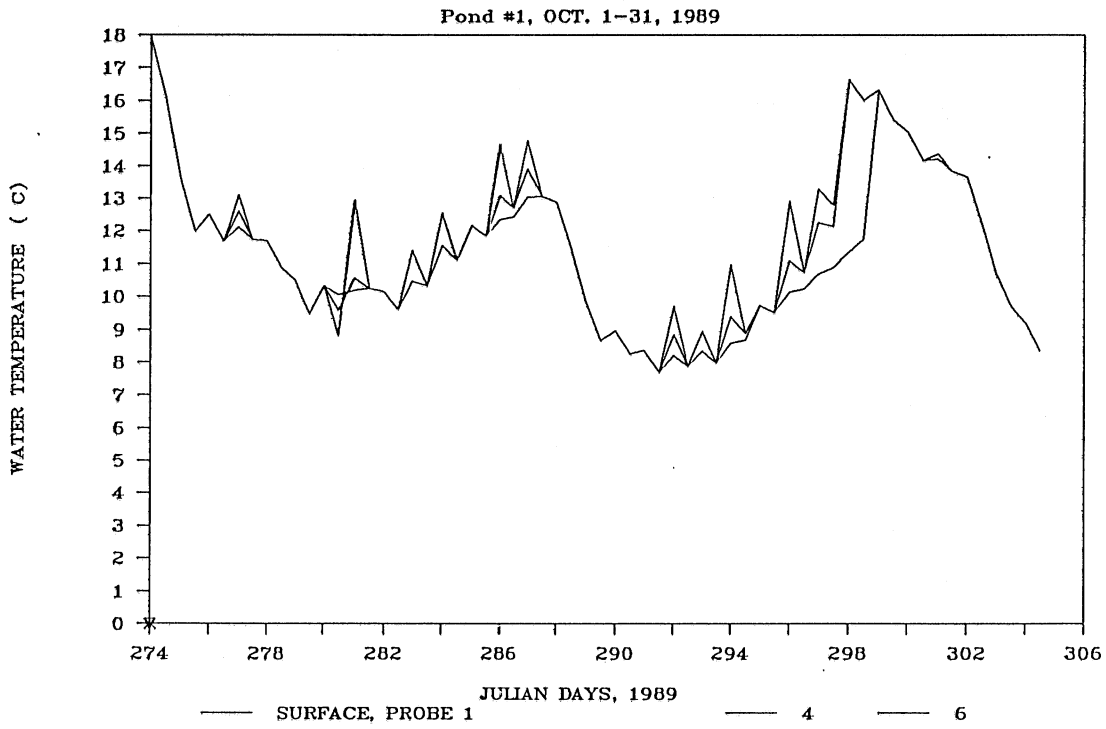


Fig. 60 Simulated water temperatures, pond 1, October, 1989

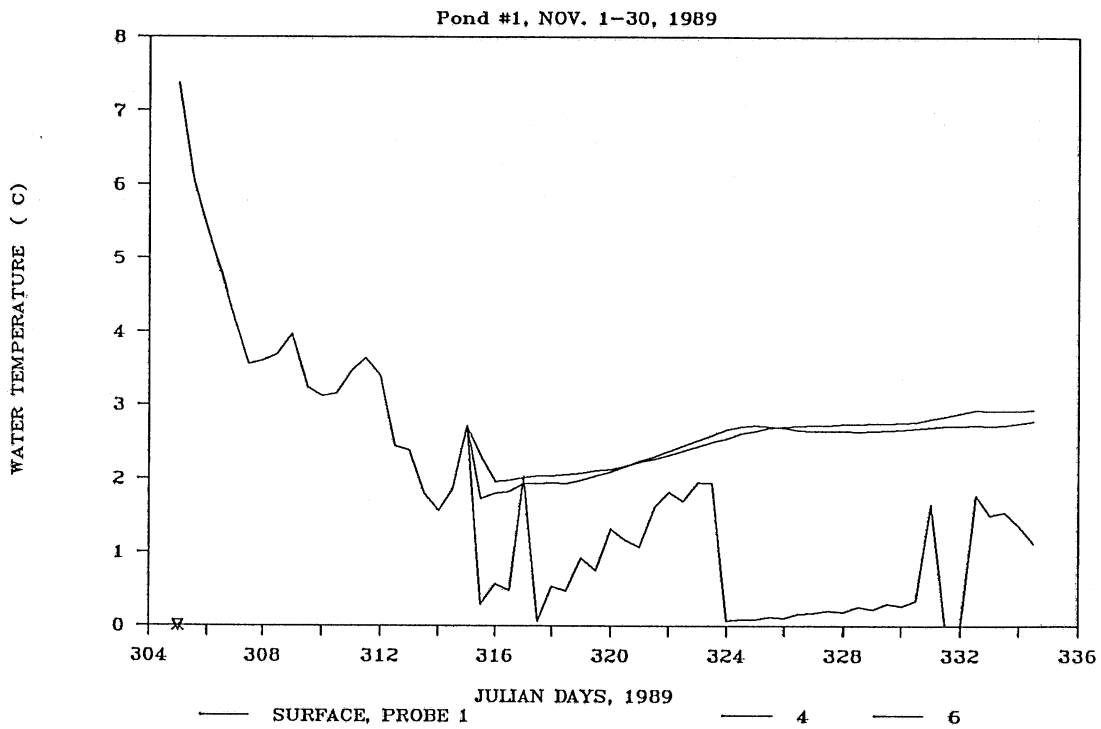


Fig. 61 Simulated water temperatures, pond 1, November, 1989

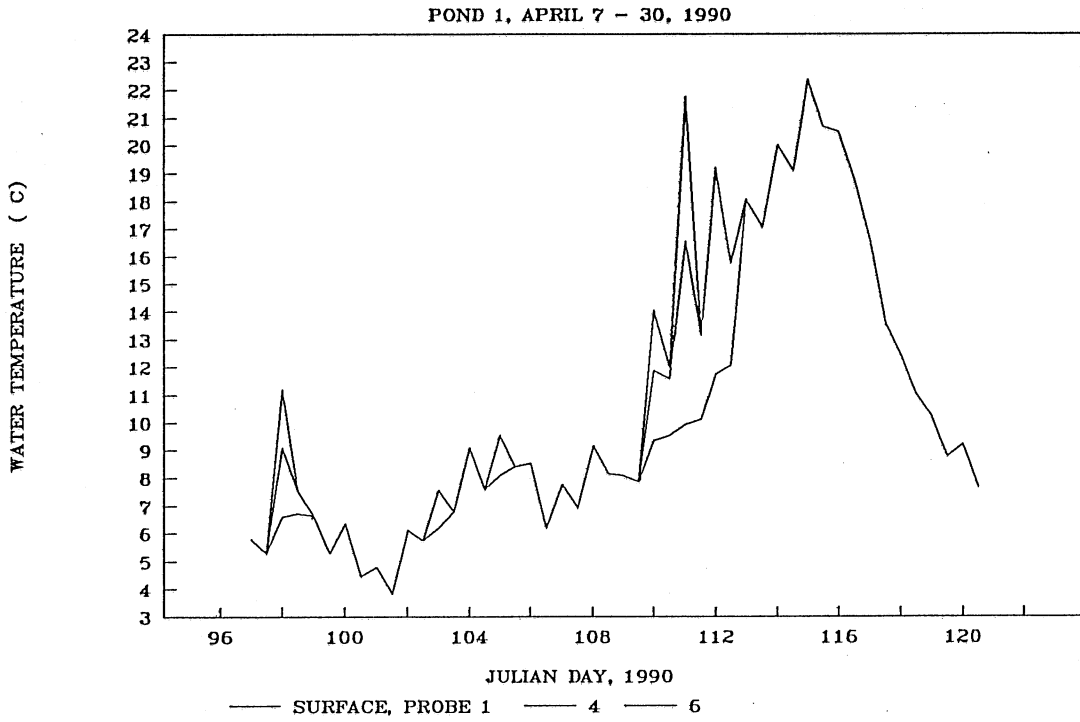


Fig. 62 Simulated water temperatures, pond 1, April, 1990

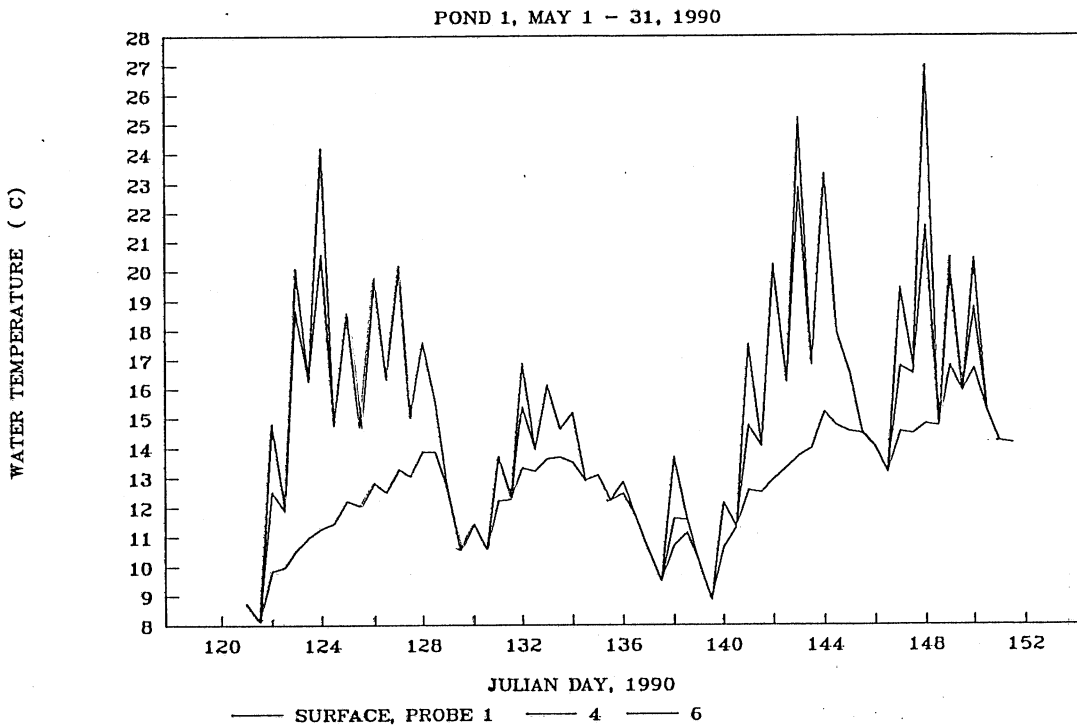


Fig. 63 Simulated water temperatures, pond 1, May, 1990

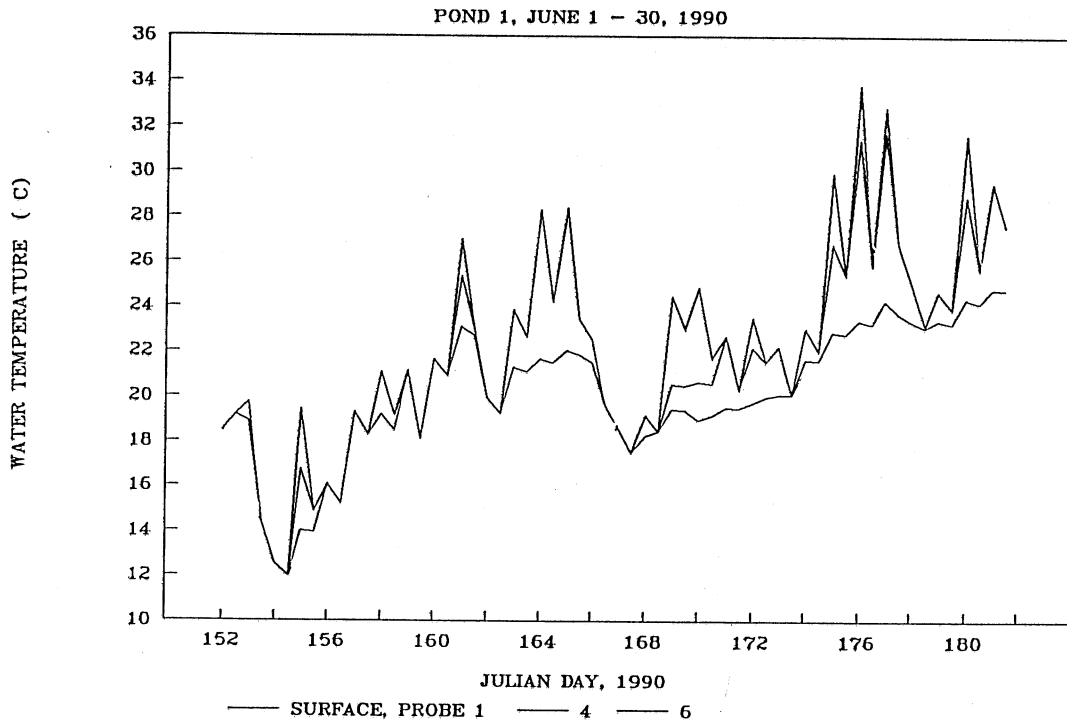


Fig. 64 Simulated water temperatures, pond 1, June, 1990

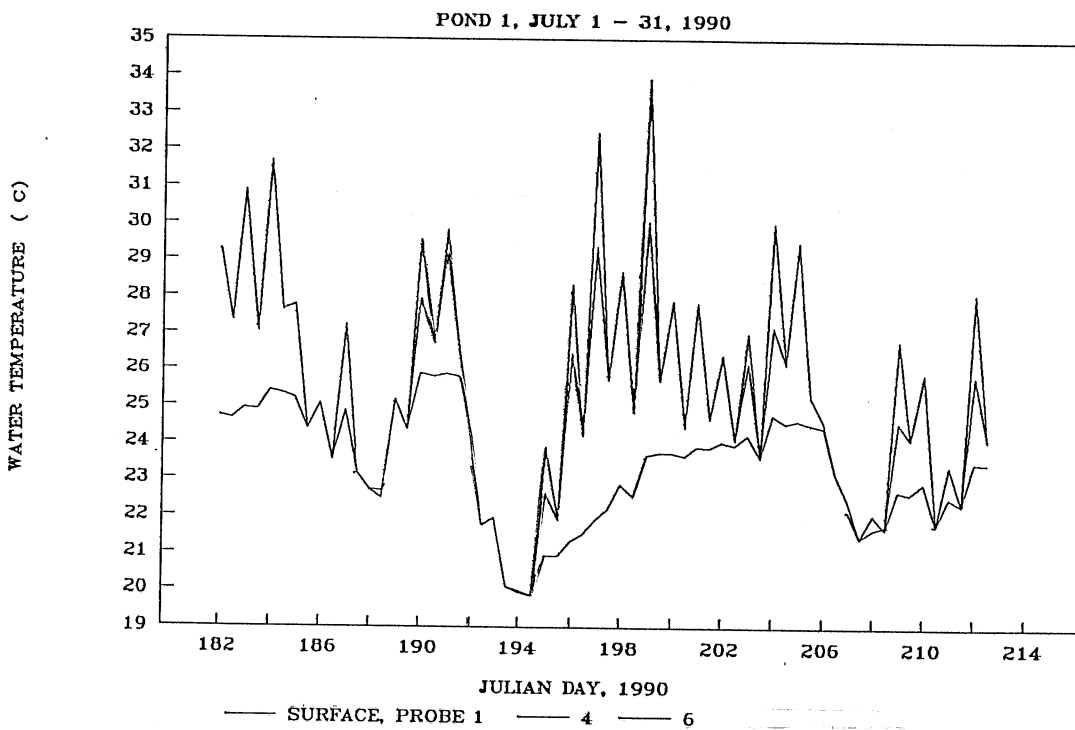


Fig. 65 Simulated water temperatures, pond 1, July, 1990

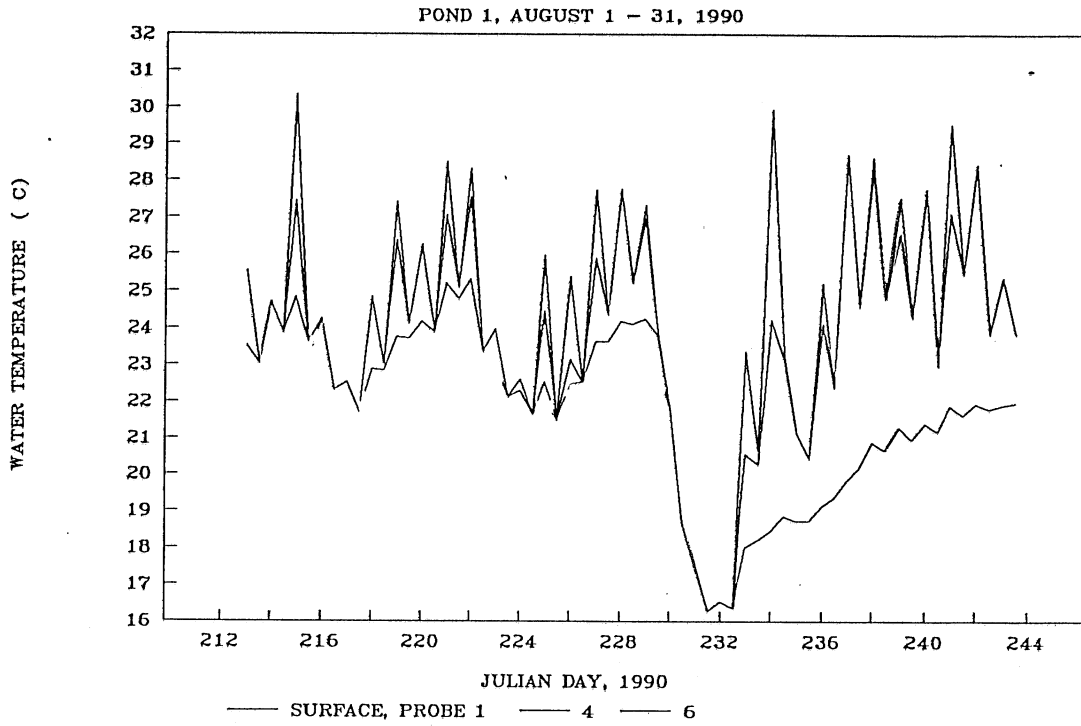


Fig. 66 Simulated water temperatures, pond 1, August, 1990

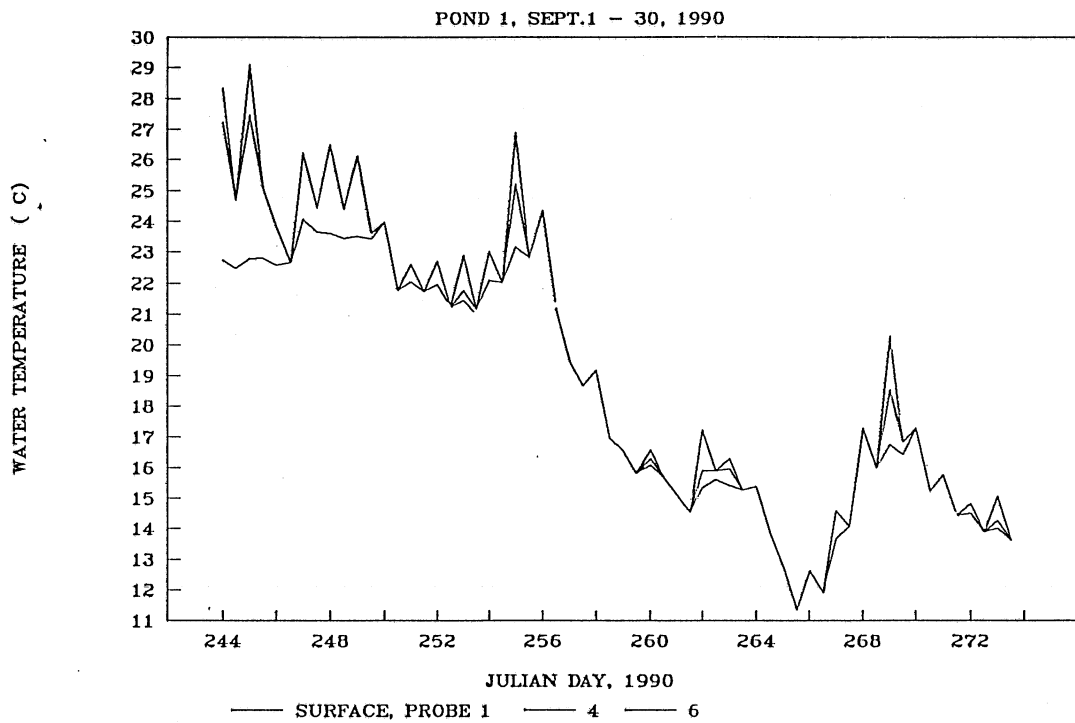


Fig. 67 Simulated water temperatures, pond 1, September, 1990

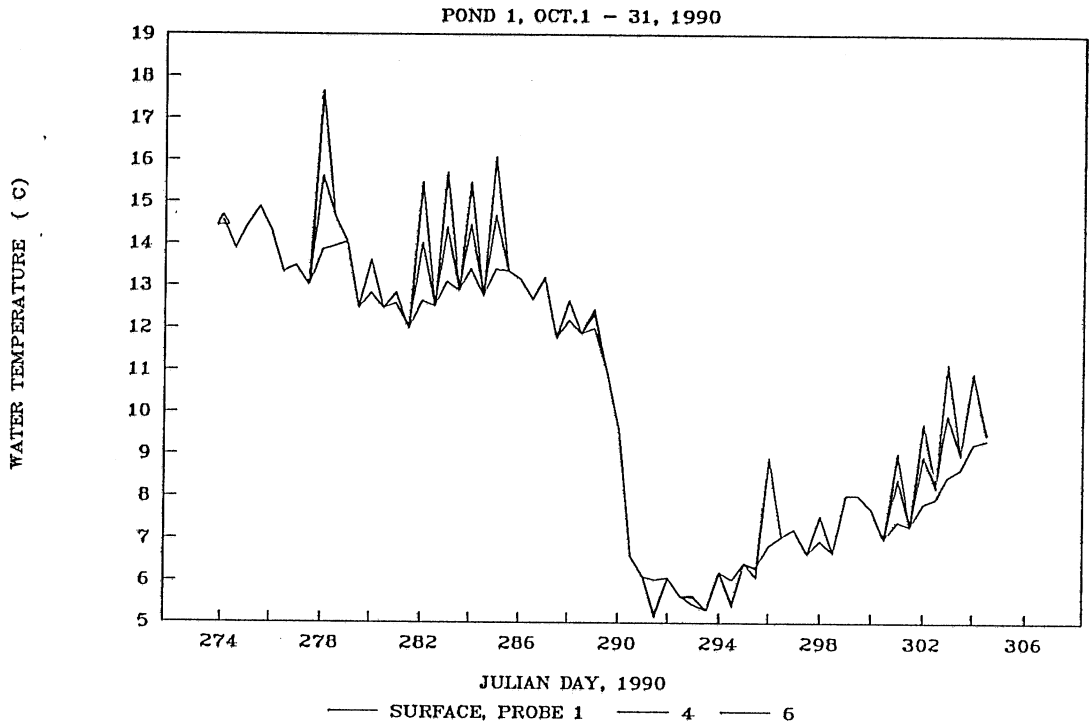


Fig. 68 Simulated water temperatures, pond 1, October, 1990

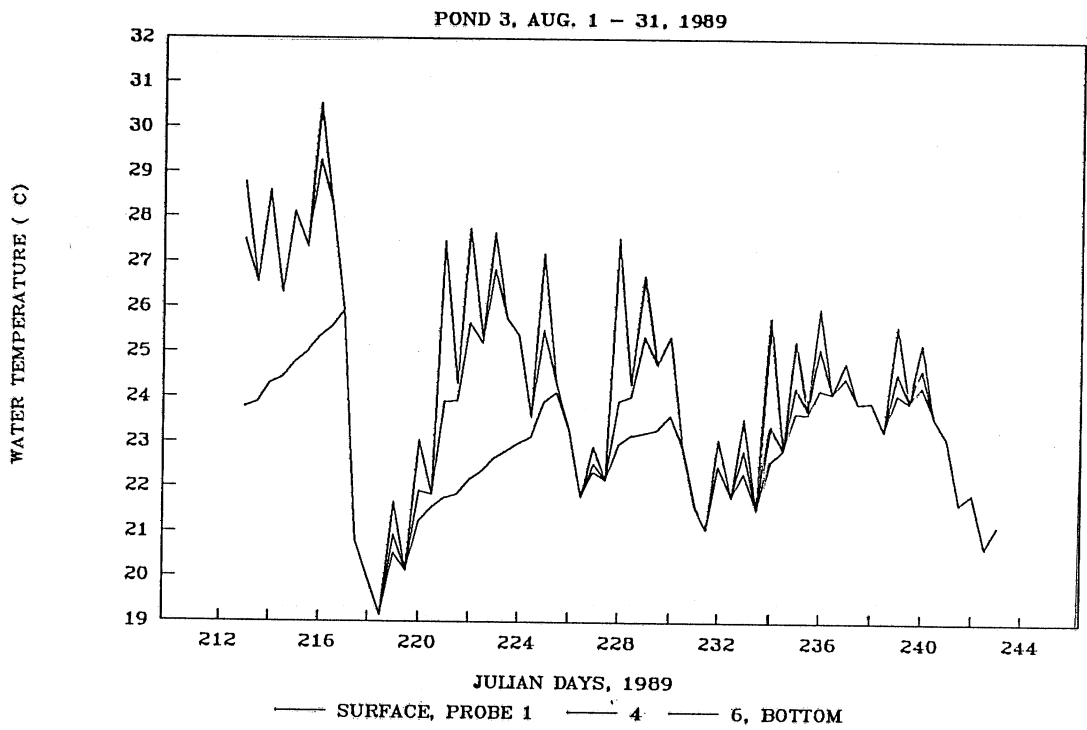


Fig. 69 Simulated water temperatures, pond 3, August, 1989

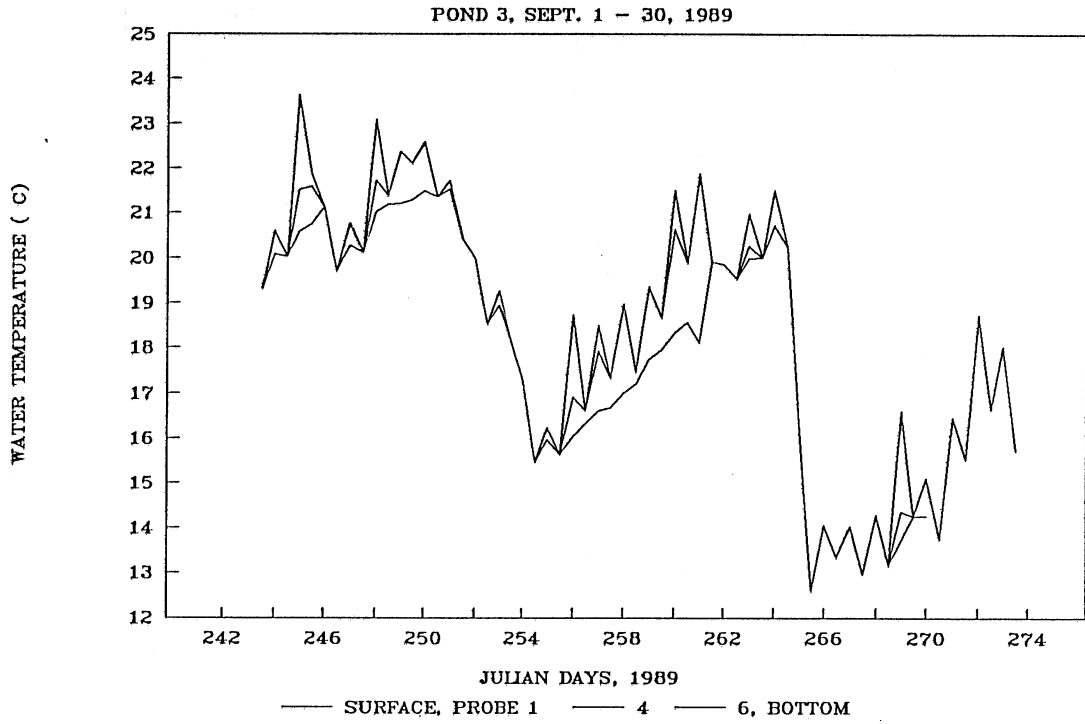


Fig. 70 Simulated water temperatures, pond 3, September, 1989

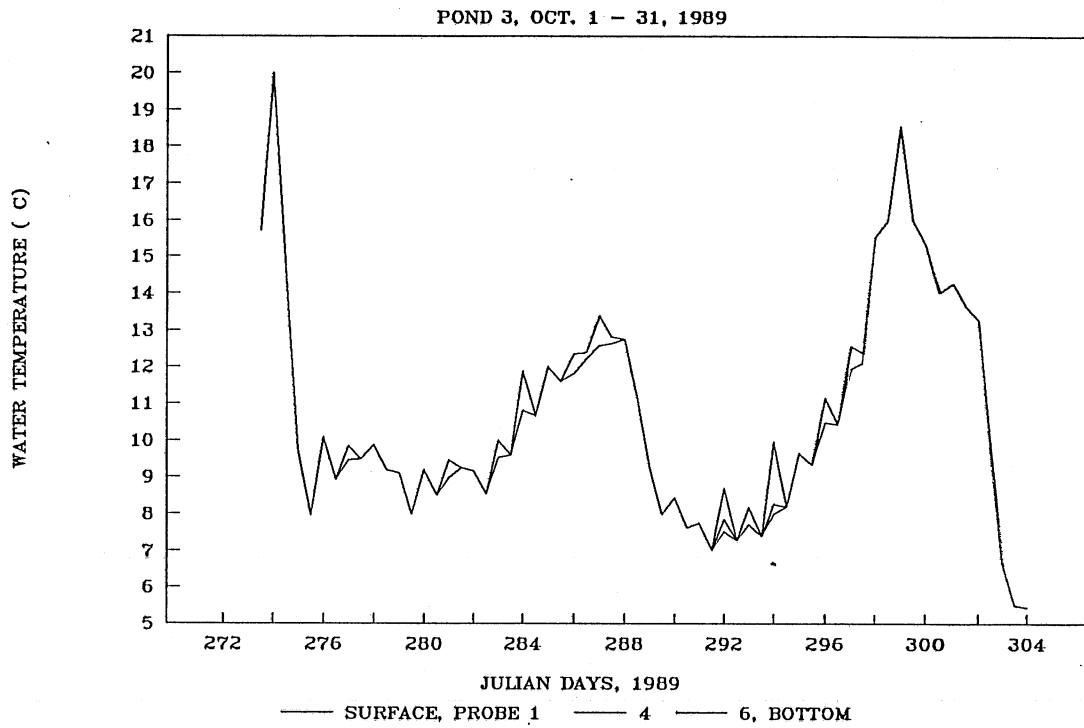


Fig. 71 Simulated water temperatures, pond 3, October, 1989

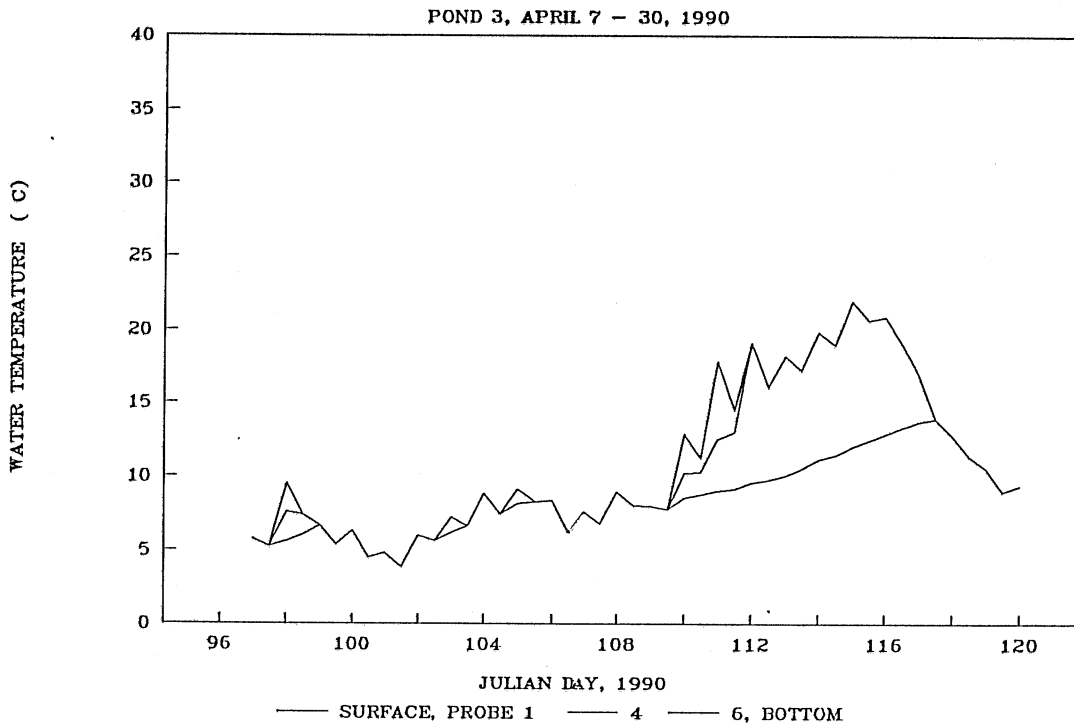


Fig. 72 Simulated water temperatures, pond 3, April, 1990

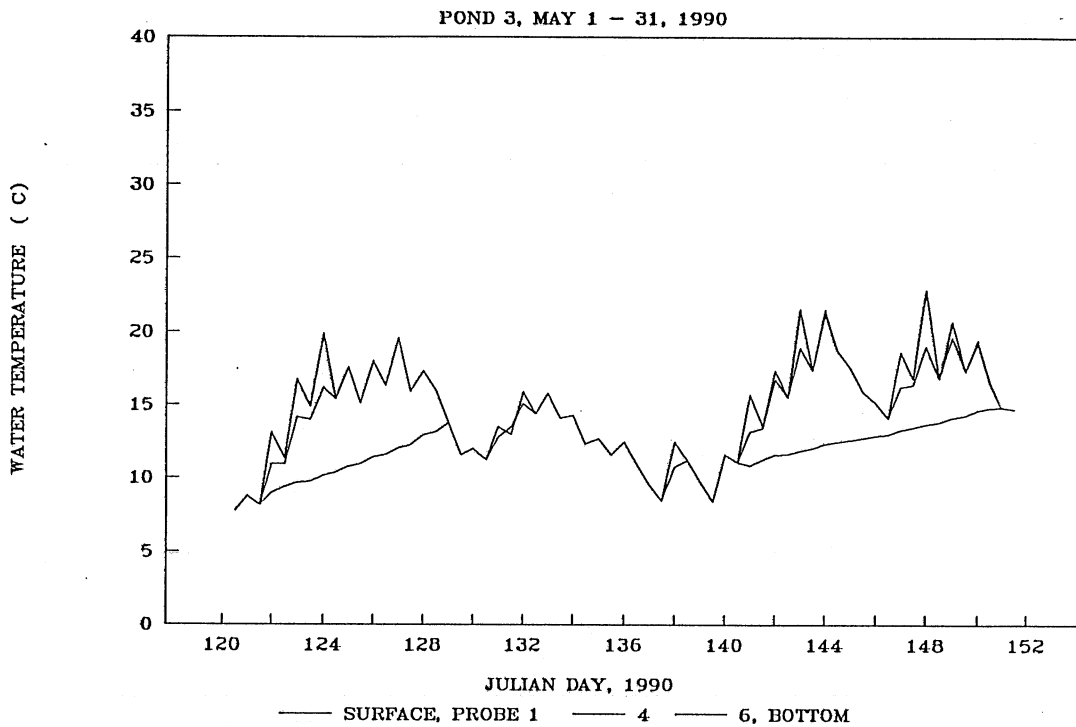


Fig. 73 Simulated water temperatures, pond 3, May, 1990



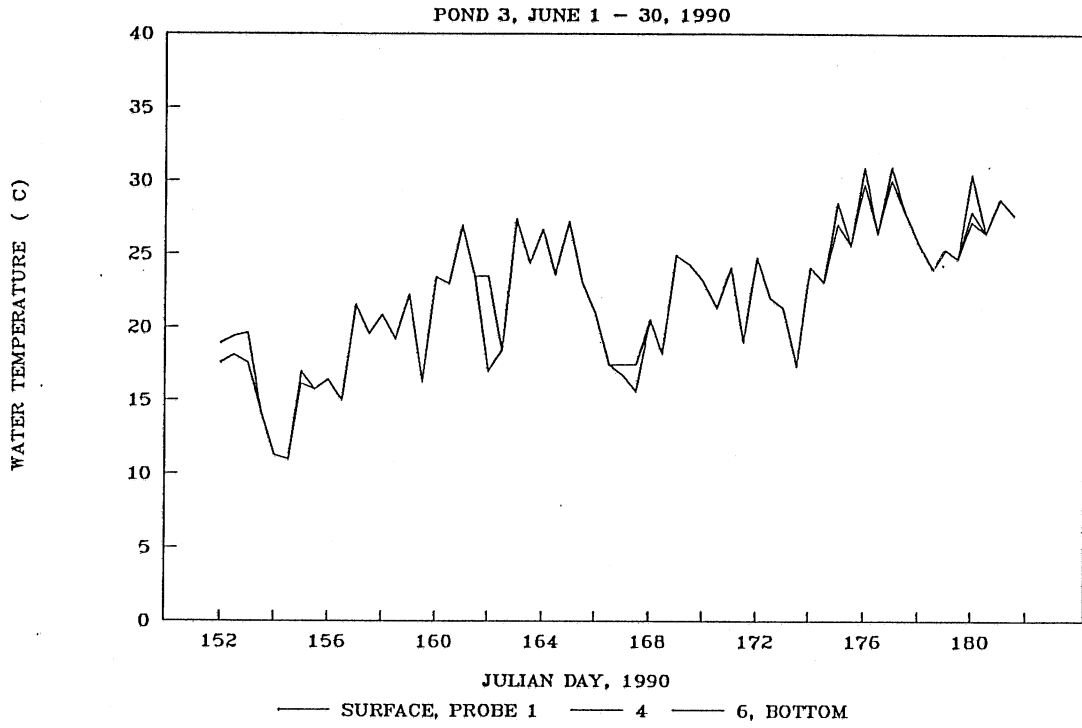


Fig. 74 Simulated water temperatures, pond 3, June, 1990

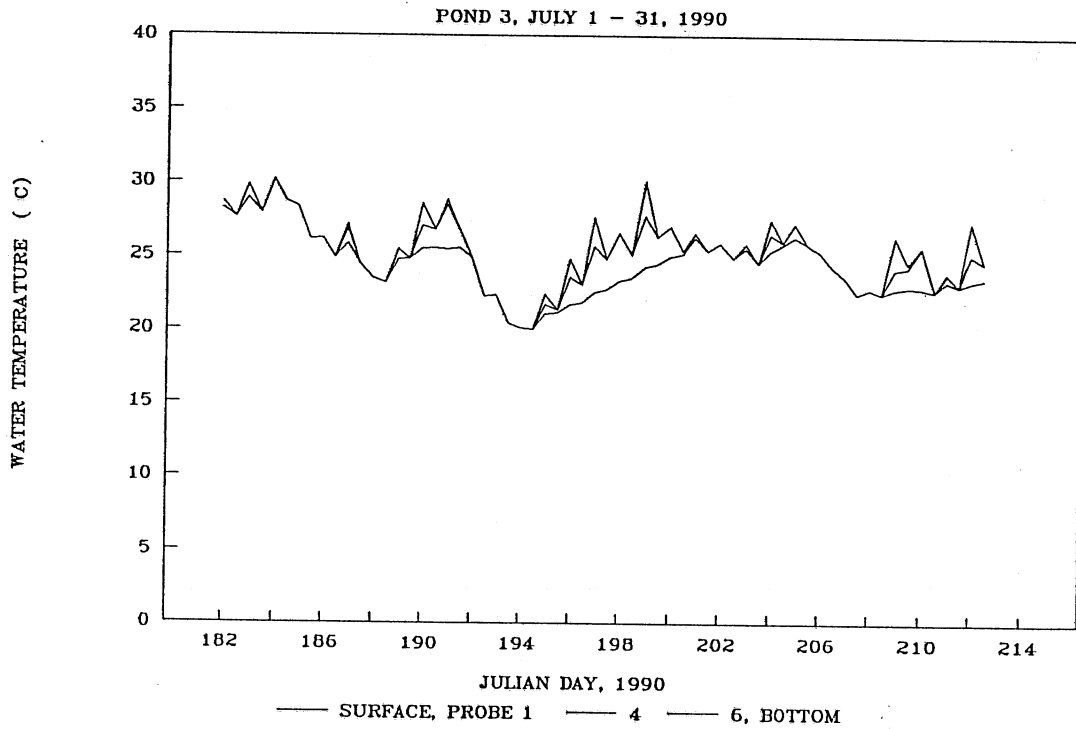


Fig. 75 Simulated water temperatures, pond 3, July, 1990

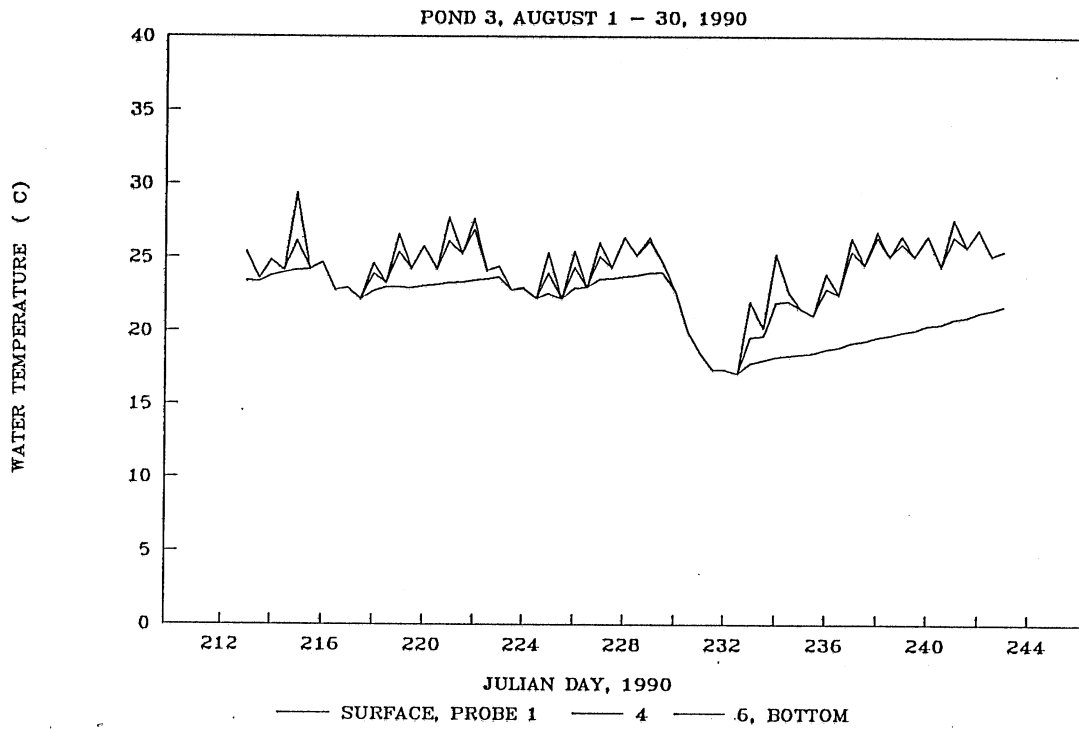


Fig. 76 Simulated water temperatures, pond 3, August, 1990

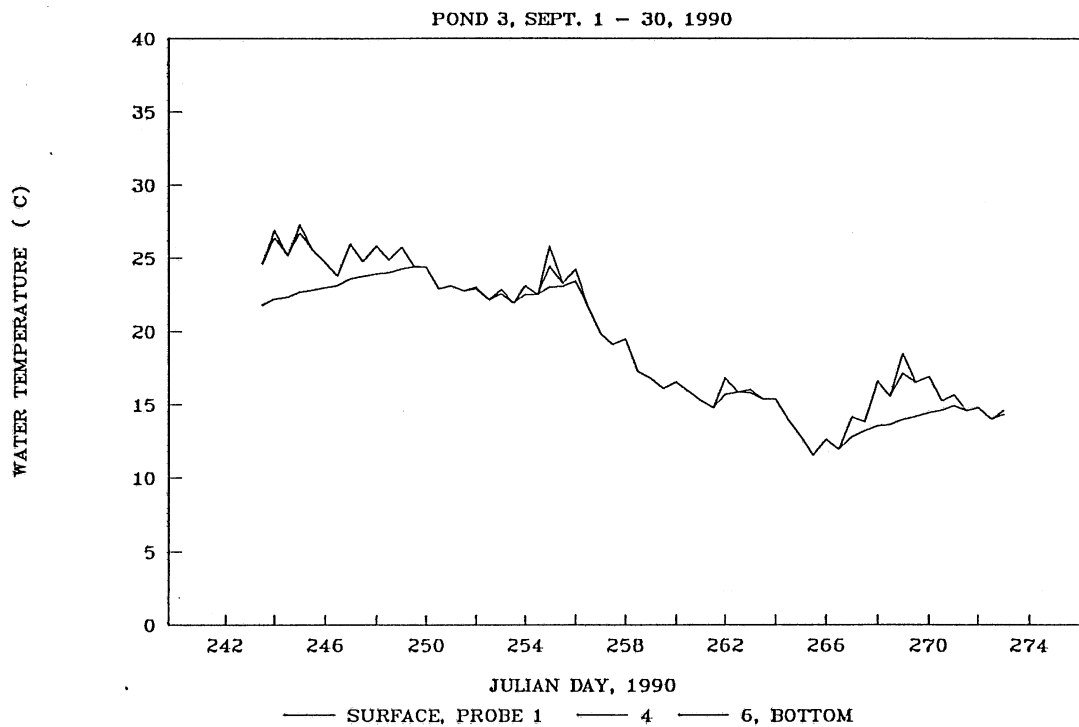


Fig. 77 Simulated water temperatures, pond 3, September, 1990

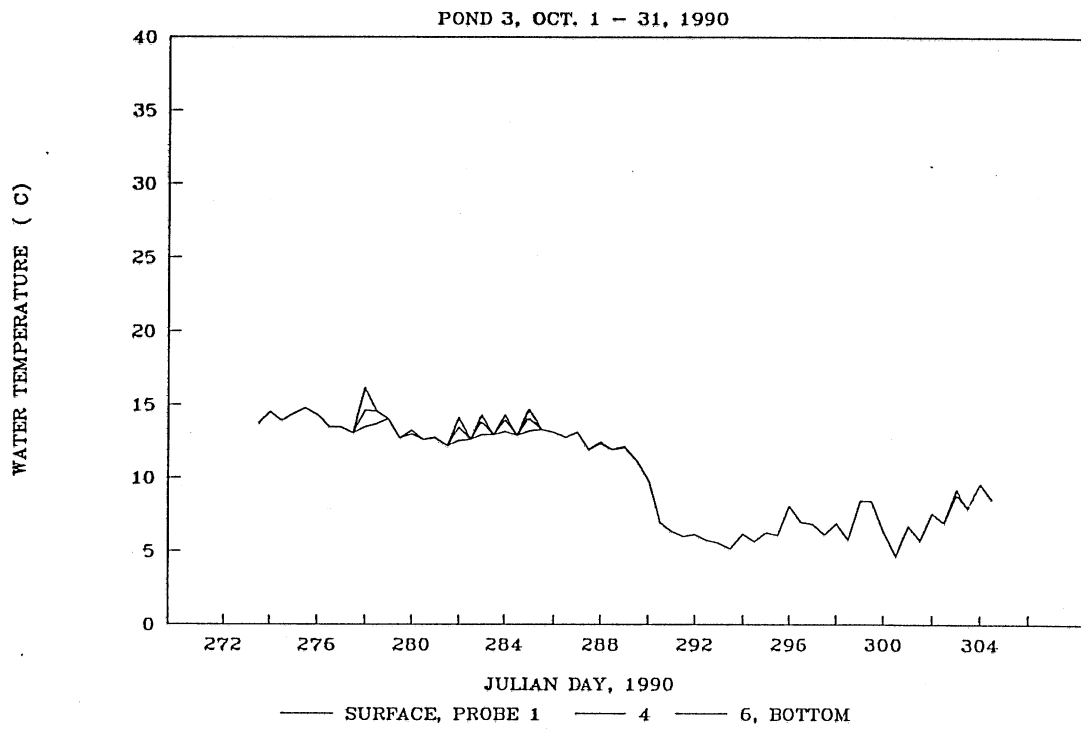


Fig. 78 Simulated water temperatures, pond 3, October, 1990

Table 3 Number of days with specific measured and simulated stratification and mixing characteristics

Year	Pond	Type	April		May		June		July		August		Sept.		Oct.		Nov.		Dec.		Total		Error	
			m	s	m	s	m	s	m	s	m	s	m	s	m	s	m	s	m	s	m	s	a	r %
1989	1	I									5	8	12	14	20	18	12	10			49	50	-1	-2
		II									17	12	16	13	9	9	0	0			42	34	8	19
		III									9	11	2	3	2	4	18	20			31	38	-7	-22
	3	I									8	10	11	10	22	23					41	43	-2	-5
		II									23	15	11	10	6	6					40	31	9	22
		III									0	6	8	10	3	2					11	18	-7	-63
1990	1	I	20	17	12	12	7	8	4	7	6	7	16	14	25	20					90	85	5	5
		II	0	3	6	5	10	6	13	9	11	10	12	11	6	10					58	54	4	6
		III	4	4	13	14	5	8	14	15	14	14	2	5	0	1					52	61	-9	-16
	3	I			12	12	29	28	12	14	5	5	7	13	23	23					88	95	-7	-8
		II			1	1	1	2	17	11	0	0	6	4	4	4					29	22	7	23
		III			18	18	0	0	2	6	26	26	17	13	2	2					65	65	0	0

Note: "m", "s", "a" and "r" indicate measured, simulated, absolute and relative values, respectively.

## 6. Summary

A dynamic water temperature simulation model was developed for the simulation of temperature stratification in the Harris wastewater stabilization ponds. A variable timestep option instead of a fixed one day time interval was incorporated into the program. Simulations with the one-half day timestep give details of stratification features within a daily cycle. To match the computational 12-hour timescale, the weather and flow input data files had to be rearranged into steps of 12 hours. The level of agreement between field measurements and numerical simulations demonstrates that water temperatures and stratification dynamics in a pond, with a small surface area and shallow depth, can be simulated on a diurnal timescale.

The model was calibrated against temperature data for the summer of 1989. Model verification was made against temperature data for spring and summer of 1990. The model for pond 1 (1989 and 1990) incorporates jet mixing and water transfer. Thermal stratification for a full one year period, including winter, may be predicted using submodels for ice and snow.

The simulation of intermittent stratification and destratification laid a necessary base for further simulation of other water quality parameters. The adaptation of the temperature simulation to other chemical and biological parameters, such as dissolved oxygen, suspended solids, phosphorus and chlorophyll is in progress and follows the procedures used in MINLAKE. Additional components such as hydrogen ion, alkalinity, inorganic carbon, and daphnia are being incorporated through new subroutines and will be reported at a later time.

The purpose of the overall study is to simulate conditions in ponds under different management and operation alternatives. This may serve to improve the pond performance and water quality in ponds where water quality standards for the discharged water are difficult to meet. The Harris ponds are not in that category but were chosen for study because they had well-defined boundary and inflow conditions, were easier to monitor than larger ponds and were considered typical of a small community.

### References:

- Albertson, M. L., Dai, Y. B., Jensen, R. A. and Rouse, H. "Diffusion of submerged jets," *Transactions, ASCE*, 115:639-664.
- Baker, D G. and Haines, D. A., Solar Radiation and Sunshine Duration Relationships in the North-central Region Alaska: Basic Computation. Agricultural Experiment Station, University of Minnesota.
- Baker, D G. and Enz, Y. W., The Availability and Dependability of Solar Radiation at St. Paul, Minnesota, Climate of Minnesota, Part XI, Agricultural Experiment Station, University of Minnesota, Technical Bulletin 316, 1979.
- Filatov, N. N., Rjanzhin, S. V., and Zaycev, L. V., Investigation of Turbulence and Langamir Circulation in Lake Ladoga. *Journal of Great Lakes Research*, Vol. 17, No. 1, pp. 1-6, 1981.
- Ford, D and Stefan, H. G., Thermal prediction using integral energy model. *Jour. of Hydraulic Div.*, ASCE, Vol. 106, HY 1, pp. 39-55, 1980
- Gu, R. and Stefan, H. G., Year-round Temperature Simulation of Cold Climate Lakes. *Cold Regions Science and Technology*, 18, pp. 147-160, 1990.
- Hondzo, M., Ellis, C., and Stefan, H. G., Vertical Diffusion in a Small Stratified Lake: Estimation and Error Analysis. *Journal of Hydraulic Engineering*, ASCE, 1991 (to be printed).
- Jasby, A. and Powell, T., Vertical Patterns of Eddy Diffusion During Stratification in Castle Lake, California, *Limnology and Oceanography*, Vol. 20, No. 4, pp. 530-543, 1975.
- Lee, J.H.W. "Stability and mixing of a round buoyant discharge in shallow water," *Proceedings, Second International Symposium on Stratified Flows*, Int'l. Assoc. for Hydraulic Research, Trondheim, Norway, 1980.
- Luck, F. N. and Stefan, H. G., Physical Limnology of the Harris Wastewater Stabilization Ponds: July 1989 to October 1990. Project Report No. 309, St. Anthony Falls Hydraulic Laboratory, University of Minnesota. 1990
- Minnesota Pollution Control Agency and Consulting Engineers Council of Minnesota, Report on Evaluation of Minnesota Water Balance Test, April. 1989.
- Riley, J. M. and Stefan, H. G., MINLAKE: a dynamic lake water quality simulation model. *Ecol. Modeling*, 43: 155-182, 1988.

- Riley, J. M. and Stefan, H. G., Dynamic Lake Water Quality Simulation Model "MINLAKE". Project Report No. 263, St. Anthony Falls Hydraulic Laboratory, University of Minnesota, 1987.
- Riley, J. M., User's Manual for the Dynamic Lake Water Quality Simulation Program "MINLAKE". External Memorandum No. 213, St. Anthony Falls Hydraulic Laboratory, University of Minnesota, 1988.
- Stefan, H. G., Dhamotharan, S and Schiebe, F. R. Temperature/sediment model for a shallow lake. *Jour. of Environmental Engineering Div., ASCE*, Vol. 108, No. EE 4, Aug. 1982.
- Stefan, H. G. and Ford, D. Temperature dynamics in dimictic lakes. *Jour. of the Hydraulic Division, ASCE*, Vol. 101, No. HY1, pp. 97-114, 1975
- Stefan, H. G. and Gu, R., "Efficiency of jet-mixing of temperature-stratified water, *Jour. of Environmental Engineering, ASCE*, accepted 1990.
- Ward, P. R. B., Diffusion in Lake Hypolimnia. Proceeding of 17th Congress of the International Association for Hydraulic Research, Vol. 2, Aug. 15-19, 1977, Baden-Baden, Germany.

## APPENDICES



## APPENDIX A

### Statistical parameters of error analysis

Several statistics were considered in the simulations for calibration and/or verification purposes (Riley, 1988). All parameters measure agreement or disagreement between field data and simulated model results. A constrained regression was chosen as providing the most useful information. The goodness of fit in the calibration and/or verification was primarily measured by the regression. The regression is constrained through the origin to provide a direction regression of field data to model results.

The slope of the regression, which indicates if the model is overpredicting (slope < 1.0) or underpredicting the field data, is defined as

$$s_r = \frac{\sum_{i=1}^n (y_i x_i)}{\sum_{i=1}^n (x_i)} \quad (\text{A.1})$$

where  $y_i$ ,  $x_i$  and  $n$  are field data, prediction and number of pairs of data, i.e. data points ( $y_i$ ,  $x_i$ ), respectively. The objective value of this parameter for calibration is 1.0.

The regression coefficient is the ratio of variance in the field data explained by the regression to the total variance in the field data. It is expressed as

$$r^2 = 1 - \frac{s_e^2}{\sigma^2} \quad (\text{A.2})$$

where  $s_e$  and  $\sigma$  are standard error of estimate and standard deviation of the mean of data, respectively, given as

$$s_e^2 = \frac{\sum_{i=1}^n (y_i - x_i)^2}{n} \quad (\text{A.3})$$

and

$$\sigma^2 = \frac{\sum_{i=1}^n (y_i - \bar{y})^2}{n} \quad (\text{A.4})$$

where  $\bar{y}$  is the mean of data

$$\bar{y} = \frac{\sum_{i=1}^n y_i}{n} \quad (\text{A.5})$$

The calibration objective is that  $r^2$  approaches 1.0 and  $s_e$  goes to 0.0.

## APPENDIX B

### Definitions and Values of Model Coefficients

- (1) Vertical turbulent diffusivity in hypolimnion

$$K_z = \min [K_{z_{\max}}, K_{z_{\max}} CN^{-1}]$$

$$\text{where } N = \left[ \frac{g}{\rho} \frac{d\rho}{dz} \right]^{\frac{1}{2}} \text{ and } C = 8.66 \times 10^{-3} \text{ s}^{-1}$$

- (2) Evaporative and convective surface heat losses  $H_e$  and  $H_c$

$$H_e = kW (e_s - e_a)$$

$$H_c = 0.618W (T_s - T_a)$$

where  $W = WCOEF$ , and  $u =$  the average wind speed over the time interval  $\Delta t$ , m/s

- (3) Stability criterion for determining the extent of wind mixing

$$\sigma = \frac{\int_A WSTR \cdot \rho \Delta t u_*^3 dA}{V_m \Delta \rho g (z_m - z_g)} \geq 1$$

$$\sigma = \frac{\text{Turbulent Kinetic Energy}}{\text{Potential Energy}}$$

### Epilimnetic Diffusivity

$$(4.1) \quad K_e = 28 W^{1.3} \text{ in MINLAKE}$$

where  $W$  = wind speed (mph)

$$(4.2) \quad K_e = \frac{u_*}{\left(\frac{1}{c}\right) + \left(\frac{\sigma}{c}\right)R_i}$$

where

$c = H/34$ ,  $H$  = total depth

$\sigma = 0.1$

$u_*$  = wind induced water shear velocity

$R_i$  = Richardson number defined as

$$R_i = \frac{g \frac{d\rho}{dz}}{\rho \frac{\partial u}{\partial z}} \quad \text{and used as}$$

$$R_i = \alpha k^2 g \left( \frac{\partial T}{\partial z} \right) / u_*^2$$

Appendix B Maximum hypolimnetic diffusivity, epilimnetic diffusivity constant, wind function coefficient and wind sheltering coefficient used for lakes and ponds

Lake or pond	Mean depth	Max. depth	Sur-face area	Epil. diff. const.	Max. hypol. diff. coeff.	Wind func-tion coeff.	Wind shel-tering coeff.	Attenua-tion Coeff.		Chl-a	Reference or modeler
	H	H <sub>max</sub>		C <sub>k</sub>	K <sub>zmax</sub>	Wcoef	Wstr	ε <sub>w</sub>	ε <sub>c</sub>		
	m	m	(km) <sup>2</sup>		m <sup>2</sup> /day			1/m	1/m	μg/l	
Harris	1.8	1.8	0.0077	0.2	0.10	20.0	0.10				Gu (1990)
Holland		18.8	0.14	28	0.10	25.0	0.30	0.65	16	28	Hondzo
Round			0.125	28	0.08	25.6	0.30	0.65	16		Gu (1990)
Long		7.5	0.73	28	0.50	25.6	0.60	0.65	16		Riley
Square		20.0	0.85	28	0.30	24.0	0.80	0.65	8.65	2	Hondzo
Fish		8.20	1.16	28	0.50	25.0	0.70	0.65	8.65	48	Hondzo
Riley		15.0	1.20	28	0.20	25.6	0.55	0.65	16		Riley
Elmo		41.8	1.23	28	0.90	26.0	0.50	0.65	8.65	9	Hondzo
Calhoun	10.0	27.0	1.71	28	0.30	22.0	0.35	0.65	16		Gu (1990)
Calhoun		24.0	1.71	28	0.70	24.0	0.60	0.65	8.65	40	Hondzo
Waconia		11.0	10.0	28	1.90	27.0	0.90	0.65	8.65	23	Hondzo

APPENDIX C  
PROGRAM LISTING

DEFINITIONS OF VARIABLES USED

IN POND SIMULATION:

CQJET2 = C2 IN EQ. 3.7 (FOR ENTRAINMENT RATE)  
 DOJET = PIPE DIAMETER (M)  
 ITPT = INDEX OF LAYER TO WHICH THE INTERFLOW (JET) INTRUDES  
 QEEE(I) = VOLUME OF ENTRAINED WATER FROM LAYER I (M\*\*3)  
 QJ = JET DISCHARGE RATE (M\*\*3/S)  
 QT = FLOWRATE OF THE INTERFLOW (INTRUDING FLOW) (M\*\*3)  
 TDEPS = MEASURED TOTAL POND DEPTH (M)  
 TDISCH = MEASURED INFLOW TEMPERATURE INTO POND 1 ( C)  
 TMSTEP = TIME STEP (HOURS)  
 TPT = TEMPERATURE OF THE INTERFLOW (INTRUDING FLOW) ( C)  
 TPUMP = PUMPING DURATION (HOURS)  
 ZWITH = WITHDRAWAL OR DISCHARGE DEPTH FOR SUBSURFACE INFLOW  
 OR OUTFLOW (M)

IN YEAR-ROUND SIMULATIONS:

AHTBTM = SEDIMENT CONDUCTIVITY  
 ALFICE = ICE REFLECTIVITY  
 ALFSNOW = SNOW REFLECTIVITY  
 BTICE = ICE ASORPTION COEFFICIENT  
 BTSNOW = SNOW ABSORPTION COEFFICIENT  
 CDISO = ICE CONDUCTIVITY  
 CFSNOW = SNOW COMPACTION FACTOR  
 CNFSNWO = SNOW CONDUCTIVITY  
 DZSL = SPACE STEP IN SEDIMENT TEPERATURE CALCULATION (M)  
 GMICE = ICE ATTENUATION COEFFICIENT  
 GMSNOW = SNOW ATTENUATION COEFFICIENT  
 HTBTM = HEAT FLUX FROM SEDIMENT TO WATER  
 IZSLT = NUMBER OF LAYERS OF SEDIMENTS  
 QWATER = HEAT FLUX FROM WATER TO ICE  
 SNOWMELT = SNOW MELTING (M)  
 TWAICE = DEPTH MEAN TEMPERATURE AT WHICH LAKE STARTS TO FREEZE OVER  
 TAIRICE = AIR TEMPERATURE AT WHICH LAKE START TO FREEZE OVER ( C)  
 THICE = ICE THICKNESS (M)  
 THSNOW = SNOW THICKNESS (M)  
 TSLMEAN = ANNUAL MEAN SEDIMENT TEMPERATURE ( C)  
 TSL = SEDIMENT TEMPERATURE ( C)  
 ZSLT = DEPTH OF SEDIMENT (M)  
 ZSL = DEPTH FROM THE LAKE BOTTOM

```

C *** This program is for Harris pond simulations ***
$DEBUG
$NOFLOATCALLS
$STORAGE:2
  SUBROUTINE LAKE(ZD,DUM,NFLOW,ID)
  REAL*8 A,V,TV,ATOP,AK,BK,CK,DK,SVOL,DUM
  CHARACTER*20 STFILE
  COMMON/MTHD/TAIR(31),TDEW(31),RAD(31),CR(31),WIND(31),
+ PR(31),DRCT(31)
  COMMON/RESULT/ T2(40),CHLATOT(40),PA2(40),PTSUM(40),BOD2(40),
+DSO2(40),C2(40),CD2(40),XNO2(40),XNH2(40),CHLA2(3,40),
+PC2(3,40),XNC2(3,40),T20(40),SI2(40)
  COMMON/SOURCE/RM(3,40),PROD(40),XMR(3,40),PRODSUM(40)
  COMMON/FLOW/HMK(41),QE(40),FVCHLA(5),PE(5,41)
  COMMON/YIELD/YCA,YCHO2,Y2CHO2,YCBOD,YPBOD,YZW,YPZP,YNZP,YZDO,
+YSCHL,YNHBOD,BRNO,BRNH,XKNNH,THNNH,YPCHLA,BODK20,SB20,BRR
  COMMON/PHYTO/PDEL(3),PMA(3),PMIN(3),THR(3),THM(3),XKR1(3),
+XKR2(3),XKM(3),HSCPA(3),HSC1(3),HSC2(3),UPMAX(3),THUP(3),
+GROMAX(3),TMAX(3),TOPT(3),XNMAX(3),XNMIN(3),UNMAX(3),THUN(3),
+HSCN(3),HSCNH(3),XNDEL(3),IDIATOM,CHLMEAN,CHLMAX,SECCHI
  COMMON/ZOOPL/IZ,MINDAY,MAXDAY,ZP,ZPMIN,PRMIN,PRMAX,PREDMIN,XIMIN,
+XIMAX,XKRZP,GRAZMAX(3),THGRAZ(3),ASM,THRZP,HSCGRAZ(3),CHLAMIN(3),
+REPRO,XI,XKMZ,GRAZE(3,40)
  COMMON/TEMP/PARIO(4),PCDUM(3,40),XNHD(40),XNOD(40),
+ CHLADUM(3,40),XNCD(3,40),PADUM(40),SID(40)
  COMMON/VOL/ZMAX,DZ(40),Z(40),A(40),V(40),TV(40),ATOP(41),DBL
  COMMON/SUB/SDZ(60),SZ(60),LAY(40),AVGI(4,60),SVOL(60)
  COMMON/CHOICE/MODEL,NITRO,IPRNT(6),NDAYS,NPRNT(30),NCLASS,PLT(30)
  COMMON/WATER/BETA,EMISS,XK1,XK2,HKMAX,WCOEF,WSTR
  COMMON/CHANNEL/WCHANL,ELCB,ALPHA,BW,WLAKE
  COMMON/STEPS/DZLL,DZUL,MBOT,NM,NPRINT,MDAY,MONTH,ILAY,DY
  COMMON/STAT/SUMXY(10),SUMX(10),SUMY(10),XSQ(10),
+YSQ(10),RSQ(10),RMS(10),RELM(10),MTHREL(10),MDAYREL(10),ZREL(10),
+ZRELM(10),RS(10),REL(10),MTHRMS(10),MDAYRMS(10),ZRS(10),ZRMS(10)
  COMMON/INFLOW/QIN(5),TIN(5),PAIN(5),BODIN(5),DOIN(5),CIN(5),
+CDIN(5),XNHIN(5),XNOIN(5),CHLAIN(3,5)
  COMMON/FIELD/ IFLAG(10),FLDATA(10,50),DEPTH(50),NFLD(10),SD
  COMMON/FILE/ DIN,MET,FLO,TAPE8,TAPE1,IREC
  COMMON/TITL/ TITLE
  COMMON/EPDIF/ WINDKM
  COMMON/PREVA/ HED,P
  COMMON/SNICE/ THICE,THSNOW,BTICE,ALFICE,GMICE,
+ BTSNOW,ALFSNOW,GMSNOW,QWATER,HTBTM,HSTMP,TMSTEP
  COMMON/BOTT/ SNOWFL(300),TSL(21),ZSL(21),TSLP(21)
  COMMON/CR/ TWAICE,TAIRICE
  COMMON/ZWIS/ZWITH(5)
  DIMENSION ZS(7),TS(7),QEEE(40)
  CHARACTER*16 DIN,MET,FLO,TAPE8,TAPE1
  GOTO (100,200,300,400,500,600,700,800,900,1000,1100,1200,1300) ID
C***** AREA COMPUTATION SECTION *****
100 CONTINUE
  DUM=54.6*92.4+8.0*(54.6+92.4)*ZD+64.0*ZD**2
  RETURN
C***** FETCH COMPUTATION SECTION *****
200 CONTINUE
  ZD=SQRT(4./3.1459*7090.0)
  RETURN
C***** VOLUME COMPUTATION SECTION *****
300 CONTINUE
  DUM=(54.6*92.4+4.0*(54.6+92.4)*zd+64.0/3.*zd**2)*ZD
  RETURN
C***** COMPUTE DEPTH FROM VOLUME *****
400 CONTINUE
  ahh=54.6
  bhh=92.4
  chh=4.0

```



```

dhh=1.0
dumtmp=abs(dum)
dhs=4.*chh**2/3./dhh**2
chs=-dumtmp/dhs
bhs=ahh*bhh/dhs
ahs=(ahh+bhh)*chh/dhh/dhs
pss=-ahs**2/3.+bhs
qss=chs-bhs*ahs/3.+2.*ahs**3/27.
ypow=1./3.
yyy1=(-qss/2.+sqrt(qss**2/4.+pss**3/27.))**ypow
+      +(-qss/2.-sqrt(qss**2/4.+pss**3/27.))**ypow
ZD=yyy1-ahs/3.
RETURN
C***** TREATMENT SECTION *****
500 WRITE(*,*) MONTH,MDAY,MBOT
RETURN
C***** PHOSPHORUS SOURCES/SINKS *****
600 RETURN
C***** NO2-NO3 SOURCES SINKS
700 RETURN
C***** NH4 SOURCES/SINKS *****
800 RETURN
C***** O2 SOURCES/SINKS *****
900 RETURN
C***** OUTFLOW COMPUTATION *****
1000 CONTINUE
C READ MEASURED TOTAL DEPTH AND CHANGE IN STORAGE
READ(16,*) JULDAY,VZND,TDEPS,QIN(1)
C READ JET INFLOW TEMPERATURE AND PUMPING DURATION (POND 1 ONLY)
READ(17,*) JULD,PVZND,TDISCH,TPUMP
TPUMP=TPUMP*3600.0
NFLOW=1
C WATER BALANCE CALCULATION
ZZMB=Z(MBOT)+0.5*DZ(MBOT)
VDUMZ1=(54.6*92.4+4.0*(54.6+92.4)*ZZMB+64.0/3.
+ *ZZMB**2)*ZZMB
IF(TDEPSP.LE.0) TDEPSP=ZZMB
VDUMZ2=(54.6*92.4+4.0*(54.6+92.4)*TDEPSP+64.0/3.
+ *TDEPSP**2)*TDEPSP
HEVOL=ATOP(1)*HED
PRVOL=ATOP(1)*P
QJVOL=QJ*TPUMP
VMDIFF=-VDUMZ1+VDUMZ2
QIN(1)=QIN(1)-VDUMZ1+VDUMZ2+HEVOL-PRVOL-QJVOL
T2C2=T2(1)
DO 1011 I=1,MBOT-1
ZINCH=0.5*(ZMAX-0.61)+0.61
ZWITH(1)=ZMAX-ZINCH
IF(ZMAX-Z(I).GT.ZINCH.AND.ZMAX-Z(I+1).LE.ZINCH) T2C2=T2(I)
1011 CONTINUE
TIN(1)=T2C2
TDEPSP=TDEPS
C
C***** VERTICAL INFLOW JET SUBMODEL (POND 1 ONLY) ***
C
TT2MAX=T2(1)
TT2MIN=T2(1)
DO 1305 I=1,MBOT
IF(Z(I).LT.0.11*ZMAX.AND.Z(I+1).GE.0.11*ZMAX) IEN=I
IF(T2(I).GT.TT2MAX) TT2MAX=T2(I)
IF(T2(I).LT.TT2MIN) TT2MIN=T2(I)
1305 CONTINUE
ZQ=ZMAX-Z(IEN)+DZ(IEN)/2.0
QT=QJ*(1+1.013*CQJET2*ZQ/DOJET+1.97*(CQJET2*ZQ/DOJET)**2)
QESUM=0.0
DO 1306 I=IEN,MBOT

```

```

      QEEE(I) = -(QT-QJ)*TPUMP*DZ(I)/ZQ
1306 QESUM=QESUM-QEEE(I)*T2(I)
      TPT=(QESUM+TDISCH*QJ*TPUMP)/(QT*TPUMP)
C      ITPT=INT(MBOT/3)
      IF(TPT.GT.TT2MAX) ITPT=IEN
      IF(TPT.LT.TT2MIN) ITPT=MBOT-1
      DO 1307 I=1,MBOT-1
1307 IF(T2(I).GT.TPT.AND.T2(I+1).LE.TPT) ITPT=I+1
      CONTINUE
      DO 1308 I=1,MBOT
      V(I)=V(I)+QEEE(I)
      IF(V(I).LE.0.0) THEN
      IF(I.EQ.1) THEN
      V(2)=V(2)+V(1)
      ENDIF
      IF(I.GE.2) THEN
      V(I-1)=V(I-1)+V(I)
      ENDIF
      V(I)=0.00001
      ENDIF
1308 CONTINUE
      T2(ITPT)=(T2(ITPT)*V(ITPT)+QT*TPUMP*TPT)/
+ (V(ITPT)+QT*TPUMP)
      V(ITPT)=V(ITPT)+QT*TPUMP
      RETURN
C***** GROUNDWATER FLOW COMPUTATION *****
1100 CONTINUE
      RETURN
C***** INPUT REQUEST OR MODIFICATION ****
C      AS THIS SUBROUTINE IS CALED JUST ONCE, IN THE BEGINNING,
C      IT IS CONVENIENT TO WRITE HERE ALL THE VALUES WHICH ARE
C      GOING TO BE UNCHANGED
1200 CONTINUE
      OPEN(13,FILE='SIWOUT')
      OPEN(14,FILE='SEDOUT')
      OPEN(15,FILE='TOUT')
      OPEN(16,FILE='QINZD1')
      OPEN(17,FILE='PLJET')
      OPEN(18,FILE='HMK')
      OPEN(12,FILE='ICEP1')
      READ(12,*) DZSL,ZSLT,IZSLT,IZSLTH,AHTBTM,TSLMEAN,ETAB,ISEDMENT
      READ(12,*) cfsnow,CDISO,CNDSNWO,CNDWI,CONSQW,DEPTHC,
+ ICEMNS,ICEDAY,IOPNMNS,IOPNDY
      READ(12,*) HKMXSP,WCFSP,WSSP,HKMXSM,WCFSM,WSSM,WINDKM
      READ(12,*) HKMXFW,WCFW,WSFW,HKMXIS,WCFIS,WSIS
      READ(12,*) BTICE,ALFICE,GMICE,BTSNOW,ALFSNOW,GMSNOW
      READ(12,*) TWAICE,TAIRICE,TMSTEP
      read(12,*) mnsnow,mdysnow,NDYSTL
      READ(12,*) QJ,CQJET2,DOJET
C      READ(12,*) (SNOWFL(I),I=1,NDYSTL)
      NDYSNW=0
      NDAYST=DY
      THSNOW=0.0
      THICE=0.0
      ifreeze=0
      HSTMSUM=0.0
      QWATSUM=0.0
      HTBTSUM=0.0
      HTICSUM=0.0
C
C      THIS INITIAL CONDITION IS VALID FOR JAN.-APRIL (MINIMUM BOTTOM TEMP)
C      AND AUG.-OCT. (MAXIMUM BOTTOM TEMP.)
      DZSL=ZSLT/FLOAT(IZSLT-1)
      DO 5 I=1,IZSLT
      ZSL(I)=FLOAT(I-1)*DZSL
      TSL(IZSLT-I+1)=T2(MBOT)*EXP(-ETAB*ZSL(I))+

```

```

+          (1.0-EXP(-ETAB*ZSL(I)))*TSLMEAN
TSLP(IZSLT-I+1)=TSL(IZSLT-I+1)
5 CONTINUE
C
WRITE(13,901)
WRITE(13,1613)
WRITE(13,1615) cfsnow,CDISO,CNDSNW0,CNDWI,DEPTHC,ICEMNS,ICEDAY,
+ IOPNMNS,IOPNDY
WRITE(13,1616) HKMXSP,WCFSP,WSSP,HKMXSM,WCFSM,WSSM
WRITE(13,1616) HKMXFW,WCFFW,WSFW,HKMXIS,WCFIS,WSIS
WRITE(13,1614) BTICE,ALFICE,GMICE,BTSNOW,ALFSNOW,GMSNOW
WRITE(13,1600)
WRITE(14,1629)
WRITE(14,1621) DZSL,ZSLT,IZSLT,AHTBTM,TSLMEAN,ETAB
WRITE(14,1631)
WRITE(13,1600)
WRITE(13,1618)
WRITE(13,251)
WRITE(14,*)
WRITE(14,1619) MONTH,MDAY,(ZSL(I),I=1,IZSLT,1)
WRITE(14,1619) MONTH,MDAY,(TSL(IZSLT-I+1),I=1,IZSLT,1)
C
251 FORMAT('IDAY MON DAY ',3X,'QWAT',2X,'QWSUM',
+ 3X,'HTBTM',3X,'HTSUM',5X,'HS',5X,'HSSUM',3X,'THICE',
+ 1X,'THSNO',2X,'SNOWF',3X,'HSA',3X,'HKMAX',4X,'RAD',3X,'HCNDISO')
901 FORMAT('INPUT DATA:')
1600 FORMAT(' ')
1613 FORMAT(3X,'CFSNOW CDISO CNDSNW0 CNDWI DEPTHC ICEMNS ICEDAY',1X,
+ 'IOPNMNS IOPNDY')
1614 FORMAT(2X,'B,A,G(ICE,SNOW)= ',6F8.3)
1615 FORMAT(2X,F6.2,1X,F5.2,1X,F7.2,1X,F5.2,1X,F6.1,1X,I6,1X,I6,1X,
+ I7,1X,I6)
1616 FORMAT(2X,'HKMAX,WCOEF,WSTR = ',2X,3F8.3)
1618 FORMAT('RESULTS OF SIMULATION:')
1619 FORMAT(1X,2I4,1X,20F6.2)
1621 FORMAT(2X,2F8.1,2X,I4,2X,'AHTBTM, TSLMEAN= ',2F10.5,2X,F6.3)
1629 FORMAT('TEMPERATURE DISTR. IN THE SEDIMENT BELOW LAKE BOTTOM:')
1631 FORMAT(2X,'DEPTH BELOW BOTTOM',8X,'TEMPERATURE')
RETURN
C***** POST DAILY SIMULATION TREATMENT AND COMPUTATIONS *****
C-----
1300 CONTINUE
WRITE(18,*)
WRITE(18,1335) MONTH,MDAY,(Z(I),I=1,MBOT,2)
WRITE(18,1333) MONTH,MDAY,(HMK(I),I=1,MBOT,2)
WRITE(18,1332) MONTH,MDAY,(T2(I),I=1,MBOT,2)
1335 FORMAT(1X,2I4,3X,'Z',20F6.3)
1332 FORMAT(1X,2I4,2X,'T2',20F6.2)
1333 FORMAT(1X,2I4,1X,'HMK',20F6.3)
C*****
WRITE(*,1627) RAD(MDAY),CR(MDAY)
1627 FORMAT(2X,'RAD= ',F6.1,2X,'CR= ',F8.2)
IF(ISEDMENT.EQ.1) THEN
CALL BOTTOM(DZSL,IZSLT,AHTBTM)
HTBTM=HTBTMP
HTBTMP=0.0
DO 1628 I=1,IZSLT
IF(I.EQ.1.OR.I.EQ.IZSLT) DZSLLL=.5*DZSL
HTBTMP=HTBTMP+500.0*DZSLLL*(TSLP(I)-TSL(I))*TMSTEP/24.0
TSLP(I)=TSL(I)
DZSLLL=DZSL
1628 CONTINUE
ENDIF
IF(MONTH.GE.ICEMNS+4) THEN
HKMAX=HKMXSM
WCOEF=WCFSM

```

```

WSTR=WSSM
ENDIF
IF (MONTH.EQ.MNSNOW.AND.MDAY.GE.MDYSNOW.AND.THICE.EQ.0.0) THEN
HKMAX=HKMXFW
WCOEF=WCFWF
WSTR=WSFW
ENDIF
IF (MONTH.GT.MNSNOW.AND.THICE.EQ.0.0) THEN
HKMAX=HKMXFW
WCOEF=WCFWF
WSTR=WSFW
ENDIF
IF (THICE.GT.0.0) THEN
HKMAX=HKMXIS
WCOEF=WCFIS
WSTR=WSIS
ENDIF
IF (MONTH.LT.ICEMNS+4.AND.THICE.EQ.0.0) THEN
HKMAX=HKMXSP
WCOEF=WCFSP
WSTR=WSSP
ENDIF
C IF (MONTH.GT.ICEMNS.AND.MONTH.LT.MNSNOW) RETURN
CALL SNOW(CFSNOW,MNSNOW,MDYSNOW,NDYSNW)
CALL ICE(IFREEZE,CDISO,CNDSNW0,DEPTHC,ICEMNS,ICEDAY,
+ IOPNMNS,IOPNDY,NDYSNW,NDAYST,HKMAX,MNSNOW,CNDWI,CONSQW)
ZST=Z(MBOT)+DZ(MBOT)/2.0
ZS(7)=ZST
ts(7)=t2(mbot-1)+(ZS(7)-z(mbot-1))*
+ (t2(mbot)-t2(mbot-1))/(z(mbot)-z(mbot-1))
IF (ZST.GE.1.0) THEN
ZS(1)=0.04
ZS(2)=0.20
ZS(3)=0.40
ZS(4)=0.60
ZS(5)=0.80
ZS(6)=1.00
ENDIF
DO 1821 I=1,6
IF (ZST.LT.1.0) THEN
ZS(I)=ZST-(1.04-FLOAT(I-1)*0.2)
ZS(6)=ZS(7)
ENDIF
DO 1823 J=1,MBOT-1
if (z(J).le.ZS(I).and.z(J+1).gt.ZS(I)) ts(I)=t2(J)+(ZS(I)-z(J))*
+ (t2(J+1)-t2(J))/(z(J+1)-z(J))
1823 CONTINUE
IF (ZS(I).LT.0) THEN
ZS(I)=0
TS(I)=0.0
ENDIF
1821 CONTINUE
IF (ZS(1).LT.Z(1)) TS(1)=T2(2)-(T2(2)-T2(1))/(Z(2)-Z(1))
+ *(Z(2)-ZS(1))
TSOMIT=0.0
ZJITPT=Z(ITPT)/ZMAX
QTLES=QT/QJ
IF (ZST.GE.1.0) WRITE(15,1825) NDAYST,(Ts(I),I=1,7),QIN(1),
+ TIN(1),TDEPS,ZST,QTLES,TPT,ZJITPT,HEVOL,PRVOL,QJVOL,VMDIFF
IF (ZST.LT.1.0) WRITE(15,1825) NDAYST,TSOMIT,(Ts(I),I=1,6),QIN(1),
+ TIN(1),TDEPS,ZST,QTLES,TPT,ZJITPT,HEVOL,PRVOL,QJVOL,VMDIFF
1825 FORMAT(1X,I4,1X,7F6.2,1X,F8.1,1X,F4.1,2F5.2,1X,F6.2,
+ 1X,F4.1,1X,F6.3,1X,3F6.1,1X,F6.1)
RETURN
END
C *****

```

```

SUBROUTINE SNOW(CFSNOW,MNSNOW,MDYSNOW,NDYSNW)
REAL*8 A,V,TV,ATOP,AK,BK,CK,DK,SVOL,DUM
COMMON/RESULT/ T2(40),CHLATOT(40),PA2(40),PTSUM(40),BOD2(40),
+DSO2(40),C2(40),CD2(40),XNO2(40),XNH2(40),CHLA2(3,40),
+PC2(3,40),XNC2(3,40),T20(40),SI2(40)
COMMON/VOL/ZMAX,DZ(40),Z(40),A(40),V(40),TV(40),ATOP(41),DBL
COMMON/MTHD/TAIR(31),TDEW(31),RAD(31),CR(31),WIND(31),
+ PR(31),DRCT(31)
COMMON/STEPS/DZLL,DZUL,MBOT,NM,NPRINT,MDAY,MONTH,ILAY,DY
COMMON/SNICE/ THICE,THSNOW,BTICE,ALFICE,GMICE,
+ BTSNOW,ALFSNOW,GMSNOW,QWATER,HTBTM,HSTMP,TMSTEP
COMMON/BOTT/ SNOWFL(300),TSL(21),ZSL(21),TSLP(21)
C SNOW ACCUMULATION FROM THE PRECIPITATION
IF(MNSNOW.EQ.MONTH.AND.MDAY.EQ.MDYSNOW) NDYSNW=1
IF(NDYSNW.GT.0) THEN
THSNOW=THSNOW+SNOWFL(NDYSNW)/(12.0*3.2808)*CFSNOW
NDYSNW=NDYSNW+1
ENDIF
C SNOW MELT
HTLTNT=80.0
DENSNOW=300.0
HTSNOW=RAD(MDAY)*10.0*(BTSNOW+(1.0-BTSNOW)*(1.0-ALFSNOW)*
+ (1.0-EXP(-GMSNOW*THSNOW)))
CPOWER=-0.0000156*800.0
TDEWMLT=TDEW(MDAY)
CPW2=7.45*TDEWMLT/(235.0+TDEWMLT)
EA=6.035*10.0**CPW2
TSNW=32.0+9.0*TAIR(MDAY)/5.0
SNOWMELT=WIND(MDAY)*(0.00736*(TSNW-32.0)*10**CPOWER
+ 0.0231*(EA-6.11))
SNOWMELT=SNOWMELT/(12.0*3.2808)
IF(TAIR(MDAY).GT.0.0) THEN
SNOWMELT=SNOWMELT+PR(MDAY)*TAIR(MDAY)*3.0/80.0*0.0254
SNOWMELT=SNOWMELT+HTSNOW/(DENSNOW*HTLTNT)
ENDIF
SNOWMELT=TMSTEP/24.0*SNOWMELT
IF(SNOWMELT.LE.0.0) SNOWMELT=0.0
THSNOW=THSNOW-SNOWMELT
IF(THSNOW.LE.0.0) THSNOW=0.0
IF(THICE.LE.0.0) THSNOW=0.0
RETURN
END
C *****
SUBROUTINE ICE(IFREEZE,CDISO,CNDSNWO,DEPTHC,ICEMNS,ICEDAY,
+ IOPMNS,IOPNDY,NDYSNW,NDAYST,HKMAX,MNSNOW,CNDWI,CONSQW)
REAL*8 A,V,TV,ATOP,AK,BK,CK,DK,SVOL,DUM
COMMON/RESULT/ T2(40),CHLATOT(40),PA2(40),PTSUM(40),BOD2(40),
+DSO2(40),C2(40),CD2(40),XNO2(40),XNH2(40),CHLA2(3,40),
+PC2(3,40),XNC2(3,40),T20(40),SI2(40)
COMMON/VOL/ZMAX,DZ(40),Z(40),A(40),V(40),TV(40),ATOP(41),DBL
COMMON/MTHD/TAIR(31),TDEW(31),RAD(31),CR(31),WIND(31),
+ PR(31),DRCT(31)
COMMON/STEPS/DZLL,DZUL,MBOT,NM,NPRINT,MDAY,MONTH,ILAY,DY
COMMON/SNICE/ THICE,THSNOW,BTICE,ALFICE,GMICE,
+ BTSNOW,ALFSNOW,GMSNOW,QWATER,HTBTM,HSTMP,TMSTEP
COMMON/BOTT/ SNOWFL(300),TSL(21),ZSL(21),TSLP(21)
COMMON/CR/ TWAICE,TAIRICE
DLTIME=TMSTEP/24.0
CNDICE=0.85984*24.0*CDISO
DENICE=920.0
HTLTNT=80.0
DENSNOW=300.0
CNDSNOW=CNDSNWO*0.85984*24.0
TMELT=0.0
HTSNIS=RAD(MDAY)*10.0*(1.0-BTSNOW)*(1.0-ALFSNOW)*
+ EXP(-GMSNOW*THSNOW)

```

```

HTICE=HTSNIS*(BTICE+(1.0-BTICE)*(1.0-ALFICE)*(1.0-
+ EXP(-GMICE*THICE)))
HSA=0.33*117.0*WIND(MDAY)
AC=THICE/CNDICE
BC=THSNOW/CNDSNOW
CC=1.0/HSA
DC=DLTIME/(DENICE*HTLTNT)
EC=TMELT-TAIR(MDAY)
DO 20 I=1,MBOT-1
IF(Z(I+1).GE.DEPTH.C.AND.Z(I).LT.DEPTH.C) THEN
TCHAR=T2(I)+(T2(I+1)-T2(I))*(DEPTH.C-Z(I))/(Z(I+1)-Z(I))
ENDIF
20 CONTINUE
QWATER=CNDWI*(TCHAR-TMELT)/DEPTH.C
IF(QWATER.LE.0.0) QWATER=0.0
IF(THICE.LE.0.0) QWATER=0.0
HCNDISO=EC/(AC+BC+CC)
THICE=THICE+DC*(EC/(AC+BC+CC)-QWATER)
if(tair(mday).le.0.0) ifreeze=1

C
IF(THICE.LE.0.0) THICE=0.0
IF(THICE.EQ.0.0) GOTO 92
IF(THSNOW.GT.0.0) GOTO 92
IF(TAIR(MDAY).GT.0.0) THEN
THICE=THICE-PR(MDAY)*TAIR(MDAY)*0.0254/80.0*TMSTEP/24.0
THICE=THICE-HTICE*DC
ENDIF

C
92. IF(THICE.LT.0.0) THICE=0.0
IF(IFRUP.EQ.1) GO TO 50
HTSUM=0.0
VSUM=0.0
DO 53 I=1,MBOT
HTSUM=HTSUM+T2(I)*A(I)*DZ(I)
53 VSUM=VSUM+A(I)*DZ(I)
TWAVE=HTSUM/VSUM
IF(TWAVE.LE.TWAICE.AND.TAIR(MDAY).LE.TAIRICE) THEN
IOPNMNS=MONTH
IOPNDY=MDAY
IFRUP=1
ENDIF
50 CONTINUE
60 IF(MONTH.EQ.IOPNMNS.AND.MDAY.LT.IOPNDY) THICE=0.0
IF(MONTH.EQ.ICEMNS.AND.MDAY.GT.ICEDAY) THICE=0.0
IF(MONTH.GT.ICEMNS.AND.MONTH.LT.IOPNMNS) THICE=0.0
if(ifreeze.eq.1) then
dgrdy=dgrdy+ec*dlttime
endif
HSTMSUM=HSTMSUM+HSTMP
QWATSUM=QWATSUM+QWATER
HTBTSUM=HTBTSUM+HTBTM
HTICSUM=HTICSUM+HCNDISO
RADTMP=RAD(MDAY)*10.0
WRITE(13,250) NDAYST,MONTH,MDAY,QWATER,QWATSUM,HTBTM,HTBTSUM,
+HSTMP,HSTMSUM,THICE,THSNOW,HSA,HKMAX
250 FORMAT(3I4,1X,F6.2,1X,F7.2,1X,F8.2,1X,F8.2,1X,F7.1,1X,F8.1,
+1X,F5.3,1X,F6.4,1X,F6.4,1X,F6.1,1X,F6.3,1X,F7.1,1X,F10.1,1X,F16.1)
C B.C. AT WATER/ICE INTERFACE IS TEMPERATURE = 0 C
NDAYST=NDAYST+1
C QWATER=0.0
QWATER=QWATER*TMSTEP/24.0*CONSQW
IF(THICE.GT.0.0) T2(1)=0.0
RETURN
END
C *****
SUBROUTINE BOTTOM(DZSL,IZSLT,AHTBTM)

```

```

REAL*8 A, V, TV, ATOP, AK, BK, CK, DK, SVOL, DUM
COMMON/RESULT/ T2(40), CHLATOT(40), PA2(40), PTSUM(40), BOD2(40),
+DSO2(40), C2(40), CD2(40), XNO2(40), XNH2(40), CHLA2(3,40),
+PC2(3,40), XNC2(3,40), T20(40), SI2(40)
COMMON/VOL/ZMAX, DZ(40), Z(40), A(40), V(40), TV(40), ATOP(41), DBL
COMMON/MTHD/TAIR(31), TDEW(31), RAD(31), CR(31), WIND(31),
+ PR(31), DRCT(31)
COMMON/STEPS/DZLL, DZUL, MBOT, NM, NPRINT, MDAY, MONTH, ILAY, DY
COMMON/SNICE/ THICE, THSNOW, BTICE, ALFICE, GMICE,
+ BTSNOW, ALFSNOW, GMSNOW, QWATER, HTBTM, HSTMP, TMSTEP
COMMON/BOTT/ SNOWFL(300), TSL(21), ZSL(21), TSLP(21)
DIMENSION PS(21), QS(21), AS(21), BS(21), CS(21), DS(21)
PRMM=DZSL**2/(AHTBTM*TMSTEP/24.0)
DO 3 I=1, IZSLT
AS(I)=1.0
BS(I)=1.0/PRMM
CS(I)=1.0/PRMM
DS(I)=(1.0-2.0/PRMM)*TSL(I)
3 CONTINUE
PS(1)=1.0
QS(1)=0.0
PS(2)=BS(2)/(AS(2)-CS(2))
QS(2)=DS(2)/(AS(2)-CS(2))
DO 10 I=3, IZSLT-1
PS(I)=BS(I)/(AS(I)-CS(I)*PS(I-1))
QS(I)=(DS(I)+CS(I)*QS(I-1))/(AS(I)-CS(I)*PS(I-1))
10 CONTINUE
TSL(IZSLT)=T2(MBOT)
DO 15 L=1, IZSLT-1
I=IZSLT-L
TSL(I)=PS(I)*TSL(I+1)+QS(I)
15 CONTINUE
IF(MOD(MDAY,1).EQ.0) THEN
WRITE(14,1619) MONTH,MDAY,(TSL(IZSLT-I+1),I=1,IZSLT,1)
ENDIF
1623 FORMAT(1X,2I6)
1619 FORMAT(1X,2I4,1X,20F6.2)
RETURN
END

```

C \*\*\* This program is for Harris pond 3 \*\*\*

\$DEBUG

\$NOFLOATCALLS

\$STORAGE:2

```
SUBROUTINE LAKE(ZD,DUM,NFLOW,ID)
  REAL*8 A,V,TV,ATOP,AK,BK,CK,DK,SVOL,DUM
  CHARACTER*20 STFILE
  COMMON/MTHD/TAIR(31),TDEW(31),RAD(31),CR(31),WIND(31),
+ PR(31),DRCT(31)
  COMMON/RESULT/ T2(40),CHLATOT(40),PA2(40),PTSUM(40),BOD2(40),
+DSO2(40),C2(40),CD2(40),XNO2(40),XNH2(40),CHLA2(3,40),
+PC2(3,40),XNC2(3,40),T20(40),SI2(40)
  COMMON/SOURCE/RM(3,40),PROD(40),XMR(3,40),PRODSUM(40)
  COMMON/FLOW/HMK(41),QE(40),FVCHLA(5),PE(5,41)
  COMMON/YIELD/YCA,YCHO2,Y2CHO2,YCBOD,YPBOD,YZW,YPZP,YNZP,YZDO,
+YSCHL,YNHBOD,BRNO,BRNH,XKNNH,THNNH,YPCHLA,BODK20,SB20,BRR
  COMMON/PHYTO/PDEL(3),PMAX(3),PMIN(3),THR(3),THM(3),XKR1(3),
+XKR2(3),XKM(3),HSCPA(3),HSC1(3),HSC2(3),UPMAX(3),THUP(3),
+GROMAX(3),TMAX(3),TOPT(3),XNMAX(3),XNMIN(3),UNMAX(3),THUN(3),
+HSCN(3),HSCNH(3),XNDEL(3),IDIATOM,CHLMEAN,CHLMAX,SECCHI
  COMMON/ZOOPL/IZ,MINDAY,MAXDAY,ZP,ZPMIN,PRMIN,PRMAX,PREDMIN,XIMIN,
+XIMAX,XKRZP,GRAZMAX(3),THGRAZ(3),ASM,THRZP,HSCGRAZ(3),CHLAMIN(3),
+REPRO,XI,XKMZ,GRAZE(3,40)
  COMMON/TEMP/PARIO(4),PCDUM(3,40),XNHD(40),XNOD(40),
+ CHLADUM(3,40),XNCD(3,40),PADUM(40),SID(40)
  COMMON/VOL/ZMAX,DZ(40),Z(40),A(40),V(40),TV(40),ATOP(41),DBL
  COMMON/SUB/SDZ(60),SZ(60),LAY(40),AVGI(4,60),SVOL(60)
  COMMON/CHOICE/MODEL,NITRO,IPRNT(6),NDAYS,NPRNT(30),NCLASS,PLT(30)
  COMMON/WATER/BETA,EMISS,XK1,XK2,HKMAX,WCOEF,WSTR
  COMMON/CHANNEL/WCHANL,ELCB,ALPHA,BW,WLAKE
  COMMON/STEPS/DZLL,DZUL,MBOT,NM,NPRINT,MDAY,MONTH,ILAY,DY
  COMMON/STAT/SUMXY(10),SUMX(10),SUMY(10),XSQ(10),
+YSQ(10),RSQ(10),RMS(10),RELM(10),MTHREL(10),MDAYREL(10),ZREL(10),
+ZRELM(10),RS(10),REL(10),MTHRMS(10),MDAYRMS(10),ZRS(10),ZRMS(10)
  COMMON/INFLOW/QIN(5),TIN(5),PAIN(5),BODIN(5),DOIN(5),CIN(5),
+CDIN(5),XNHIN(5),XNOIN(5),CHLAIN(3,5)
  COMMON/FIELD/ IFLAG(10),FLDATA(10,50),DEPTH(50),NFLD(10),SD
  COMMON/FILE/ DIN,MET,FLO,TAPE8,TAPE1,IREC
  COMMON/TITL/ TITLE
  COMMON/EPDIF/ WINDKM
  COMMON/PREVA/ HED,P
  COMMON/SNICE/ THICE,THSNOW,BTICE,ALFICE,GMICE,
+ BTSNOW,ALFSNOW,GMSNOW,QWATER,HTBTM,HSTMP,TMSTEP
  COMMON/BOTT/ SNOWFL(300),TSL(21),ZSL(21),TSLP(21)
  COMMON/CR/ TWAICE,TAIRICE
  COMMON/ZWIS/ZWITH(5)
  DIMENSION ZS(7),TS(7),QEEE(40)
  CHARACTER*16 DIN,MET,FLO,TAPE8,TAPE1
  GOTO (100,200,300,400,500,600,700,800,900,1000,1100,1200,1300) ID
```

C\*\*\*\*\* AREA COMPUTATION SECTION \*\*\*\*\*

100 CONTINUE

DUM=54.6\*92.4+8.0\*(54.6+92.4)\*ZD+64.0\*ZD\*\*2

RETURN

C\*\*\*\*\* FETCH COMPUTATION SECTION \*\*\*\*\*

200 CONTINUE

ZD=SQRT(4./3.1459\*7090.0)

RETURN

C\*\*\*\*\* VOLUME COMPUTATION SECTION \*\*\*\*\*

300 CONTINUE

DUM=(54.6\*92.4+4.0\*(54.6+92.4)\*zd+64.0/3.\*zd\*\*2)\*ZD



```

RETURN
C***** COMPUTE DEPTH FROM VOLUME *****
400 CONTINUE
    ahh=54.6
    bhh=92.4
    chh=4.0
    dhh=1.0
    dumtmp=abs(dum)
    dhs=4.*chh**2/3./dhh**2
    chs=-dumtmp/dhs
    bhs=ahh*bhh/dhs
    ahs=(ahh+bhh)*chh/dhh/dhs
    pss=-ahs**2/3.+bhs
    qss=chs-bhs*ahs/3.+2.*ahs**3/27.
    ypow=1./3.
    yyy1=(-qss/2.+sqrt(qss**2/4.+pss**3/27.))**ypow
+      +(-qss/2.-sqrt(qss**2/4.+pss**3/27.))**ypow
    ZD=yyy1-ahs/3.
    RETURN
C***** TREATMENT SECTION *****
500 WRITE(*,*) MONTH,MDAY,MBOT
    RETURN
C***** PHOSPHORUS SOURCES/SINKS *****
600 RETURN
C***** NO2-NO3 SOURCES SINKS
700 RETURN
C***** NH4 SOURCES/SINKS *****
800 RETURN
C***** O2 SOURCES/SINKS *****
900 RETURN
C***** OUTFLOW COMPUTATION *****
1000 CONTINUE
    READ(16,*) JULDAY,VZND,TDEPS,QIN(1)
C    READ(17,*) JULD,PVZND,TDISCH,TPUMP
    TPUMP=TPUMP*3600.0
    NFLOW=1
    ZZMB=Z(MBOT)+0.5*DZ(MBOT)
    VDUMZ1=(54.6*92.4+4.0*(54.6+92.4))*ZZMB+64.0/3.
+ *ZZMB**2)*ZZMB
    IF(TDEPSP.LE.0) TDEPSP=ZZMB
    VDUMZ2=(54.6*92.4+4.0*(54.6+92.4))*TDEPSP+64.0/3.
+ *TDEPSP**2)*TDEPSP
    HEVOL=ATOP(1)*HED
    PRVOL=ATOP(1)*P
    QJVOL=QJ*TPUMP
    VMDIFF=-VDUMZ1+VDUMZ2
    QIN(1)=QIN(1)-VDUMZ1+VDUMZ2+HEVOL-PRVOL-QJVOL
    T2C2=T2(1)
    DO 1011 I=1,MBOT-1
    ZINCH=0.5*(ZMAX-0.61)+0.61
    ZWITH(1)=ZMAX-ZINCH
    IF(ZMAX-Z(I).GT.ZINCH.AND.ZMAX-Z(I+1).LE.ZINCH) T2C2=T2(I)
1011 CONTINUE
    TIN(1)=T2C2
    TDEPSP=TDEPS
C
    RETURN
C***** GROUNDWATER FLOW COMPUTATION *****
1100 CONTINUE
    RETURN

```

```

C***** INPUT REQUEST OR MODIFICATION *****
C   AS THIS SUBROUTINE IS CALED JUST ONCE, IN THE BEGINNING,
C   IT IS CONVENIENT TO WRITE HERE ALL THE VALUES WHICH ARE
C   GOING TO BE UNCHANGED
1200 CONTINUE
    OPEN(13, FILE='SIWOUT')
    OPEN(14, FILE='SEDOUT')
    OPEN(15, FILE='TOUT')
    OPEN(16, FILE='QINZD3')
    OPEN(12, FILE='ICEP3')
    READ(12, *) DZSL, ZSLT, IZSLT, IZSLTH, AHTBTM, TSLMEAN, ETAB, ISEDMNT
    READ(12, *) cfsnow, CDISO, CNDSNWO, CNDWI, CONSQW, DEPTH,
+    ICEMNS, ICEDAY, IOPNMNS, IOPNDY
    READ(12, *) HKMXSP, WCFSP, WSSP, HKMXSM, WCFSM, WSSM, WINDKM
    READ(12, *) HKMXFW, WCFFW, WSFW, HKMXIS, WCFIS, WSIS
    READ(12, *) BTICE, ALFICE, GMICE, BTSNOW, ALFSNOW, GMSNOW
    READ(12, *) TWAICE, TAIRICE, TMSTEP
    read(12, *) mnsnow, mdysnow, NDYSTL
C   READ(12, *) 'QJ, CQJET2, DOJET
C   READ(12, *) (SNOWFL(I), I=1, NDYSTL)
    NDYSNW=0
    NDAYST=DY
    THSNOW=0.0
    THICE=0.0
    ifreeze=0
    HSTMSUM=0.0
    QWATSUM=0.0
    HTBTM=0.0
    HTICSUM=0.0

C
C   THIS INITIAL CONDITION IS VALID FOR JAN.-APRIL (MINIMUM BOTTOM TEMP)
C   AND AUG.-OCT. (MAXIMUM BOTTOM TEMP.)
    DZSL=ZSLT/FLOAT(IZSLT-1)
    DO 5 I=1, IZSLT
    ZSL(I)=FLOAT(I-1)*DZSL
    TSL(IZSLT-I+1)=T2(MBOT)*EXP(-ETAB*ZSL(I))+
+    (1.0-EXP(-ETAB*ZSL(I)))*TSLMEAN
    TSLP(IZSLT-I+1)=TSL(IZSLT-I+1)
5 CONTINUE

C
    WRITE(13, 901)
    WRITE(13, 1613)
    WRITE(13, 1615) cfsnow, CDISO, CNDSNWO, CNDWI, DEPTH, ICEMNS, ICEDAY,
+    IOPNMNS, IOPNDY
    WRITE(13, 1616) HKMXSP, WCFSP, WSSP, HKMXSM, WCFSM, WSSM
    WRITE(13, 1616) HKMXFW, WCFFW, WSFW, HKMXIS, WCFIS, WSIS
    WRITE(13, 1614) BTICE, ALFICE, GMICE, BTSNOW, ALFSNOW, GMSNOW
    WRITE(13, 1600)
    WRITE(14, 1629)
    WRITE(14, 1621) DZSL, ZSLT, IZSLT, AHTBTM, TSLMEAN, ETAB
    WRITE(14, 1631)
    DO 10 I=1, IZSLT
    WRITE(14, 1619) ZSL(I), TSL(IZSLT-I+1)
10 CONTINUE
    WRITE(13, 1600)
    WRITE(13, 1618)
    WRITE(13, 251)

C
251 FORMAT('IDAY MON DAY ', 3X, 'QWAT', 2X, 'QWSUM',
+ 3X, 'HTBTM', 3X, 'HTSUM', 5X, 'HS', 5X, 'HSSUM', 3X, 'THICE',

```

```

+ 1X, 'THSN0', 2X, 'SNOWF', 3X, 'HSA', 3X, 'HKMAX', 4X, 'RAD', 3X, 'HCNDISO')
901 FORMAT('INPUT DATA:')
1600 FORMAT(' ')
1613 FORMAT(3X, 'CFSNOW CDISO CNDSNWO CNDWI DEPTHIC ICEMNS ICEDAY', 1X,
+ 'IOPNMNS IOPNDY')
1614 FORMAT(2X, 'B,A,G(ICE,SNOW)= ', 6F8.3)
1615 FORMAT(2X, F6.2, 1X, F5.2, 1X, F7.2, 1X, F5.2, 1X, F6.1, 1X, I6, 1X, I6, 1X,
+ I7, 1X, I6)
1616 FORMAT(2X, 'HKMAX, WCOEF, WSTR = ', 2X, 3F8.3)
1618 FORMAT('RESULTS OF SIMULATION:')
1619 FORMAT(12X, F8.2, 10X, F8.2)
1621 FORMAT(2X, 2F8.1, 2X, I4, 2X, 'AHTBTM, TSLMEAN= ', 2F10.5, 2X, F6.3)
1629 FORMAT('TEMPERATURE DISTR. IN THE SEDIMENT BELOW LAKE BOTTOM:')
1631 FORMAT(2X, 'DEPTH BELOW BOTTOM', 8X, 'TEMPERATURE')
RETURN
C***** POST DAILY SIMULATION TREATMENT AND COMPUTATIONS *****
C-----
1300 CONTINUE
C*****
WRITE(*, 1627) RAD(MDAY), CR(MDAY)
1627 FORMAT(2X, 'RAD= ', F6.1, 2X, 'CR= ', F8.2)
IF(ISEDNT.EQ.1) THEN
CALL BOTTOM(DZSL, IZSLT, AHTBTM)
HTBTM=HTBTMP
HTBTMP=0.0
DO 1628 I=1, IZSLT
IF(I.EQ.1.OR.I.EQ.IZSLT) DZSLLL=.5*DZSL
HTBTMP=HTBTMP+500.0*DZSLLL*(TSLP(I)-TSL(I))*TMSTEP/24.0
TSLP(I)=TSL(I)
DZSLLL=DZSL
1628 CONTINUE
ENDIF
IF(MONTH.GE.ICEMNS+4) THEN
HKMAX=HKMXSM
WCOEF=WCFSM
WSTR=WSSM
ENDIF
IF(MONTH.EQ.MNSNOW.AND.MDAY.GE.MDYSNOW.AND.THICE.EQ.0.0) THEN
HKMAX=HKMXFW
WCOEF=WCFFW
WSTR=WSFW
ENDIF
IF(MONTH.GT.MNSNOW.AND.THICE.EQ.0.0) THEN
HKMAX=HKMXFW
WCOEF=WCFFW
WSTR=WSFW
ENDIF
IF(THICE.GT.0.0) THEN
HKMAX=HKMXIS
WCOEF=WCFIS
WSTR=WSIS
ENDIF
IF(MONTH.LT.ICEMNS+4.AND.THICE.EQ.0.0) THEN
HKMAX=HKMXSP
WCOEF=WCFSP
WSTR=WSSP
ENDIF
C IF(MONTH.GT.ICEMNS.AND.MONTH.LT.MNSNOW) RETURN
CALL SNOW(CFSNOW, MNSNOW, MDYSNOW, NDYSNW)
CALL ICE(IFREEZE, CDISO, CNDSNWO, DEPTHIC, ICEMNS, ICEDAY,

```

```

+ IOPNMNS,IOPNDY,NDYSNW,NDAYST,HKMAX,MNSNOW,CNDWI,CONSQW)
ZST=Z(MBOT)+DZ(MBOT)/2.0
ZS(6)=ZST
ts(6)=t2(mbot-1)+(ZS(6)-z(mbot-1))*
+ (t2(mbot)-t2(mbot-1))/(z(mbot)-z(mbot-1))
IF(ZST.GE.1.0) THEN
ZS(1)=0.04
ZS(2)=0.25
ZS(3)=0.50
ZS(4)=0.75
ZS(5)=1.00
c ZS(6)=1.00
ENDIF
DO 1821 I=1,5
IF(ZST.LT.1.0) THEN
ZS(I)=ZST-(1.04-FLOAT(I-1))*0.25)
ZS(5)=ZS(6)
ENDIF
DO 1823 J=1,MBOT-1
if(z(J).le.ZS(I).and.z(J+1).gt.ZS(I)) ts(I)=t2(J)+(ZS(I)-z(J))*
+ (t2(J+1)-t2(J))/(z(J+1)-z(J))
1823 CONTINUE
IF(ZS(I).LT.0) THEN
ZS(I)=0
TS(I)=0.0
ENDIF
1821 CONTINUE
IF(ZS(1).LT.Z(1)) TS(1)=T2(2)-(T2(2)-T2(1))/(Z(2)-Z(1))
+ (Z(2)-ZS(1))
TSOMIT=0.0
IF(ZST.GE.1.0) WRITE(15,1825) NDAYST,(Ts(I),I=1,6),QIN(1),
+ TIN(1),TDEPS,ZST,QTLES,TPT,ZJITPT,HEVOL,PRVOL,QJVOL,VMDIFF
IF(ZST.LT.1.0) WRITE(15,1825) NDAYST,TSOMIT,(Ts(I),I=1,5),QIN(1),
+ TIN(1),TDEPS,ZST,QTLES,TPT,ZJITPT,HEVOL,PRVOL,QJVOL,VMDIFF
1825 FORMAT(1X,I4,1X,6F6.2,1X,F8.1,1X,F4.1,2F5.2,1X,F6.2,
+ 1X,F4.1,1X,F6.3,1X,3F6.1,1X,F6.1)
RETURN
END
C *****
SUBROUTINE SNOW(CFSNOW,MNSNOW,MDYSNOW,NDYSNW)
REAL*8 A,V,TV,ATOP,AK,BK,CK,DK,SVOL,DUM
COMMON/RESULT/ T2(40),CHLATOT(40),PA2(40),PTSUM(40),BOD2(40),
+DSO2(40),C2(40),CD2(40),XNO2(40),XNH2(40),CHLA2(3,40),
+PC2(3,40),XNC2(3,40),T20(40),SI2(40)
COMMON/VOL/ZMAX,DZ(40),Z(40),A(40),V(40),TV(40),ATOP(41),DBL
COMMON/MTHD/TAIR(31),TDEW(31),RAD(31),CR(31),WIND(31),
+ PR(31),DRCT(31)
COMMON/STEPS/DZLL,DZUL,MBOT,NM,NPRINT,MDAY,MONTH,ILAY,DY
COMMON/SNICE/ THICE,THSNOW,BTICE,ALFICE,GMICE,
+ BTSNOW,ALFSNOW,GMSNOW,QWATER,HTBTM,HSTMP,TMSTEP
COMMON/BOTT/ SNOWFL(300),TSL(21),ZSL(21),TSLP(21)
C SNOW ACCUMULATION FROM THE PRECIPITATION
IF(MNSNOW.EQ.MONTH.AND.MDAY.EQ.MDYSNOW) NDYSNW=1
IF(NDYSNW.GT.0) THEN
THSNOW=THSNOW+SNOWFL(NDYSNW)/(12.0*3.2808)*CFSNOW
NDYSNW=NDYSNW+1
ENDIF
C SNOW MELT
HTLTNT=80.0
DENSNOW=300.0

```

```

HTSNOW=RAD(MDAY)*10.0*(BTSNOW+(1.0-BTSNOW)*(1.0-ALFSNOW)*
+ (1.0-EXP(-GMSNOW*THSNOW)))
CPOWER=-0.0000156*800.0
TDEWMLT=TDEW(MDAY)
CPW2=7.45*TDEWMLT/(235.0+TDEWMLT)
EA=6.035*10.0**CPW2
TSNW=32.0+9.0*TAIR(MDAY)/5.0
SNOWMELT=WIND(MDAY)*(0.00736*(TSNW-32.0)*10**CPOWER
+ 0.0231*(EA-6.11))
SNOWMELT=SNOWMELT/(12.0*3.2808)
IF(TAIR(MDAY).GT.0.0) THEN
SNOWMELT=SNOWMELT+PR(MDAY)*TAIR(MDAY)*3.0/80.0*0.0254
SNOWMELT=SNOWMELT+HTSNOW/(DENSNO*HTLTNT)
ENDIF
SNOWMELT=TMSTEP/24.0*SNOWMELT
IF(SNOWMELT.LE.0.0) SNOWMELT=0.0
THSNOW=THSNOW-SNOWMELT
IF(THSNOW.LE.0.0) THSNOW=0.0
IF(THICE.LE.0.0) THSNOW=0.0
RETURN
END

```

C

```

*****
SUBROUTINE ICE(IFREEZE,CDISO,CNDSNWO,DEPTHC,ICEMNS,ICEDAY,
+ IOPNMS,IOPNDY,NDYSNW,NDAYST,HKMAX,MNSNOW,CNDWI,CONSOW)
REAL*8 A,V,TV,ATOP,AK,BK,CK,DK,SVOL,DUM
COMMON/RESULT/ T2(40),CHLATOT(40),PA2(40),PTSUM(40),BOD2(40),
+DSO2(40),C2(40),CD2(40),XNO2(40),XNH2(40),CHLA2(3,40),
+PC2(3,40),XNC2(3,40),T2O(40),SI2(40)
COMMON/VOL/ZMAX,DZ(40),Z(40),A(40),V(40),TV(40),ATOP(41),DBL
COMMON/MTHD/TAIR(31),TDEW(31),RAD(31),CR(31),WIND(31),
+ PR(31),DRCT(31)
COMMON/STEPS/DZLL,DZUL,MBOT,NM,NPRINT,MDAY,MONTH,ILAY,DY
COMMON/SNICE/ THICE,THSNOW,BTICE,ALFICE,GMICE,
+ BTSNOW,ALFSNOW,GMSNOW,QWATER,HTBTM,HSTMP,TMSTEP
COMMON/BOTT/ SNOWFL(300),TSL(21),ZSL(21),TSLP(21)
COMMON/CR/ TWAICE,TAIRICE
DLTIME=TMSTEP/24.0
CNDICE=0.85984*24.0*CDISO
DENICE=920.0
HTLTNT=80.0
DENSNO=300.0
CNDSNWO=CNDSNWO*0.85984*24.0
TMELT=0.0
HTSNIS=RAD(MDAY)*10.0*(1.0-BTSNOW)*(1.0-ALFSNOW)*
+ EXP(-GMSNOW*THSNOW)
HTICE=HTSNIS*(BTICE+(1.0-BTICE)*(1.0-ALFICE)*(1.0-
+ EXP(-GMICE*THICE)))
HSA=0.33*117.0*WIND(MDAY)
AC=THICE/CNDICE
BC=THSNOW/CNDSNWO
CC=1.0/HSA
DC=DLTIME/(DENICE*HTLTNT)
EC=TMELT-TAIR(MDAY)
DO 20 I=1,MBOT-1
IF(Z(I+1).GE.DEPTHC.AND.Z(I).LT.DEPTHC) THEN
TCHAR=T2(I)+(T2(I+1)-T2(I))*(DEPTHC-Z(I))/(Z(I+1)-Z(I))
ENDIF
20 CONTINUE
QWATER=CNDWI*(TCHAR-TMELT)/DEPTHC
IF(QWATER.LE.0.0) QWATER=0.0

```

```

IF(THICE.LE.0.0) QWATER=0.0
HCNDISO=EC/(AC+BC+CC)
THICE=THICE+DC*(EC/(AC+BC+CC)-QWATER)
if(tair(mday).le.0.0) ifreeze=1
C
IF(THICE.LE.0.0) THICE=0.0
IF(THICE.EQ.0.0) GOTO 92
IF(THSNOW.GT.0.0) GOTO 92
IF(TAIR(MDAY).GT.0.0) THEN
THICE=THICE-PR(MDAY)*TAIR(MDAY)*0.0254/80.0*TMSTEP/24.0
THICE=THICE-HTICE*DC
ENDIF
C
92 IF(THICE.LT.0.0) THICE=0.0
IF(IFRUP.EQ.1) GO TO 50
HTSUM=0.0
VSUM=0.0
DO 53 I=1,MBOT
HTSUM=HTSUM+T2(I)*A(I)*DZ(I)
53 VSUM=VSUM+A(I)*DZ(I)
TWAVE=HTSUM/VSUM
IF(TWAVE.LE.TWAICE.AND.TAIR(MDAY).LE.TAIRICE) THEN
IOPNMNS=MONTH
IOPNDY=MDAY
IFRUP=1
ENDIF
50 CONTINUE
60 IF(MONTH.EQ.IOPNMNS.AND.MDAY.LT.IOPNDY) THICE=0.0
IF(MONTH.EQ.ICEMNS.AND.MDAY.GT.ICEDAY) THICE=0.0
IF(MONTH.GT.ICEMNS.AND.MONTH.LT.IOPNMNS) THICE=0.0
if(ifreeze.eq.1) then
dgrdy=dgrdy+ec*dlttime
endif
HSTMSUM=HSTMSUM+HSTMP
QWATSUM=QWATSUM+QWATER
HTBTSUM=HTBTSUM+HTBTM
HTICSUM=HTICSUM+HCNDISO
RADTMP=RAD(MDAY)*10.0
WRITE(13,250) NDAYST,MONTH,MDAY,QWATER,QWATSUM,HTBTM,HTBTSUM,
+HSTMP,HSTMSUM,THICE,THSNOW,HSA,HKMAX
250 FORMAT(3I4,1X,F6.2,1X,F7.2,1X,F8.2,1X,F8.2,1X,F7.1,1X,F8.1,
+1X,F5.3,1X,F6.4,1X,F6.4,1X,F6.1,1X,F6.3,1X,F7.1,1X,F10.1,1X,F16.1)
C B.C. AT WATER/ICE INTERFACE IS TEMPERATURE = 0 C
NDAYST=NDAYST+1
C
QWATER=0.0
QWATER=QWATER*TMSTEP/24.0*CONSQW
IF(THICE.GT.0.0) T2(1)=0.0
RETURN
END
C *****
SUBROUTINE BOTTOM(DZSL,IZSLT,AHTBTM)
REAL*8 A,V,TV,ATOP,AK,BK,CK,DK,SVOL,DUM
COMMON/RESULT/ T2(40),CHLATOT(40),PA2(40),PTSUM(40),BOD2(40),
+DSO2(40),C2(40),CD2(40),XNO2(40),XNH2(40),CHLA2(3,40),
+PC2(3,40),XNC2(3,40),T20(40),SI2(40)
COMMON/VOL/ZMAX,DZ(40),Z(40),A(40),V(40),TV(40),ATOP(41),DBL
COMMON/MTHD/TAIR(31),TDEW(31),RAD(31),CR(31),WIND(31),
+ PR(31),DRCT(31)
COMMON/STEPS/DZLL,DZUL,MBOT,NM,NPRINT,MDAY,MONTH,ILAY,DY
COMMON/SNICE/ THICE,THSNOW,BTICE,ALFICE,GMICE,

```

```

+      BTSNOW,ALFSNOW,GMSNOW,QWATER,HTBTM,HSTMP, TMSTEP
COMMON/BOTT/ SNOWFL(300),TSL(21),ZSL(21),TSLP(21)
DIMENSION PS(21),QS(21),AS(21),BS(21),CS(21),DS(21)
PRMM=DZSL**2/(AHTBTM*TMSTEP/24.0)
DO 3 I=1,IZSLT
AS(I)=1.0
BS(I)=1.0/PRMM
CS(I)=1.0/PRMM
DS(I)=(1.0-2.0/PRMM)*TSL(I)
3 CONTINUE
PS(1)=1.0
QS(1)=0.0
PS(2)=BS(2)/(AS(2)-CS(2))
QS(2)=DS(2)/(AS(2)-CS(2))
DO 10 I=3,IZSLT-1
PS(I)=BS(I)/(AS(I)-CS(I)*PS(I-1))
QS(I)=(DS(I)+CS(I)*QS(I-1))/(AS(I)-CS(I)*PS(I-1))
10 CONTINUE
TSL(IZSLT)=T2(MBOT)
DO 15 L=1,IZSLT-1
I=IZSLT-L
TSL(I)=PS(I)*TSL(I+1)+QS(I)
15 CONTINUE
IF(MOD(MDAY,1).EQ.0) THEN
WRITE(14,1623) MONTH,MDAY
DO 20 I=1,IZSLT
WRITE(14,1619) ZSL(I),TSL(IZSLT-I+1)
20 CONTINUE
ENDIF
1623 FORMAT(1X,2I6)
1619 FORMAT(3X,2F8.3)
RETURN
END

```